2014

Effect of suction on local scour around circular bridge piers

Mohammed Jahan
University of Windsor

EFFECT OF SUCTION ON LOCAL SCOUR AROUND CIRCULAR BRIDGE PIERS

By

Mohammed Jahan

A Thesis
Submitted to the Faculty of Graduate Studies
through the Department of Civil and Environmental Engineering
in Partial Fulfillment of the Requirements for
the Degree of Master of Applied Science
at the University of Windsor

Windsor, Ontario, Canada

2014

EFFECT OF SUCTION ON LOCAL SCOUR AROUND CIRCULAR BRIDGE PIERS

by

Mohammed Jahan

APPROVED BY:

_____
R. Barron
Department of Mathematics and Statistics, University of Windsor

_____
V. Roussinova
Department of Civil and Environmental Engineering, University of Windsor

_____
R. Balachandar, Co-Advisor
Department of Civil and Environmental Engineering, University of Windsor

_____
T. Bolisetti, Advisor
Department of Civil and Environmental Engineering University of Windsor

April 23, 2014

AUTHOR'S DECLARATION OF ORIGINALITY

I hereby certify that I am the sole author of this thesis and that no part of this thesis has been published or submitted for publication.

I certify that, to the best of my knowledge, my thesis does not infringe upon anyone's copyright nor violate any proprietary rights and that any ideas, techniques, quotations, or any other material from the work of other people included in my thesis, published or otherwise, are fully acknowledged in accordance with the standard referencing practices.

I declare that this is a true copy of my thesis, including any final revisions, as approved by my thesis committee and the Graduate Studies office, and that this thesis has not been submitted for a higher degree to any other University or institution.

ABSTRACT

An experimental study was conducted in the Hydraulics Laboratory of the University of Windsor, involving analysis of local scour around circular model bridge piers placed on a non-cohesive sand bed, with suction and no suction conditions. Experiments were conducted using three model circular piers. The results show that a narrower pier will induce a large value of depth averaged channel mean velocity in comparison to a wider pier in the same flow field. Furthermore, suction generally creates larger equilibrium scour depth, and increases near bed velocity, and decreases friction velocities with increasing suction. The present results indicate that, generally, scour rate with suction at the beginning of the test is higher than the scour rate with no suction condition. It was also observed in the present study that the percentage increase of equilibrium scour depth was almost 23% for 5% suction and 42% for 10% suction in comparison to no suction conditions.

ACKNOWLEDGEMENTS

First of all, I would like to express my gratitude to Almighty ALLAH for giving His blessings to complete this thesis. I also like to express my sincere appreciation and deep sense of gratitude to my Advisor Dr. Tirupati Bolisetti for his guidance, encouragement and personal concern throughout the course of this research work. My sincere acknowledgement also goes to co-Advisor Dr. Ram Balachandar for his invaluable and helpful suggestions and guidance in this work.

Special thanks to Matt St. Louis and Mr. Prashanth for their assistance and help throughout the laboratory program of my research. I want to use this opportunity to express my sincere thankfulness to my wife, daughter and son for their constant support and encouragement.

DEDICATION

This thesis is dedicated to my late mother Mrs. Rawshan Ara Parul. The dedication also goes to my father Md. Golam Mostofa who is 83 years old and gave me continuous encouragements over the telephone from my back home country (Bangladesh).

TABLE OF CONTENTS

LIST OF TABLES

LIST OF FIGURES

NOMENCLATURE

ACRONYMS

ADV	Acoustic Doppler Velocimeter
CSU	Colorado State University
WDOT	Washington State Department of Transportation
FHWA's HEC-18	Federal Highway Administration, Hydrological Engineering Circular

SYMBOLS

d_{se}	equilibrium scour depth
D	model pier diameter
y_o	approach flow depth
y	vertical or wall normal distance
d_{50}	diameter of sand, 50% of which is finer by weight
σ_g	geometric standard deviation of sand bed particle
C_u	uniformity coefficient of sand bed particle
C_c	coefficient of gradation
U^*	shear velocity
U^+	velocity in inner coordinate (velocity scaled by the friction velocity = U/U^*)
y^+	depth in inner coordinate (or depth scaled by friction velocity = yU^*/ν)
U_e	free stream velocity
δ	boundary layer thickness
U	depth averaged approach velocity

k_s	bed roughness coefficient
U_c	critical mean flow velocity
U_c^*	critical shear velocity
$F_{doppler}$	change in received frequency (Doppler shift)
F_{source}	frequency of transmitted sound
V	velocity of source relative to receiver
C	speed of sound
τ_w	wall shear stress
ρ	density of water
γ	specific weight of water
ν	kinematic viscosity of water
U'	turbulence intensity
d_{se}	equilibrium local scour depth
d_{st}	scour depth at time t
Y	dimensionless time-dependent scour depth = d_{se}/d_{st}
T	dimensionless time = tU/D

CHAPTER 1

INTRODUCTION

1.1 Background

Bridges on a river or a stream play a vital role for economic, social and cultural improvement in any country. More than 1000 bridges have collapsed over the past 30 years in the USA, with 60% of the failures occurring due to scour. This serious problem also happens in many East Asian countries, such as Taiwan, Japan, Korea, owing to the fact that these areas are subjected to several typhoon and flood events each year during the summer and fall seasons. St. Anthony Falls Hydraulics Laboratory recently conducted an automated scour monitoring system due to recent flooding to protect Minnesota bridges in USA [50]. Scour failure tends to occur suddenly and without prior warning or sign of distress to the structure (Lin et al., 2004). According to the National Transportation Safety Board [39] the 1989 catastrophic collapse of the several bridges over the Hatchie River in Tennessee (USA) resulted in the death of eight people. In an intensive study of bridge failures in the United States, Ross et al. (1993) reported that the Federal Highways Administration in 1978 claimed that damage to bridges and highways from major regional floods in 1964 and 1972 estimated about $100 million per event.

There are mainly two types of scour; general and local. General scour occurs due to natural processes and excessive shear stress at the bottom of a channel, and this type of scour is greatly influenced by the cross-sectional shape of a river or stream (Breusers and Raudkivi, 1991). On the other hand, local scour at a bridge pier is due to the obstruction to the flow. Local scour is defined as “the abrupt decrease in bed elevation near a pier due to the erosion of the bed material by the local flow structure induced by the piers” (Shen

et al., 1969). Local scour results from the development of secondary circulation due to curvature in the stream lines around bridge pier and vertical velocity components (Herbich and Brennan, 1967). Further, local scour can be classified into two types: a) clear-water scour and b) live-bed scour. In clear-water scour the bed material upstream of the scour area remains stationary. In this case the bed shear stresses away from the structure are less than sediment critical shear stress, which is defined as the stress when sediment movement just starts On the other hand live-bed scour occurs when there is general bed load transport by the stream. Here the bed shear stresses away from the structure are greater than the critical stress. By using flow intensity (U/U_c) it is said that clear-water scour occurs when $U/U_c \leq 1$ and live-bed scour occurs when $U/U_c \geq 1$. Here, U is the depth averaged approach velocity and U_c is the critical depth averaged approach velocity.

When a bridge is constructed on a river and the flow is partially obstructed by a bridge pier, the flow pattern in the channel is significantly changed. The shear stresses around the pier increase due to the formation of vortices, which aid in scouring the bed and the bank of the channel. Accurate prediction of the scour pattern near any obstacle, such as a bridge pier, helps to compute sediment transport and bed morphodynamics around the obstacle. Scour reduces pier support and the effective length of friction bearing piles which results in pier settlement, bottom rotation and/or top rotation of the pier.

Ettema et al., (2006) noted that due to the presence of an obstruction, a complex flow field evolves with horseshoe vortices, surface rollers, and wake vortices. High concentrations of velocities, bed shear stresses, vortices, down-flows and turbulence occur at the nose of the cylinder, which propagate downstream. The combination of these

factors leads to the removal of bed sediments from around the cylinder and the development of a local scour hole.

A river bed of permeable material (e.g. cohesionless sand) induces suction, which can be defined as drawing water downward, either artificially (engineering structures such as a river intake) or naturally (surface water level of river is higher than surrounding groundwater level) through the river bed. Suction has a significant influence on the near bed flow field, which can change bed load movement and boundary stresses that may lead to scouring. The study of bed-suction effects on the structure of turbulent open channel flow has both practical and theoretical interest. Prinos (1995) found that the near bed flow field variation due to suction (in the presence of a river intake structure) increases boundary shear stresses, which may increase local scour and damage the intake structure. Prinos (1995) also noted that with increasing suction rate, near bed velocities were increased and the excess bed shear stress was calculated to be in the order of three to eight times the respective one with no suction.

Numerous laboratory investigations of local scour around structures have been reported in the hydraulics engineering literature. Nevertheless, there is no unifying theory to use with confidence for safe and economic design. One of the main reasons to study local scour around bridge piers is the uncertainty of scour failure. There is considerable uncertainty in the use of the various existing scour depth formulae to predict scour in field settings (Mia and Nago, 2003). Mohammed et al., (2006) stated that many researchers developed numerous formulae for estimating maximum local scour based on limited data, and the use of these formulae in design is uncertain because laboratory flumes are rectangular and natural channels are non-rectangular with rough and mobile

banks. Therefore, it is very important to understand the local scour phenomenon which is vital for the design of pier foundations.

1.2 Objectives

The objectives of this study are the following:

i) To review the relation between depth of flow and bridge pier diameter, and to investigate time variations of equilibrium scour depth with no suction and with suction

ii) To understand the effect of suction on equilibrium local scour depth

1.3 Scope

To achieve the objectives, the following steps are needed:

i) Review present and past experimental programs with suction

ii) Analyze scour geometry and deposit profiles obtained from experiments with no suction and with varying suction rates. As stated later, six experiments were performed for each case.

iii) Review velocity profiles with different suction rates and with no suction condition by using an acoustic Doppler velocimeter.

1.4 Organization of Thesis

Appropriate literature review of experimental study on local scour around bridge piers and seepage effect on local scour is presented in Chapter 2. The details of the acoustic Doppler velocimeter (ADV) system, experimental set-up and procedures, and the description of the flow system are provided in the Chapter 3. The results and the analysis are presented in Chapter 4. Finally, conclusions and recommendations are presented in Chapter 5.

Chapter 2

LITERATURE REVIEW

2.1 Introduction

This chapter discusses the current state of literature dealing with pier scour. The role of seepage in open channel flow is discussed and the existing literature is analyzed to evaluate the potential influence of seepage on scour. Scour around cylindrical bridge piers in a non-cohesive sediment bed has been extensively studied in the last few decades (e.g., Melville and Raudkivi, 1977; Melville and Sutherland, 1988; Chiew and Melville, 1987; Hoffmans and Pilarczk, 1995).

The National Cooperative Highway Research Program Project 24-27(01) discusses scour as a design concern (Ettema et al., 2011). In addition, the report discusses the pier scour interaction process, the influence of primary and secondary parameters, pier site complications, leading prediction formulae, proposed design methodology, and research needs for single-column piers and complex pier-forms. Some key aspects in the report are:

i) The flow field and the potential maximum scour depth change in accordance with three variable- effective pier width, undisturbed approach flow depth and erodibility of the boundary material

ii) The flow field differs substantially for narrow piers, transition pier, and wide pier categories

iii) Estimation of potential maximum scour depth is preferred rather than the entire scour geometry. Potential maximum scour depth is the greatest scour

depth attainable for a given pier flow field, and can be determined using the primary variables

iv) Flow conditions commonly vary with time

Ettema et al., (2006) suggested the need for the inclusion of Euler number (U^2/gD) effects in scour prediction methods. Parameter U^2/gD is useful for describing energy gradients for flow around a pier. It can be considered to express the ratio of stagnation head $U^2/2g$ to pier width. To preserve flow patterns, pressure head along flow paths scale directly with the geometric scale relating a model pier in the laboratory to a pier in the field. Based on their laboratory data, they defined a correction factor that could be used to account for Euler number effects in laboratory scale tests.

2.2 Seepage Effect on Local Scour

Limited literature can be found on the effect of seepage on local scour around bridge piers. Generally, seepage flow remains insignificant in comparison to the main flow. However, sometimes it may be large enough to adversely affect the existing situation of local scour. Since seepage can change the flow boundary condition and existing sediment transport, scouring of the river bed would be changed accordingly. Seepage flow which occurs at the interface between the sand-bed and the flowing water is very complex. Results of many past investigators were sometimes contradictory in nature (Francalanci et al., 2008; Liu and Chiew, 2012). The critical shear stress near a sediment bed and the boundary shear stress are the two important factors which determine increase or decrease of local scour depth under the influence of seepage. Many changes in the characteristics of the flow in the presence of seepage are interrelated and apparently difficult to comprehend.

Most researchers accept that bed suction increases the bed shear stresses as reported by Maclean and Willets (1986), Maclean (1991), Prinos (1995) and Chen and Chiew (2004), but the magnitude of the increase remains a point of contention. The extent of increase or decrease of sediment transport rate depends upon the flow regime (which relates bed-forms in alluvial channels to flow velocity). Richardson and Richardson (1985) found that for the lower flow regime the sediment transport rate increased with injection seepage. In the lower flow regime, sediment transport rate becomes very low due to flow velocity remains below critical entrainment velocity resulting in lower plane bed, ripples marks, and slightly larger dunes. Oldenziel and Brink (1974) observed that injection increased the sediment transport. Willets and Drossos (1975) concluded that suction near the sand bed enhanced the rate of sediment transport if the extent of the suction zone was limited. Seepage injection inhibits the motion of bed particles, while suction enhances it.

Using one of the flumes at the Hydraulic Engineering Laboratory at the University of Windsor, Faruque (2009) conducted experiments by introducing various degrees of suction and injection. He showed that for two different flow rates, suction increases the near-bed velocity and decreases bed shear stress, resulting in reduced bed stability. On the other hand, injection decreases the near-bed velocity and increases the bed shear stress, resulting in increased bed stability. Faruque (2009) also showed that the effect of seepage on different turbulent characteristics was not restricted to the near-bed region but could be seen throughout the flow depth. Seepage can change the rate of sediment transport and eventually affect the depth of local scour.

Chiew and Hong (2013) conducted experiments in the presence of a pier with 2% suction. The equilibrium scour depth was reduced by 50% and 30%, where suction sources were

located near the pier and 6.4D downstream distance from the pier centre repectively (D = pier diameter) in comparison with the no suction condition.

Dey and Sarker (2007) conducted an experimental study of injection seepage through the river bed downstream of an apron of a sluice gate. They found that equilibrium scour depth and many other scour geometry parameters increased with increase of injection. Francalanci et al., (2008) showed experimentally that suction caused scour and injection produced deposition. Francalanci et al., (2006) also showed that the flow field in the vicinity of bridge piers was characterized not only by highly non-hydrostatic pressure fields, but also by two dimensional patterns of boundary shear stress.

Maclean and Willetts (1986) experimentally measured the shear stress using indicator grains and reported an increase in bed shear stress over a suction zone associated with a submerged type of river intake structure. In later work, Maclean (1991) conducted laboratory experiments to determine the increase in bed shear stress and local scour with a mobile bed, and the final scour depth was found to be directly proportional to the difference between the initial bed shear stress because of suction and the threshold bed shear stress for the bed grains in the presence of suction. Prinos (1995) reported much higher bed stresses than that obtained by Maclean and Willets (1986) for the same suction rate.

The following table shows the research findings of past studies on the effect of seepage on sediment particle movement.

Table 2.1. Summary of results of previous investigations (Source: Liu and Chiew, 2012)

Source	Flume dimensions			Seepage effects					
	Length (m)	Width (m)	Seepage zone (m)	Bed shear stress		Critical shear stress		Sediment transport	
				I	S	I	S	I	S
Oldenziel and Brink (1974)	15	0.5	4	↓	-	-	-	↑	↓
Willets and Drossos (1975)	3.6	0.076	0.125	-	-	-	-	-	↑
Richardson (1985)	9.45	0.3	3	-	-	-	-	↑	-
Maclean and Willets (1986)	5	0.076	0.13	-	↑	-	-	-	↑
Maclean (1991)	5	0.075	0.13	-	↑	-	-	-	↑
Rao et al. (1994)	14.16	0.615	1.275	↑	↑	-	-	-	-
Prinos (1995)	-	-	-	-		-	-	-	-
Cheng and Chiew (1999)	7.6	0.21	0.5	-	-	↓	-	-	-
						-	-	-	
Ali et al. (2003)	5.5	0.6	1	↓	-	↓	-	↓	-
Chen and Chiew (2004)	30	0.7	2	-	↑	-	-	-	-
Dey and Zanke (2004)	-	-	-	-	-	↓	-	-	-
Xie et al. (2009)	-	-	-	-	-	↓	-	-	-
Dey and Nath (2010)	12	0.6	2	↓	↑	-	-	-	-

Letter ‘I’ denotes Injection and ‘S’ denotes Suction, and ↑ means increasing and ↓ means decreasing.

2.3 Scouring Processes

When a structure is placed in a current, the flow is accelerated around the structure and the vertical velocity gradient of the flow is transformed into a pressure gradient on the leading edge of the structure. This pressure gradient results in a downward flow that impacts the bed. At the base of the structure, this downward flow forms vortices whose ends are swept around and downstream of the structure by the surrounding flow field (Fig. 2.1). The downward flow velocity at the nose of a bridge pier and a vortex system (comprised of a horseshoe-vortex, a wake vortex and a surface roller) are the basic components of flow fields that cause local river-bed scour at or near bridge piers.

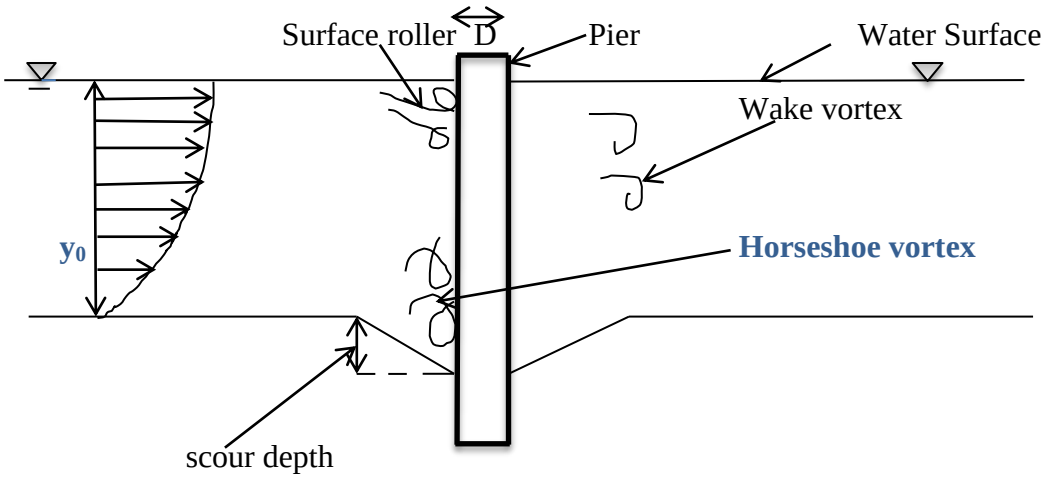

Fig. 2.1. Definition sketch of flow field in the vicinity of a pier

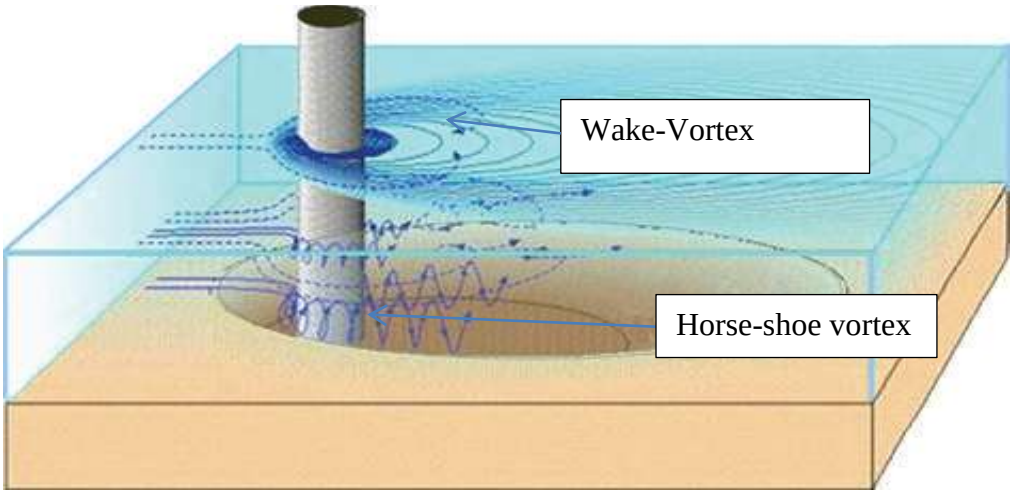

Fig. 2.2. Schematic of local scour showing horseshoe and wake vortices around cylindrical piers (adapted from Yu and Yu, 2010)

According to Muzzammil and Gangadhariah (2003), the power of the vortices in front of the pier is proportional to the mean flow velocity, U. The vortices contain an energy that is dissipated in the following form:

Power per unit mass = $\frac{dv^2}{dt} = A_p \frac{v^3}{l_v}$ (1)

Where *v* is the mean velocity of the vortex, l_v is the length defined as the vortex size, and A_p is constant of the order one, independent of the Reynolds number.

The relationship between the vortex velocity and the flow velocity is nearly constant in a circular pier. The mean velocity of the flow can be expressed as:

$U = q/ (y_0 + d_{se})$ (2)

Here, y_0 is the water depth, d_{se} is the equilibrium scour depth measured from the bed level and q is the unit flow discharge

Experiments by Ettema (1980) revealed that for a circular cylinder and no scour hole, the maximum downward velocity is approximately 40% of the mean approach velocity. When scour occurs, the maximum downward velocity is about 80% of U.

The maximum scour depth has been the primary concern in the study of local scour around bridges and most researchers have concentrated on this measurement, which has been expressed as the relative scour depth, d_{se}/D for clear-water and live-bed scour. Many researchers, e.g., Shen et al., (1969), and Jain and Fischer (1980) have recognized the two independent components of scour depth: i) scour depth due to pier, and ii) change in bed elevation due to bed features.

2.4 Prediction Methods for Bridge Pier Scour

By conducting extensive research with laboratory and field data, various prediction methods for bridge pier scour have been developed, (e.g. Melville and Sutherland, 1988; Mia and Nago, 2003; Ashtiani et al., 2009). More than 35 different formulae have been proposed for scour estimation since 1949. Hopkins et al., (1980) stated that over the past century many investigators attempted to develop a simple scour prediction formula, and it appeared that a set of variables were arbitrarily selected and data collected over a limited range to determine their relationship to scour depth. This approach has left engineers with a large number of sometimes conflicting formulae to predict scour.

Breusers et al., (1977) identified many variables which influence local scour. To lessen cost and complexities, Copp and Johnson (1987) limited these variables to eight considering alluvial, non-cohesive, uniform particle-sized bed materials, and working with single piers that were perfectly smooth and aligned with the approach flow and without scour protection systems. The functional relationship was expressed as:

$$d_{se} = f(\rho, \upsilon, g, d, \rho_s, y_0, U, D) \qquad (3)$$

Where ρ is the density of water, υ is the kinematic viscosity of water, g is the acceleration due to gravity, d is the grain diameter, ρ_s is the density of sediment, y_0 is the approach flow depth and D is the diameter of pier.

2.5 Some Important Scour Equations

Dimensional analysis provides (Breusers, 1967)

$$\frac{d_{se}}{D} = f\left[\frac{U_* d}{\upsilon}, \frac{{U_*}^2}{\sqrt{\Psi g d}}, \frac{y_0}{D}, \frac{d}{D}, \frac{\rho_s - \rho}{\rho}\right] \quad (4)$$

Where U_* is the friction velocity and Ψ is a constant

Truc and Khai (1982) used the diameter of the primary forced vortex, $d_f = 0.25\, D^{0.8} y_0^{0.2}$ and available experimental and field data to develop a new practical design relation.

$$d_{se} = K y_0^{0.2} D^{0.8} \left(\frac{U}{V_c}\right)^n k_d k_\alpha k_{sh} \quad (5)$$

Where U is the mean velocity of flow directly upstream of pier(m/s), V_c is the tangential velocity at the edge of the vortex, k_d is the relative sediment factor = $1+\frac{1}{2.7}(D/y_0)^{1/6}$, V_c = $\sqrt[3]{gh\omega_d}(y_0/D)^{0.06}$ (m/s), ω_d is the circular characteristic velocity with sediment, K = 0.93, n = 1.5 for V≥ V_c, and K = 1.21, n = 0.57 for V< V_c, and k and k_{sh} = correction factors for angle of attack and pier shape respectively

Hafez (2004) developed an equation using energy balance theory. The energy balance theory assumes that at the equilibrium geometry of the scour hole, the work done by the attacking fluid flow upstream the bridge pier is equal to the work done in removing the volume of the scoured bed material. The work done by the fluid flow of the horizontal jet

coming from upstream of the bridge pier in the stagnation symmetry plane was expressed as:

$$W = \frac{\rho V_x^2 y_o d\eta^2}{(1-D/B)^2}(y_0/2 + d_{se}/2) \quad (6)$$

Where V_x is the longitudinal flow velocity of the jet attacking the bridge in the direction normal to the pier, d is the bed material sediment diameter, η is the transfer coefficient of the horizontal momentum into a vertical momentum in the downward direction, and B is the channel width

The work done in removing the bed material from the scour hole is equal to:

$$W = \frac{1}{2}\left(\frac{d_{se}}{tan\varphi}\, d\right)\frac{d_{se}}{3}(1-\Theta)(\gamma_s - \gamma) \quad (7)$$

Where φ is the slope of the scour hole in symmetry plane, Θ is bed material porosity, γ_s is bed material unit weight, and γ is fluid unit weight

This equation yielded much superior agreement with field data than any other existing empirical equation when applied to the average and maximum of 515 field data. It showed better results than many other equations when applied to Imbaba and El-Tahreer bridges near Cairo, Egypt.

In the late twentieth century the Washington State Department of Transportation (WDOT) utilized the Laursen and Toch (1956) equation to estimate scour depth:

$$d_{se}/D = 1.5\,(y_0/D) \quad (8)$$

Ettema et al., (2001) developed an equation for the scour depth as:

$$\left(\frac{d_{se}}{D}\right) = \left(\frac{y_o}{D}\right)^{0.62}\left(\frac{U}{(gy_o)^{0.5}}\right)^{0.2}\left(\frac{D}{d_{50}}\right)^{0.08} \quad (9)$$

Where d_{50} is the diameter of sand bed, 50% of which is finer by weight.

The Federal Highway Administration's Hydraulic Engineering Circular No.18 (HEC-18) U.S. Department of Transport (1993) recommends the use of the local scour formula of Colorado State University (CSU):

$$\frac{d_{se}}{y_o} = 2.0\ K_1K_2\left(\frac{D}{y_o y}\right)^{0.65} Fr_1^{\ 0.43} \qquad (10)$$

Where K_1 is correction factor for pier nose shape, K_2 = correction factor for angle of attack, Fr_1= Froude number at upstream of the pier and y is the vertical or wall normal distance.

Melvile and Sutherland (1988) developed a scour formula based on extensive laboratory experimentations. The formula is:

$$d_{se} = K_lK_dK_yK_aK_sD \qquad (11)$$

Where K_l is the flow intensity factor, K_d is the sediment size factor, K_y is the flow depth factor, K_a is the pier-alignment factor and K_s is the pier-shape factor.

2.6 Past Experimental Studies

Hodi (2009) studied the effect of blockage and densimetric Froude number on bridge pier local scour by doing experimental studies. Experiments were conducted in two flumes of different widths utilizing piers of various diameters. Significant blockage effect (greater difference in scour geometry) was observed increasing the blockage ratio from 2.2% to 5%. Further he noted that small changes in the absolute value of densimetric Froude number can have a large influence on maximum scour depth and scour geometry.

Mohamed et al., (2006) carried out laboratory experiments and field data studies to obtain pier scour information. They compared the measured scour depths obtained from the laboratory experiments with computed scour depths using selected formulae. It appears that Laursen and Toch (1956) and the CSU formulae give reasonable prediction, while

Melvile and Sutherland (1988) formulae appear to over-predict the depth of scour for both the laboratory model and field prototype. The over prediction in the case of field results is even greater compared with that of the laboratory model.

Ettema et al., (2006) experimentally established a direct trend (values of normalized scour depth increased when cylinder diameter decreased) between equilibrium scour depth and the intensity and frequency of large-scale turbulence shed from each vertical cylinder in a sand bed. Carollo et al., (2008) described the results of the turbulence intensity in gravel bed channels by using an acoustic Doppler velocimeter (ADV) in a laboratory flume. The collected data allowed the velocity fluctuations to be measured and the large-scale turbulent structure to be analyzed. On the basis of their measurements, the writers observed an ordered sequence of long-term large-scale vortices moving downstream with the same velocity as the mean, and producing a motion of fluid toward both the bed and the free surface, involving the whole flow depth. Moving from the bed towards the free surface, even if the size of the large scale vortices increases, the turbulence phenomenon intensity decreases. The longitudinal turbulence intensity decreased progressively as the distance from the bed increases, with the exception of the thin layer close to the wall (depth scaled by friction velocity = $yU^*/\nu = y^+ \leq$ 10-20) , where the viscous effects exceed the turbulent fluctuations (Nezu and Nakagawa 1993).

Ettema et al., (2001) presented the data suggesting that the scour depth at piers did not scale linearly with pier width unless there was more-or-less complete geometric similitude of pier, flow and bed sediment particles. The non-linearity can result in laboratory flume studies of local scour (at scale-reduced model piers) leading to deeper scour holes relative to pier width than any likely to occur in the field. The energy

associated with turbulence structures in the pier flow field can be characterized in terms of a pier Euler number, Eu = $\frac{U^2}{gD}$, and the frequency of vortex formation and break-up or shedding in terms of pier Reynolds number, which influences the frequency of shedding. They noted that smaller cylinders in the same flow generate eddies at a greater rate.

Clark (1968) found that the distribution of turbulence intensity does not depend on either the Reynolds number or the Froude number and can be described by a single curve. In the three- dimensional case, because of the influence of the walls, the maximum value of flow velocity appears at a distance from the bed, δ smaller than the water depth, y_0.

Liu and Chiew (2012) conducted laboratory experiments with different suction to show suction effects on sediment entrainment quantitatively. When the hydrodynamic forces exerted on the sediment particles just exceed the resistive forces, particles begin to move. This phenomenon is defined as the "incipient motion" or "threshold condition". Only visual observation is not sufficient to determine the precise threshold condition for a specific case. Therefore, various investigators have conducted different methods to identify the incipient motion. By using $q_b = 0.0432 \times 10^{-6}$ m^2/s as the bed load transport rate at the threshold condition, Liu and Chiew (2012) showed that the suction velocities (V_s) help to initiate sand particle movement. The combined results provide an overall view on suction effects on the initiation of cohesionless sediment motion, showing that the downward seepage (suction) increases the critical shear velocity.

Chen and Chiew (2004) conducted experiments using a laser Doppler velocimeter by Dantec, with and without suction, and suction rates were 1.53% and 0.86%. The measured data confirmed a significant increase in the near bed velocity and the reduction of velocity near the water surface resulted in the formation of a more uniform velocity

distribution with comparison to no suction condition. Schematic diagram of velocity profile is shown in the following figure.

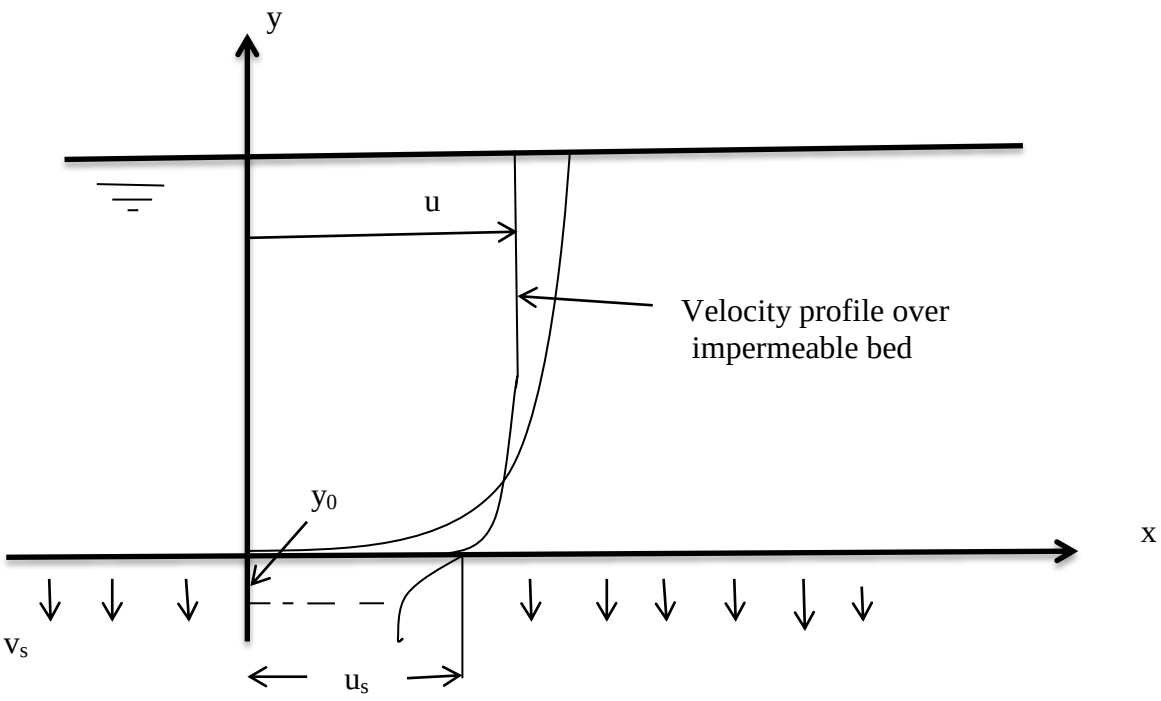

Fig. 2.3. Schematic diagram of velocity profile over permeable bed with suction

Where, u is the time-average streamwise velocity at a distance y from the boundary, y_0 is vertical displacement of the origin of the mean velocity profile, u_s is slip velocity at the bed surface and v_s is suction velocity

2.7 Issues with Experimental Studies

Depending on the water level and scour around the foundation, the flow field in the vicinity of the pier may vary significantly. The inherent difficulty of scaling y_0, D, and d_{50} makes hydraulic modeling intrinsically approximate. After reviewing some past experimental studies on bridge piers local scour, some similarity in the formulae for predicting potential maximum scour depth can be observed. Although the forms of these

equations are similar, their results differ widely from each other when applied to a specific case. As there is no single, universally accepted equation was reported to date because of the complexity of local scour. The choice of a scour prediction equation is also subject to an unknown level of uncertainty. Experimental studies have been conducted by considering only certain aspects of the problem and accepting the other parameters as constants. Experimental relationships may be inadequate because of the large number of parameters that affect scour. Potential maximum local scour depth from experimental studies in the laboratory may vary significantly in real field because of the following reasons:

i) Formulae are based on limited data
ii) Simplified conditions in the lab
iii) Generally laboratory flumes are rectangular in cross section and these have smooth and fixed walls
iv) In real field situations, channels are non-rectangular in cross section with mobile banks and over bank flow occurs frequently and lateral flow distribution is non-uniform
v) Generally predictive scour equations from laboratory flume tend to estimate excessive pier scour than real field
vi) Complexities of flow field
vii) Variation in channel boundary materials

Most of the investigators established scour equations based on the experiments carried out in fixed wall laboratory flumes, which do not represent the real situation in the field. To minimize the error the experiments are carried out in a ‘regime’ flume where the

experimental conditions are close to the field situation. The results from the experimental approach should be compatible with the present-day theories of fluid mechanics and sediment transportation. The factors affecting the scour phenomenon can be controlled in the laboratory to an extent that is not possible in the field.

Melville and Chiew (1999) stated that due to poor correlation between scour-depths observed in the field and these measured in the laboratory, and in order to achieve equilibrium conditions in small-scale laboratory experiments of clear-water scour depth development at bridge foundation, it was necessary to run the experiments for several days. Data obtained after lesser time, say 10 to 12 h, can exhibit scour-depth less than 50% of the equilibrium depth. The time for equilibrium depth of scour to develop and the equilibrium depth of local scour at a circular pier are inherently interdependent. In the literature there are limited information concerning the required time to reach the equilibrium state under clear water conditions.

CHAPTER 3

EXPERIMENTAL SETUP AND PROCEDURE

3.1 Experimental Setup

Experiments were conducted in a horizontal flume of 9.0 m long, 1.10 m wide, and 0.920 m deep at the University of Windsor. The bottom of the flume was made of aluminum and the flume sides were made of Plexiglas supported by a metal frame. A schematic of the side view of the experimental setup including sand bed, pier model and flume is shown in Fig.3.1.

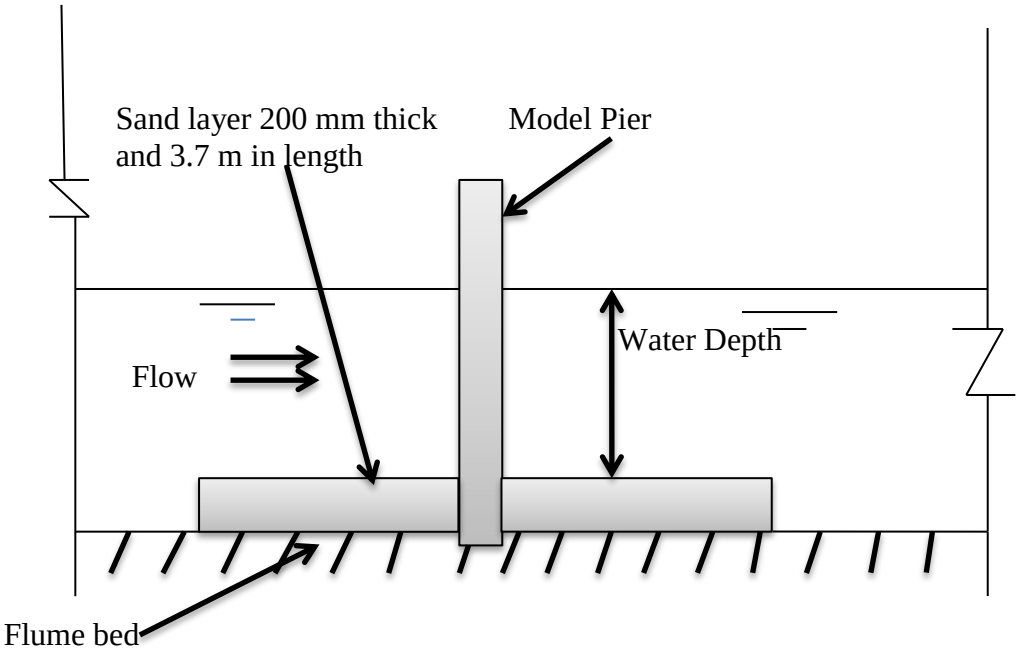

Fig. 3.1. Schematic profile for the flume and pier model

Twelve experimental runs were conducted in this proposed study. The experiments utilized three different circular test cylinders with diameters of 51, 38 and 30 mm and a range of water depths (50-100 mm). To minimize the effect of secondary currents and to

make the flow two-dimensional the value of aspect ratio, B/y_o (channel width/flow depth) was maintained greater than 11, and velocity measurements were conducted along the centerline of the flume (Nezu, 2005). Blockage ratio, D/B (model pier diameter/channel width) was restricted to less than 5% (i.e. 2%- 4%) to reduce the blockage effect. Uniform flow is achieved in the flume by using a variable speed pump, distribution manifold and flow straighteners. The sand bed is 3.7 m long, 0.20 m deep and spans the entire width of flume. The sieve analysis of the sand is shown in Fig. 3.2.

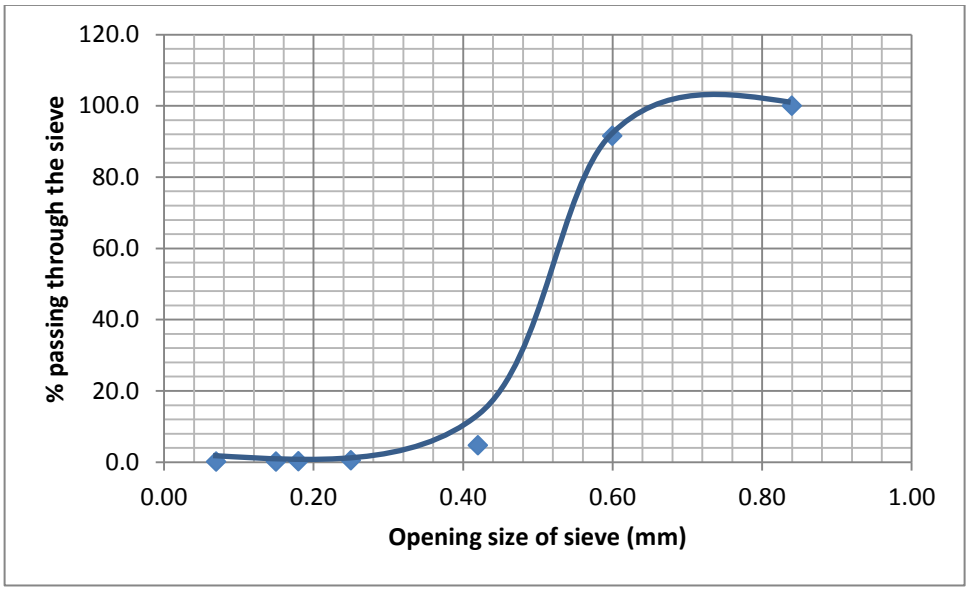

Fig. 3.2. Sieve analysis of sand

The mean particle size of sediment, d_{50} = 0.51 mm, was taken as the representative particle size of the sediment. The sand size was selected to maintain D/d_{50} greater than 50 to overcome the influence of sediment size on local scour depth (Ettema, 1980). The geometric standard deviation, σ_g, the uniformity coefficient, C_u, and coefficient of gradation, C_c were calculated using following equations (Terzaghi et al., 1996).

$$\sigma_g = \left(\frac{d_{84}}{d_{16}}\right)^{0.5} \quad (12)$$

$$C_u = \frac{d_{60}}{d_{10}} \quad (13)$$

$$C_c = \frac{(d_{30})^2}{d_{60} d_{10}} \quad (14)$$

From the sieve analysis, σ_g, C_u and C_c have been found to be 1.14, 1.36, and 1.11, respectively. A bed material is considered uniform when σ_g less than 1.5. Sand with C_u less than 4 is considered uniform soil and C_c = 1 regarded as well graded soil (Das, 2005). The physical characteristics of the sand are given below.

i) Specific gravity : 2.65

ii) Porosity : 39%

iii) Acid solubility : 1%

iv) Hardness (MOH) : 7

v) Grain shape : Round to sub-angular

Seepage effects on local scour were studied only for suction. The suction zone was 2.4 m long, 1.10 m wide and 0.125 m deep, and consisted of natural sand bed, seepage console, fifteen parallel perforated pipes, perforated plates, filter net, two separate pumps, two flow meters with valves, and common feeder pipe with valve. The longitudinal and plan view of a model pier in the suction zone are shown in Fig. 3.3 and Fig. 3.4.

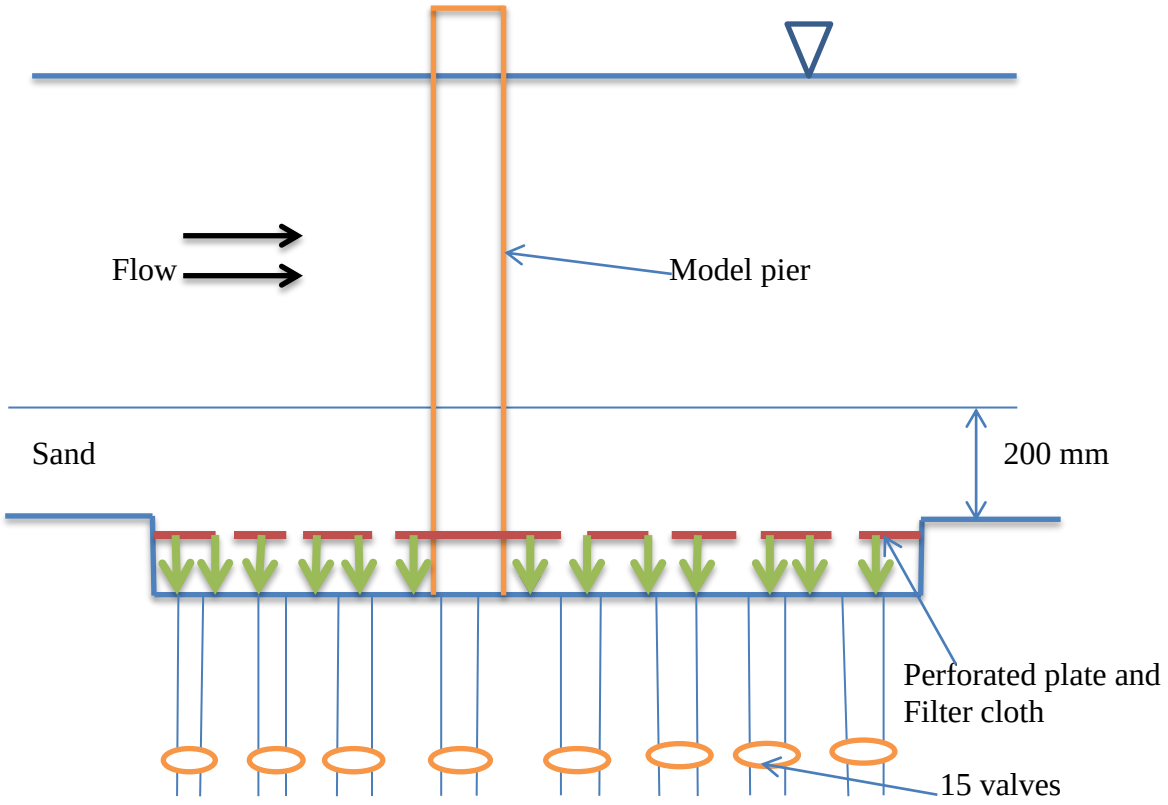

Fig.3.3. Longitudinal view of model pier in suction zone

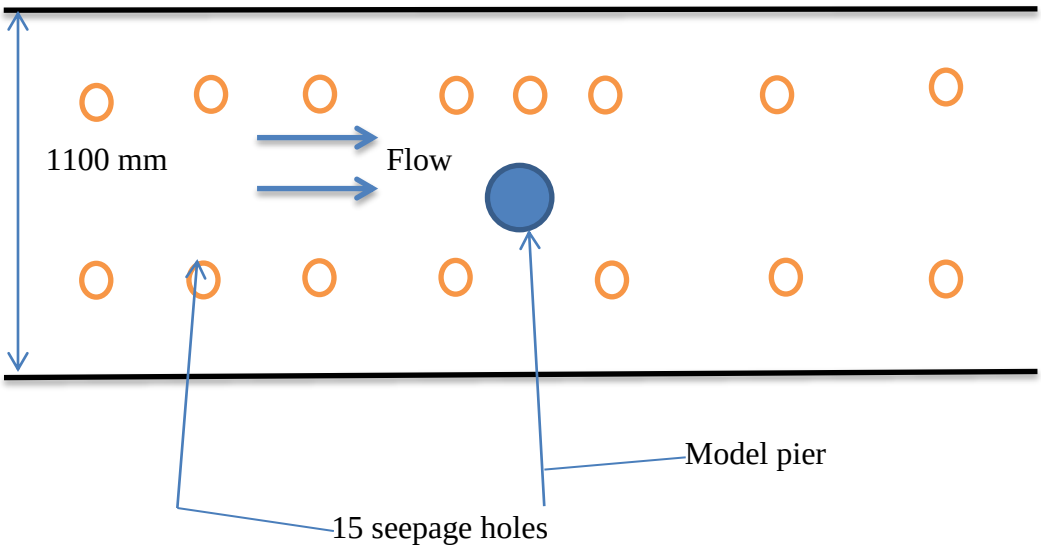

Fig.3.4. Plan view of model pier in suction zone

Uniform seepage velocity was maintained over the entire sand bed by using a seepage console and controlling valves on each drainage pipe. One pump at the upstream and another pump at the downstream location were installed to remove water from the flume bed to maintain the flow rate for suction, which was monitored using flow meters. The model pier is located 7.2 m from the upstream end of the flume. Perforated pipes are used to withdraw water from the sand bed by creating suction. Filter net is used to prevent the sediment particles from falling down.

3.2 Test Procedure and Details of acoustic Doppler velocimeter

Before starting the test, the model pier and sand bed were carefully examined. The model pier was placed centrally and vertically in the working section so that movement does not occur during the test. The sand bed was levelled. To protect sediment movement and to remove trapped air bubbles among sediment grains, the flume was slowly filled with water and the pump was started only after one hour. For each experimental run, the flume was allowed to drain slowly after completing the test and detailed photographs of the scour hole and deposit were taken with a digital camera. Scour hole and sediment deposit measurements were accomplished using a manual traverse (point gauge). Scour hole formation is frustum shaped around the pier's upstream perimeter due to downflow at the pier face creating a groove. As the groove deepens, it triggers the formation of the scour hole. A deposition dune or mound forms downstream of the pier due to deceleration of the sediment particles entrained from the region of high bed shear stress and pressure fluctuations. All tests were run for a period of 48 hours, and experiments 2 and 11 which were run for different durations (1, 4, 8, 24 and 48 hours) to understand the temporal effect of local scour.

Using acoustic Doppler velocimeter (ADV), the approach flow velocity profiles for each experiment were measured at the centreline of the flume and the ADV instrument was set at 1.25 m from pier centre in the upstream direction. For each profile, velocities were recorded at various depths (from approximately 7 mm near the bed level up to the water surface). ADV operates by the principle of Doppler shift. This shift in frequency can be calculated using the following equation.

$$F_{doppler} = - F_{source} V/C \qquad (15)$$

where, $F_{doppler}$ is the change in received frequency (doppler shift), F_{source} is the frequency of transmitted sound, V is the velocity of source relative to receiver and C is the speed of sound.

The ADV uses this principle to measure the velocity of water in three dimensions. The device sends out a beam of acoustic waves at fixed frequency from a transmitter probe. The receiver arm of ADV receives Doppler shift measurements from a small volume in space referred to the sample volume. The ADV then calculates the velocity components of the water in the x, y, and z direction. Vectrino Velocimeter (Nortek AS 2004) measured 3D flow in a cylindrical sampling volume of 7 mm diameter, located about 50 mm from the sidelooking probe. The error in velocity measurements depend on variability in the equipment, the processes, the environment, and other sources.

Vectrino software was installed on a computer before its use in the experimental runs. After installing the software, a functional check has been done by selecting serial port and communication and accepting the default baud rate (9600). Probe check was accomplished for inspecting the region where ADV makes its measurement by showing how the signal varies with time. For performing functional test of this Vectrino, particles

have been added for checking the transducer functional capability. While transducers are in the air, the velocity measurement will look like random noise. After immersing the transducers in the water the graphical view of the velocity has been changed to smooth signal. This phenomenon has been explained in Fig. 3.5. One of the most important parameters in the measurement is Signal-to-Noise Ratio (SNR) which is defined by the following formula.

$$SNR = 20log_{10}(\frac{Amplitude_{signal}}{Amplitude_{noise}}) \qquad (16)$$

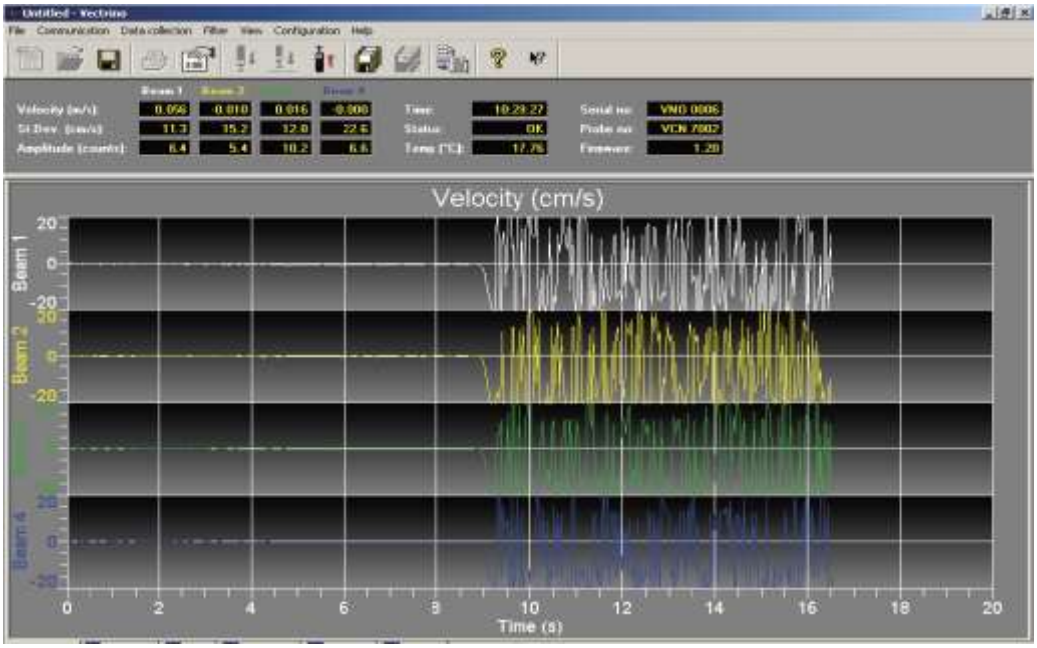

Fig. 3.5. Velocity in water (left part) and in air (right part)

Uncertainty analysis of VectrinoVelocimeter was done using the specifications given by the manufacturer. To perform the uncertainty analysis the bias limit i.e., the design stage uncertainty, the product of student‘t’ value at the assigned probability P%, and precision index i.e., the estimate of precision error at 95% confidence were calculated. This confidence interval is a quantified measure of the random error in the estimate of the true

value of the velocity. Gratiot et al., (2000) stated that the ADV uses acoustic techniques to measure the velocity in a remotely sensed volume so that the measured flow is undisturbed by the presence of the probe. The primary use of the ADV in the present research study was to measure the vertical velocity profile along the water depth around piers, and initial velocity measurement is possible 7 mm from the flume bed. Laser Doppler Velocimeter was used to measure the velocity very near flume bed which is not possible with the use of ADV. Experiments on scour were performed near threshold condition i.e. $\frac{U}{U_c}$ = 0.8 (U is the approach velocity and U_c is the critical velocity for the sediment movement).

3.3 Experimental Program

The experiments were conducted by using a visualization technique and measuring the flow velocity by an acoustic Doppler velocimeter (ADV). In these experimental studies only clear-water conditions with a flat sand bed were considered. No sediment inflow was allowed into the scour hole from upstream. Several tests were performed to visualize the influence of flow shallowness or relative approach flow depth (y_0/D) on local scour depth and to understand the effect of time on the development of depth of scour at circular piers considering no suction. After introducing suction, changes in local scour were examined experimentally. The flow shallowness ratio (y_0/D) ranged from 0.98 to 3.33. A total of twelve experimental runs comprising piers with diameter of 51, 38 and 30 mm, approach flow depth 0.05 m - 0.1 m and bed material size, d_{50} as 0.51 mm were carried out. Table 3.1 and 3.2 summarize the test conditions, and Table 3.3 shows summary data on experimental runs.

Table 3.1: Experimental program: effect of flow shallowness

Experiment No	Pier Diameter, D (mm)	Approach flow depth, y_0 (mm)	$\frac{y_0}{D}$	D/d_{50}	Test condition
1	51	50	0.98	100	No suction
2	30	50	1.67	59	No suction
3	30	75	2.50	59	No suction
4	30	100	3.33	59	No suction
5	38	100	2.63	75	No suction
6	38	75	1.97	75	No suction
7	38	75	1.97	75	2% suction
8	30	50	1.67	59	5% suction
9	38	75	1.97	75	7% suction
10	30	50	1.67	59	6% suction
11	30	50	1.67	59	7% suction
12	30	50	1.67	59	10% suction

Table 3.2: Experimental program: temporal effect on the local scour depth

Exp No.	y_o	D	Test condition	Test duration(hrs)
2	50	30	no suction	1
2	50	30	no suction	4
2	50	30	no suction	8
2	50	30	no suction	24
2	50	30	no suction	48
11	50	30	7% suction	1
11	50	30	7% suction	4
11	50	30	7% suction	8
11	50	30	7% suction	24
11	50	30	7% suction	48

Table 3.3: Summary data of Experimental runs

Experiment No.	y_0 (mm)	D (mm)	Q (L/s)	U* (m/s)	D/d_{50}	y_0/D	B/y_0
1	50	51	9.03	0.028	100	0.98	22
2	50	30	9.03	0.028	59	1.67	22
3	75	30	17.81	0.012	59	2.50	15
4	100	30	21.93	0.015	59	3.33	11
5	100	38	21.93	0.015	75	2.63	11
6	75	38	17.81	0.021	75	1.97	15
7	75	38	18.70	0.031	75	1.97	15
8	50	30	9.84	0.023	59	1.67	22
9	75	38	19.94	0.019	75	1.97	15
10	50	30	9.93	0.016	59	1.67	22
11	50	30	10.11	0.012	59	1.67	22
12	50	30	10.38	0.011	59	1.67	22

CHAPTER 4

RESULTS AND ANALYSIS

4.1 Introduction

The primary objectives of this research study were to review the effect of flow shallowness and temporal effect on local scour depth with and without suction by conducting a physical hydraulic model study in the hydraulics lab of the University of Windsor. In this chapter the results obtained from the experiments are presented. First six experiments were conducted without suction conditions, and the remaining six experiments were conducted with different suction rates conditions (2% to 10%). To show the temporal behaviour of local scour features and profiles without suction and with suction, two experiments were conducted with different time durations (1, 4, 8, and 24 hours). Experiments were conducted for three water depths (50, 75, and 100 mm), and three model piers (51, 38, and 30 mm) in turbulent flow and clear-water scouring conditions. The detailed measurement of scour hole and deposit profiles were accomplished by using manual traverse. The following Fig. 4.1 shows the schematic diagram of measurement system.

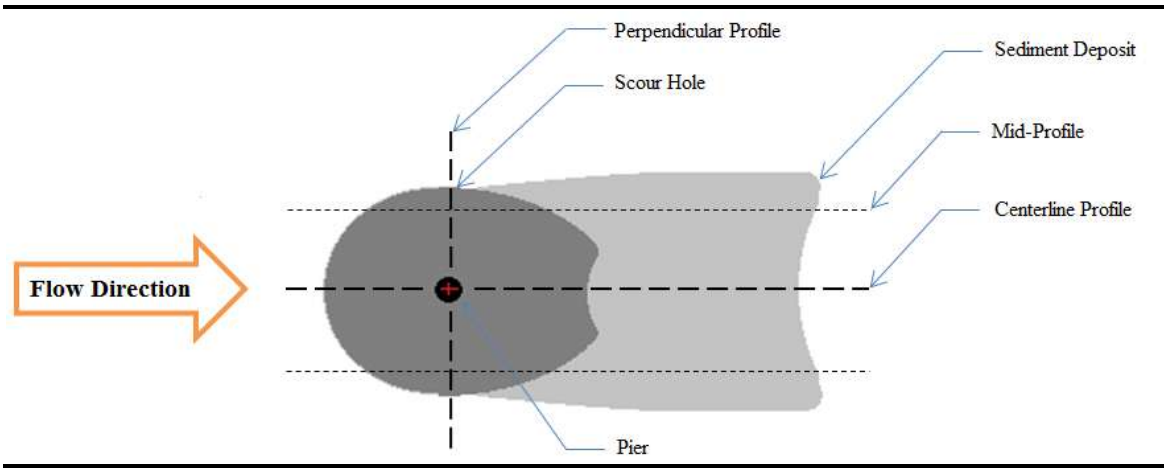

Fig. 4.1. Schematic diagram of measurement system for scour features and profiles

The issue of initiation of sediment motion was also experimentally studied. For each test, it was observed that small ripples formed on the sand bed of the flume, centerline starting from the upstream end and progressing downstream toward the pier study area. A photograph showing the ripples is shown in Fig. 4.2.

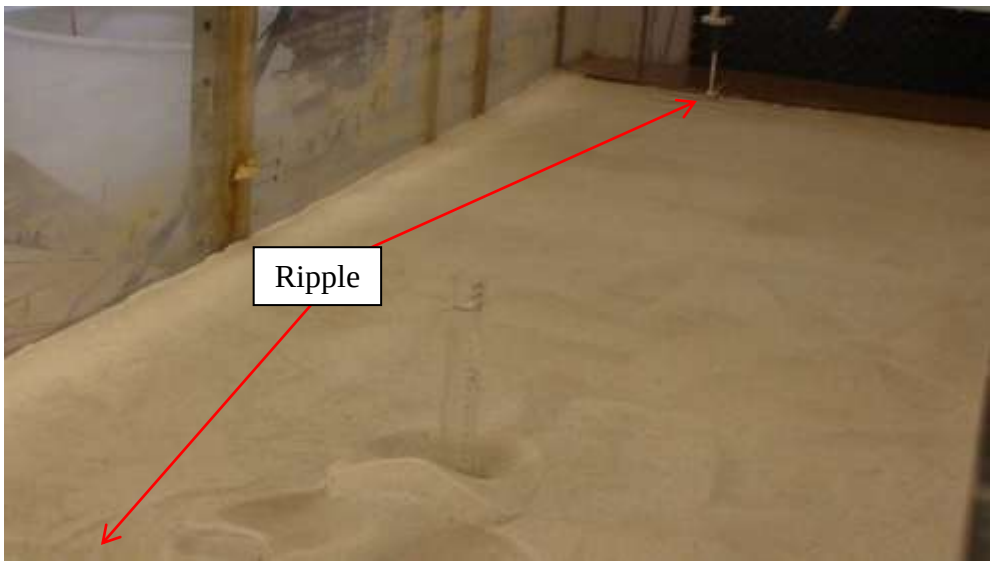

Fig. 4.2. Ripple formation at locations far upstream and downstream of the pier study area

The clear-water scour condition would not be applicable when the ripples reached the pier study area and the particular test was stopped. For ripple-forming sediments, which are classified as sediments having d_{50} less than 0.7 mm, it is seldom possible a plane bed condition (Breusers and Raudkivi, 1991). It might be noted that the sand used in the current study had a median grain size of 0.51 mm.

For different y_0/D, the experimental velocity profiles and the distribution of turbulence intensities with no suction condition are shown. The changes in equilibrium scour depth with Euler number and y_0/D for no suction and with suction were found by conducting twelve experiments. To show temporal effect on local scour, two experiments (one with suction and another with no suction) were conducted for different time durations illustrating dimensional and non dimensional centerline profiles for scour hole and deposit. Mean velocity profiles, dimensional and non dimensional scour hole and deposit profiles were found by conducting six experiments with no suction and another six experiments with different suction rates.

4.2 Effect of flow shallowness

For different y_0/D, vertical velocity profiles, and turbulence intensity along the water depth are analyzed experimentally by measuring velocity at different water depth with an acoustic Doppler velocimeter (ADV). For experiment 1 (y_0 = 50 mm), 3 (y_0 = 75 mm) and 4 (y_0 = 100 mm), the velocity profiles in the outer layers are shown by plotting y/y_o versus U/U_e in the Fig. 4.3. For the shallow water depth (y_o = 50 mm) the higher gradient of velocity and shear stress attained near the bottom compared to deep water depth (y_o = 100 mm). Irrespective of water depth the maximum velocity occurs below the water

surface. For $0.2 < y/y_0 < 0.6$ gradually increasing velocity and for $0.6 < y/y_0 < 0.9$ an upward distribution appear for the velocity profiles. According to Pope (2000), the outer layer corresponds roughly $y^+ > 50$, where $y^+ = yU^*/\nu$ is a sort of local Reynolds number, and a depth scaled by friction velocity. Its value is a measure of the relative importance of viscous and turbulent transport at different distance from the wall. Free stream velocity (U_e) and approach flow depth (y_o) are used to non-dimensionalize the mean velocity (U) and the wall normal distance (y). Faruque (2009) experimentally showed that, in the outer region, each velocity profile shows a slight dip where the maximum velocity (U_{max}) occurs slightly below the free surface, and this velocity dip would be the largest for the sand bed among smooth, continuous roughness, and distributed roughness surface. Roussinova et al. (2006) stated that velocity dip would not be significant when measurements were made in the centre of the channel and the geometric channel aspect ratio (channel width/ flow depth) is greater than five. It might be noted that the channel aspect ratios for the experiment 1, 3, and 4 were 22, 14.67, and 11, respectively.

The velocity profiles for these three experiments in inner layers are shown in Fig. 4.4. According to Pope (2000), the inner layer corresponds roughly to $y/\delta < 0.1$ or the region over which the shear stress is approximately constant, where δ = boundary-layer thickness. In the inner region, the flow depends on the wall shear stress (τ_w), the density (ρ), the viscosity (μ) and the distance from the wall (y). For the region close to the bed, the shear velocity is given by:

$$U^* = \left(\frac{\mu_w}{\rho}\right)^{1/2} \qquad (17)$$

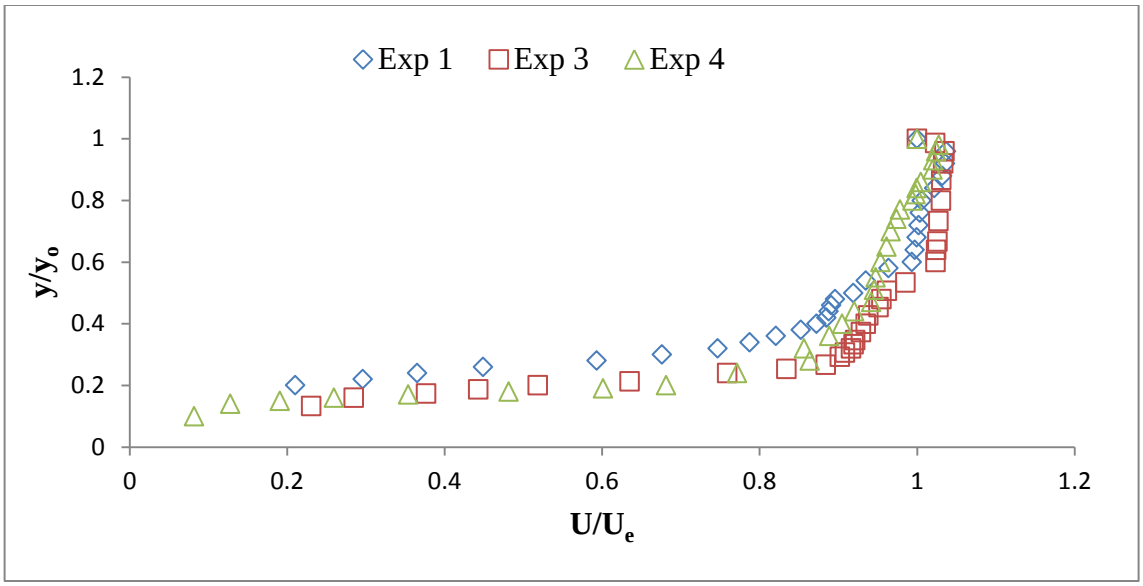

Fig. 4.3. Experimental velocity profiles for experiment 1, 3 and 4 in outer layer

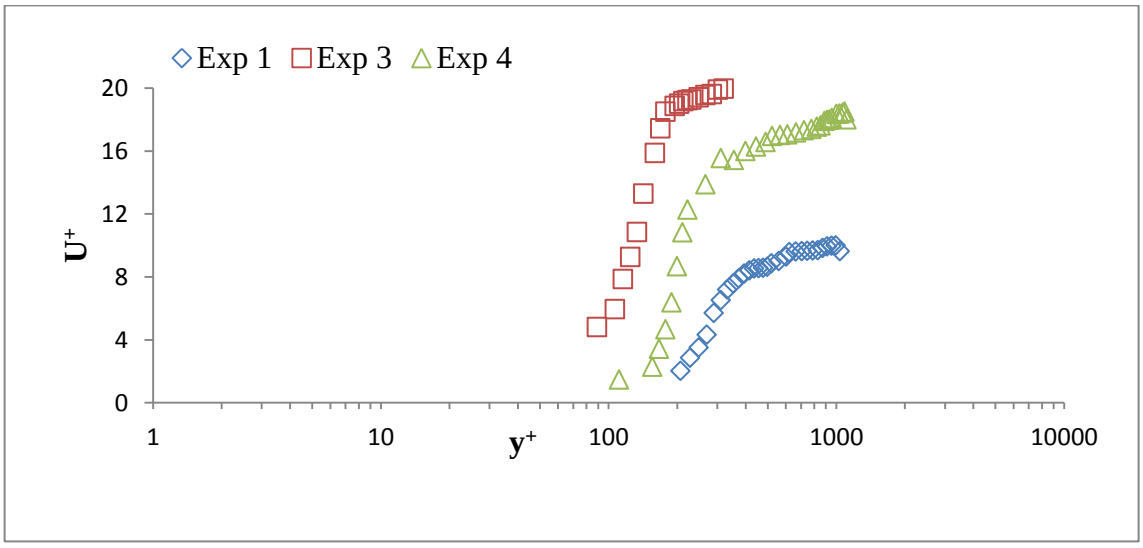

Fig. 4.4. Experimental velocity profiles for experiment 1, 3 and 4 in inner layer

The friction velocity may be calculated for smooth and rough beds using the Clauser method by fitting the mean velocity profiles with the classical log law, $U^+ = \kappa^{-1} \ln y^+ + B - \Delta U^+$. Here, $U^+ = U/U^*$, $y^+ = yU^*/\nu$, $\kappa = 0.41$ and $B = 5$ are log-law constants and ΔU^+ is the roughness function representing the downward shift of the velocity profile (Faruque,

2009). The shear velocity U^* was computed from the velocity profiles measured along the centre-line of the suction zone. The critical shear velocity was calculated by using Shields (1936) entrainment function for the d_{50} of bed material and using some empirical formulae. The relation between critical shear velocity and mean grain size can be expressed as:

$$U_c^* = 0.03\ (d_{50}) \qquad (18)$$

$$U_c^* = 0.0115 + 0.0125(d_{50}) \qquad (19)$$

where, U_c^* is in m/s and d_{50} is in mm

The velocity profiles are fully developed because these profiles do not change with downstream distance. Fully developed flows are encountered in long, straight channels and pipes. The open channel flow is typically turbulent, and the flow is fully developed by the time uniform flow is established.

In the same flow field, irrespective of no suction or with suction condition (from 5% suction to 10% suction) from the same $y_0/D = 1.67$, relative equilibrium scour depths are increasing with the increase in Euler number. This phenomenon can be explained from the following Fig. 4.5, and it shows that minimum Euler number attains for no suction condition and maximum Euler number attains for 10% suction condition. The following Fig. 4.6 shows that for the same $y_0/D = 1.97$, relative equilibrium scour depth is reduced for 2 % suction condition and increased for 7% suction condition in comparison to no suction condition. Ettema et al.'s (1998) data show that scour depth relative to pier width, may increase with pier Euler number.

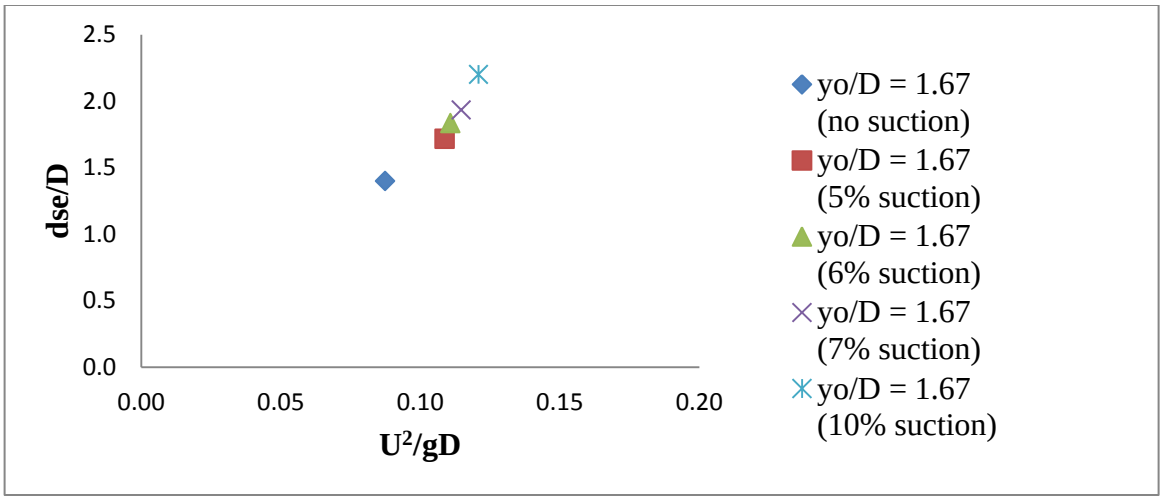

Fig. 4.5. Variation of d_{se}/D with Euler number (U^2/gD) for the same y_0/D = 1.67 with suction and no suction

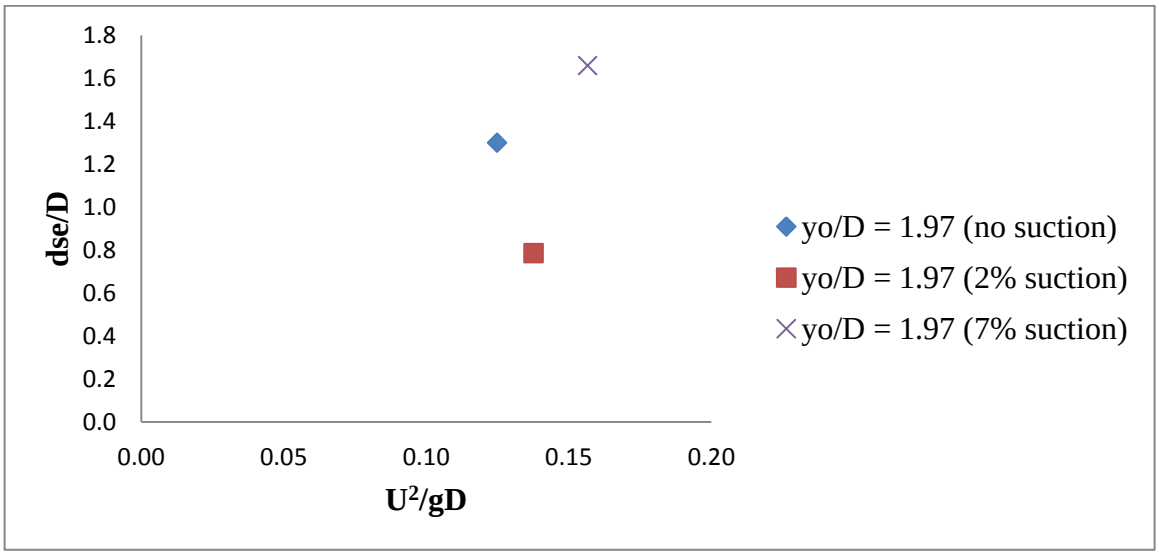

Fig. 4.6. Variation of d_{se}/D with Euler number (U^2/gD) for the same y_0/D = 1.97 with suction and no suction

For the same y_0/D (1.97 and 1.67) the equilibrium scour hole and deposit dimension in y-direction versus equilibrium scour hole and deposit in x- direction for no suction and with 2% through 10% suction have been plotted in the following Fig. 4.7 through 4.10. These figures indicate that 2% suction creates reduced scour hole perimeter and deposit expansion compared to no suction condition, and 7% suction creates more scour hole perimeter comparison to 2% suction condition, and larger deposit expansion compared to no suction condition. Maximum and minimum scour hole perimeter occur for 10% suction and 5% suction conditions, respectively. Scour hole perimeter with no suction condition remains second largest among 5% suction through 10% suction conditions (shown in Fig. 4.9). Maximum and minimum deposit expansion occur for 10% suction and no suction condition, respectively. The deposit expansions are gradually increasing from 5% suction condition to 10% suction condition (shown in Fig.4.10).

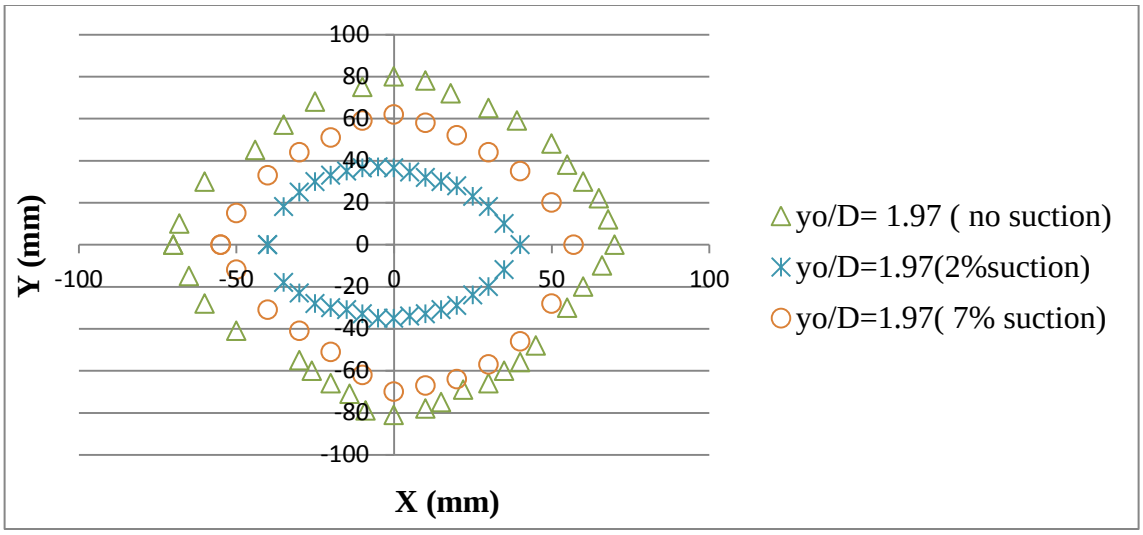

Fig. 4.7. Variation of scour hole with suction and no suction for $y_0/D = 1.97$

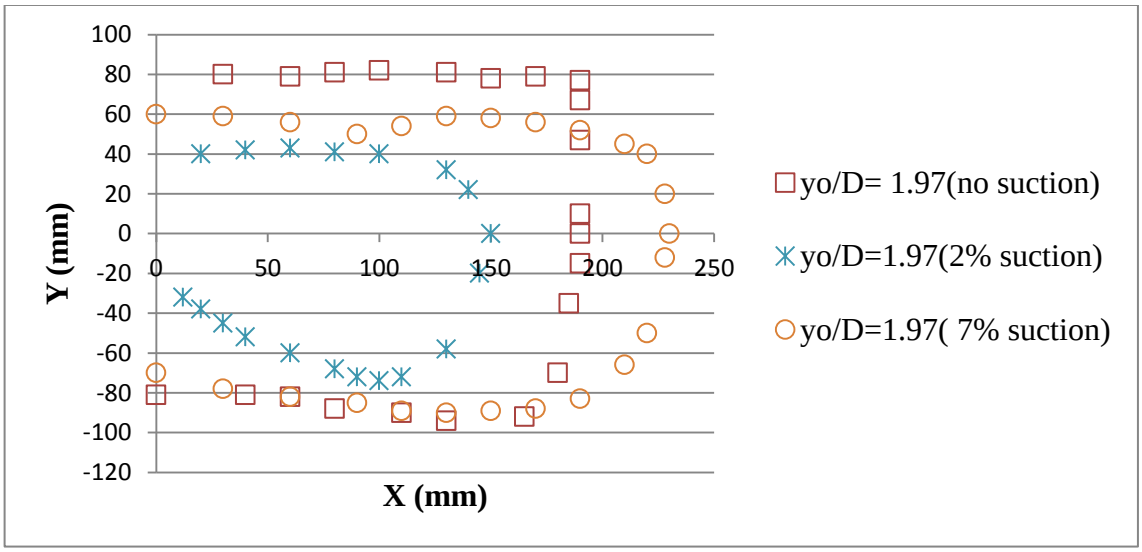

Fig. 4.8. Variation of deposit with suction and no suction for $y_0/D = 1.97$

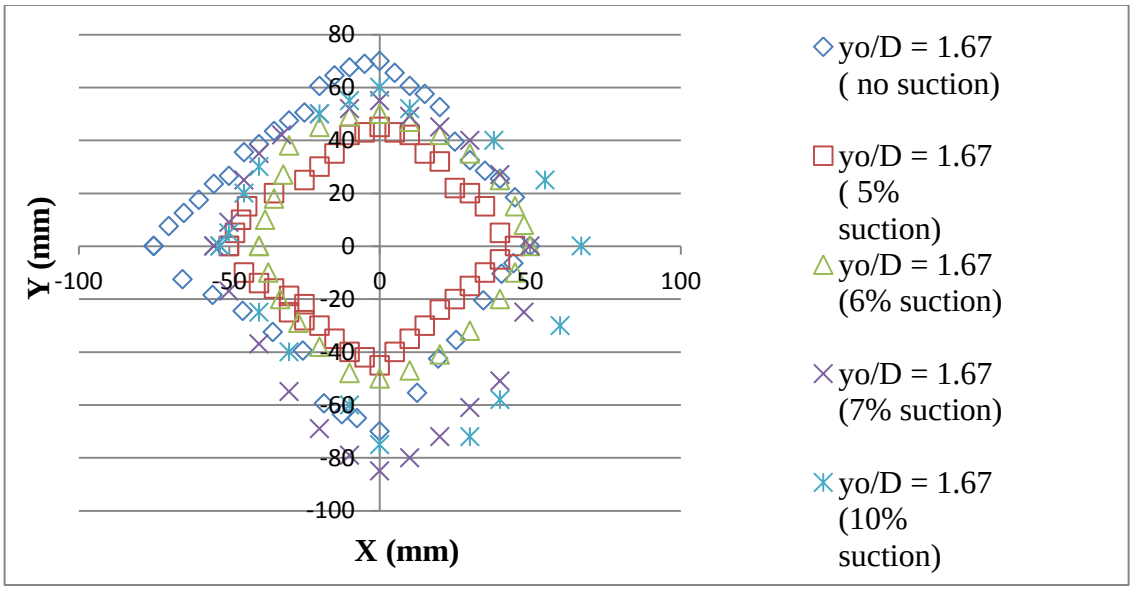

Fig. 4.9. Variation of scour hole with suction and no suction for $y_0/D = 1.67$

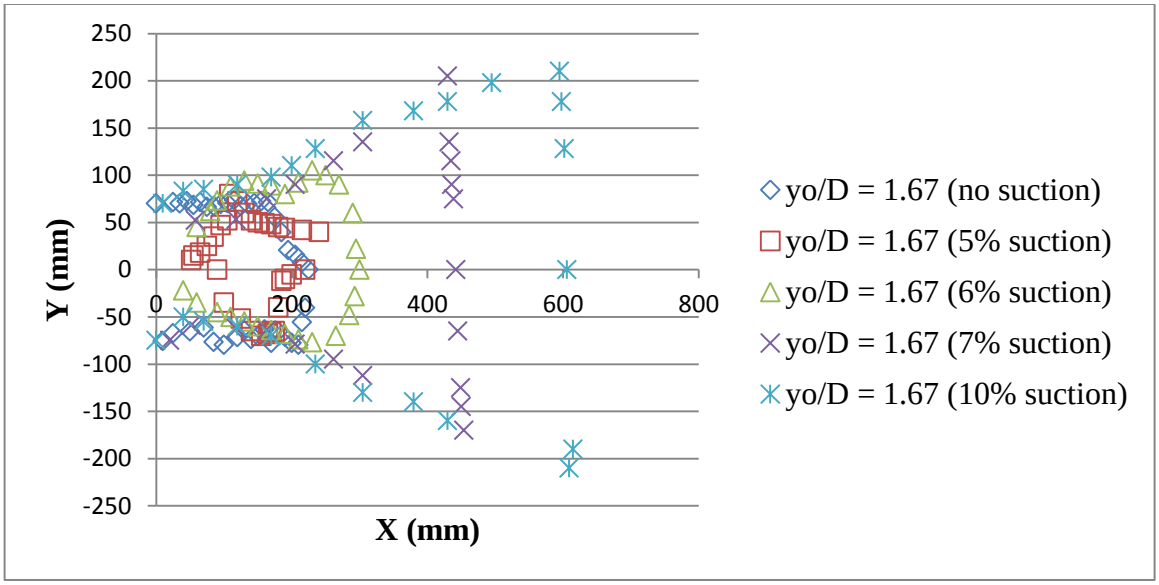

Fig. 4.10. Variation of deposit with suction and no suction for $y_0/D = 1.67$

For experiments with no suction condition, the highest and the lowest scour hole area produce in case of y_0/D = 1.97 and 3.33 respectively, but in case of deposit the opposite scenario happened (shown in the Fig. 4.11 and 4.12). Ettema et al. (2011) stated that widening of the deposition bar behind the pier occurred and scour hole might be deepening further, its slope would remain relatively steep in the case of y_o/D is less than 1.

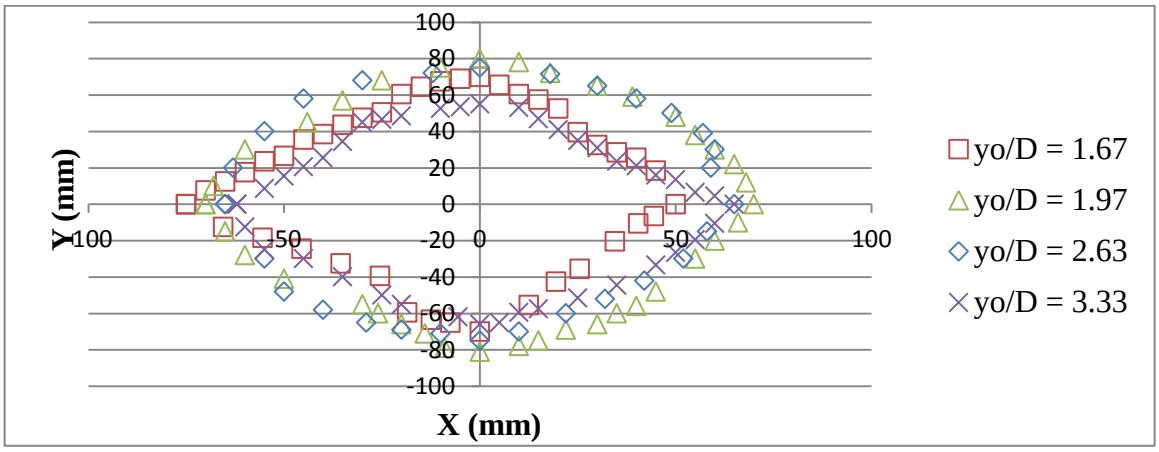

Fig. 4.11. Variation of scour hole for different y_0/D with no suction

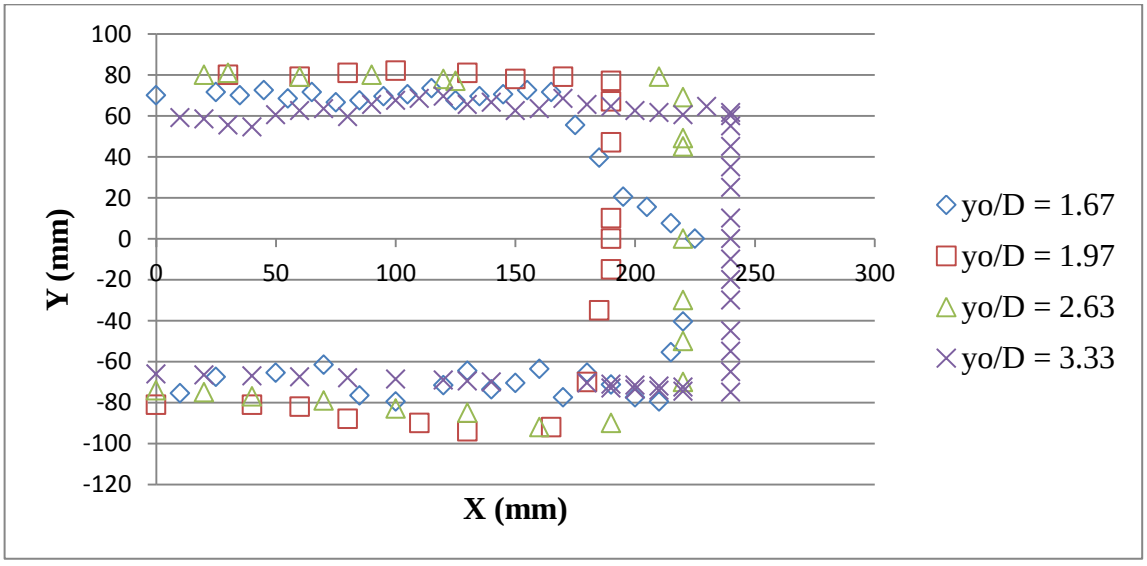

Fig. 4.12. Variation of deposit for different y_0/D with no suction

The equilibrium local scour depth, expressed as d_{se}/D, versus y_0/D for different experiments is shown in the following Fig. 4.13. It is very clear from this figure that irrespective of no suction and with suction condition, the equilibrium scour depth depends on both water depth and pier diameter. It also shows that in case of no suction condition, the maximum equilibrium scour depth attains for y_o/D = 3.33. For the same y_o/D, the equilibrium scour depth becomes the least for 2% suction condition, and the scour depths are found to be gradually increasing from 5% to 10% suction conditions. Generally suction creates larger equilibrium scour depth in comparison to no suction condition. For larger water depth (i.e. deep flow) the scour depth becomes independent of flow depth but depends on the pier diameter. So the equilibrium local scour depth, $d_{se,}$ would be directly proportional to pier diameter when D/y_0 < 0. 7 according to the classification of local scour processes at bridge pier foundations (Melville and Coleman, 2000).

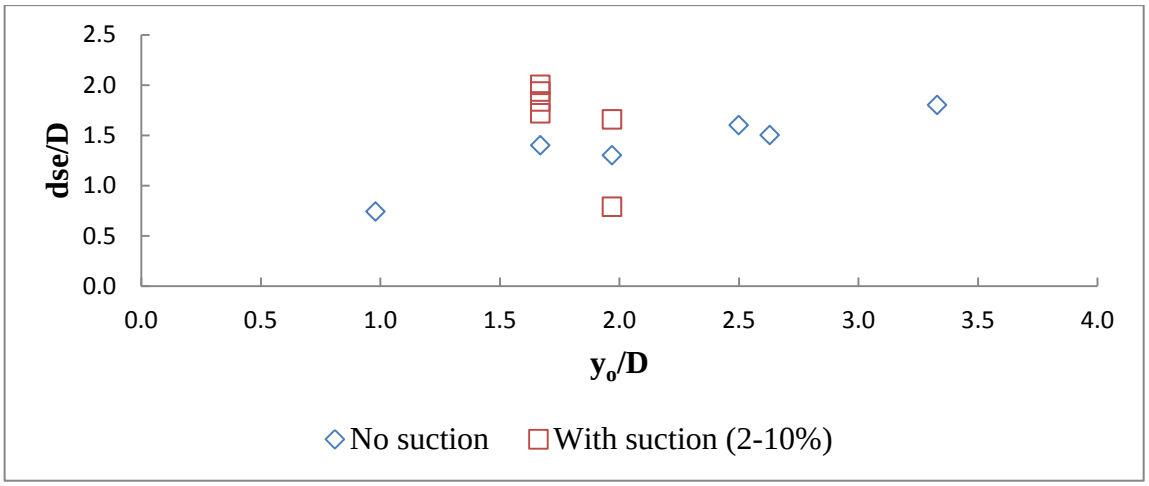

Fig. 4.13. Influence of y_0/D on local scour depth expressed as d_{se}/D

Experiment 1 was conducted with no suction condition, and average flow velocity was measured as 0.1642 m/sec. Scour hole approximate centerline profile diameter was 190 mm. Deposit formation extends 145 mm downstream from the model pier face. The maximum equilibrium scour depth was measured as 37.5 mm.

The experiment 2 was also conducted with no suction, and average flow velocity was measured by using acoustic Doppler velocimeter was 0.1604 m/sec. According to centerline profile for scour hole and deposit, centerline approximate diameter of scour hole was 120 mm, and it expands 75 mm upstream and 45 mm downstream from model pier face. The maximum equilibrium scour depth was measured as 42 mm.

Experiment 3 was conducted by using 30 mm model pier diameter and maintaining water depth of 75 mm with no suction condition. The depth average velocity was measured as 0.2158 m/sec by using acoustic Doppler velocimeter.According to the centerline profile for scour hole and deposit features, the maximum equilibrium scour depth found at 5 mm downstream from pier face measured as 48 mm. Scour depths are gradually decreasing from pier face to downstream and upstream direction. Scour hole expands 58 mm upstream, 57 mm downstream, 60 mm up and 57 mm down from pier face. Deposit profile expand 260 mm downstream from pier face along centerline, and maximum deposit height measured as 20.5 mm located 150 mm downstream from pier face.

Experiment 4 was carried out by using $y_0/D = 3.33$ with no suction. The depth average velocity was measured as 0.1974 m/s by using acoustic Doppler velocimeter, and the maximum equilibrium scour depth measured as 54 mm. According to scour hole and deposite outlines, scour hole expands 62 mm upstream, 65 mm downstream, 55 mm up,

and 62 mm down from pier face, and deposit expands upto 240 mm downstream along centerline from pier face.

Experiment 5 was carried out by using $y_0/D = 2.63$ with no suction. The depth average velocity was measured as 0.1994 m/s by using acoustic Doppler velocimeter, and the maximum equilibrium scour depth measured as 57 mm. According to scour hole and deposite outlines, scour hole expands 65 mm upstream, 65 mm downstream, 75 mm up, and 75 mm down from pier face, and deposit expands upto 220 mm downstream along centerline from pier face.

Experiment 6 was carried out by using $y_0/D = 1.97$ with no suction. The depth average velocity was measured as 0.1619 m/s by using acoustic Doppler velocimeter, and the maximum equilibrium scour depth measured as 49.4 mm. According to scour hole and deposite outlines, scour hole expands 70 mm upstream, 70 mm downstream, 80 mm up, and 70 mm down from pier face, and deposit expands upto 190 mm downstream along centerline from pier face.

Experiment 7 was conducted by using 38 mm model pier diameter and maintaining water depth of 75 mm introducing 2% suction. The depth average velocity was measured as 0.1689 m/sec by using acoustic Doppler velocimeter. According to the centerline profile for scour hole and deposit features, the maximum equilibrium scour depth found at 10 mm downstream from pier face measured as 29.89 mm. Scour depths are gradually decreasing from pier face to downstream and upstream direction. Scour hole expands 40 mm upstream, 40 mm downstream, 36.5 mm up and 35 mm down from pier face. Deposit profile expand 150 mm downstream from pier face along centerline, and maximum deposit height measured as 19.6 mm located 95 mm downstream from pier face.

Experiment 8 was conducted by using 30 mm model pier diameter and maintaining water depth of 50 mm introducing 5% suction. The depth average velocity was measured as 0.1768 m/sec by using acoustic Doppler velocimeter. According to the centerline profile for scour hole and deposit features, the maximum equilibrium scour depth found at 20 mm downstream from pier face measured as 51.5 mm. Scour depths are gradually decreasing from pier face to downstream and upstream direction. Scour hole expands 50 mm upstream, 50 mm downstream, 45 mm up and 45 mm down from pier face. Deposit profile expand 240 mm downstream from pier face along centerline, and maximum deposit height measured as 44.5 mm located 150 mm downstream from pier face.

Experiment 9 was conducted by using 38 mm model pier diameter and maintaining water depth of 75 mm introducing 7% suction. The depth average velocity was measured as 0.2242 m/sec by using acoustic Doppler velocimeter. According to the centerline profile for scour hole and deposit features, the maximum equilibrium scour depth found at 10 mm downstream from pier face measured as 63 mm. Scour depths are gradually decreasing from pier face to downstream and upstream direction. Scour hole expands 55 mm upstream, 57 mm downstream, 62 mm up and 55 mm down from pier face. Deposit profile expand 230 mm downstream from pier face along centerline, and maximum deposit height measured as 39.9 mm located 120 mm downstream from pier face.

Experiment 10 was conducted by using 30 mm model pier diameter and maintaining water depth of 50 mm introducing 6% suction. The depth average velocity was measured as 0.1540 m/sec by using acoustic Doppler velocimeter. According to the centerline

profile for scour hole and deposit features, the maximum equilibrium scour depth found at the face of pier measured as 54.98 mm. Scour depths are gradually decreasing from pier face to downstream and upstream direction. Scour hole expands 40 mm upstream, 50 mm downstream, 50 mm up and 40 mm down from pier face. Deposit profile expand 300 mm downstream from pier face along centerline, and maximum deposit height measured as 51.26 mm located 110 mm downstream from pier face.

Experiment 11 was conducted by using 30 mm model pier diameter and maintaining water depth of 50 mm introducing 7% suction. The depth average velocity was measured as 0.1797 m/sec by using acoustic Doppler velocimeter. According to the centerline profile for scour hole and deposit features, the maximum equilibrium scour depth found at the face of pier measured as 57.22 mm. Scour depths are gradually decreasing from pier face to downstream and upstream direction. Scour hole expands 55 mm upstream, 55 mm downstream, 55 mm up and 85 mm down from pier face. Deposit profile expand 430 mm downstream from pier face along centerline, and maximum deposit height measured as 27.58 mm located 210 mm downstream from pier face.

Experiment 12 was conducted by using 30 mm model pier diameter and maintaining water depth of 50 mm introducing 10% suction. The depth average velocity was measured as 0.1878 m/sec by using acoustic Doppler velocimeter. According to the centerline profile for scour hole and deposit features, the maximum equilibrium scour depth found at the face of pier measured as 59.56 mm. Scour depths are gradually decreasing from pier face to downstream and upstream direction. Scour hole expands 53 mm upstream, 80 mm downstream, 75 mm up and 53 mm down from pier face. Deposit

profile expand 595 mm downstream from pier face along centerline, and maximum deposit height measured as 34.59 mm located 170 mm downstream from pier face.

4.3 Temporal Effect on Local Scour Depth

For experiment 2 with no suction (y_0 = 51 mm and D = 30 mm) and experiment 11 with 7% suction, the tests were done for different time durations (t = 1, 4, 8, 24, and 48 hours). In Fig. 4.14 shows a schematic illustration of the scour hole development pattern with time. In Fig. 4.14a symbol 1 refers to scour starting region or region 1, symbol 2 refers to upstream face of the pier region or region 2, symbol 3 refers to immediately downstream from the pier region or region 3, and symbol 4 refers to further downstream of the pier region or region 4.

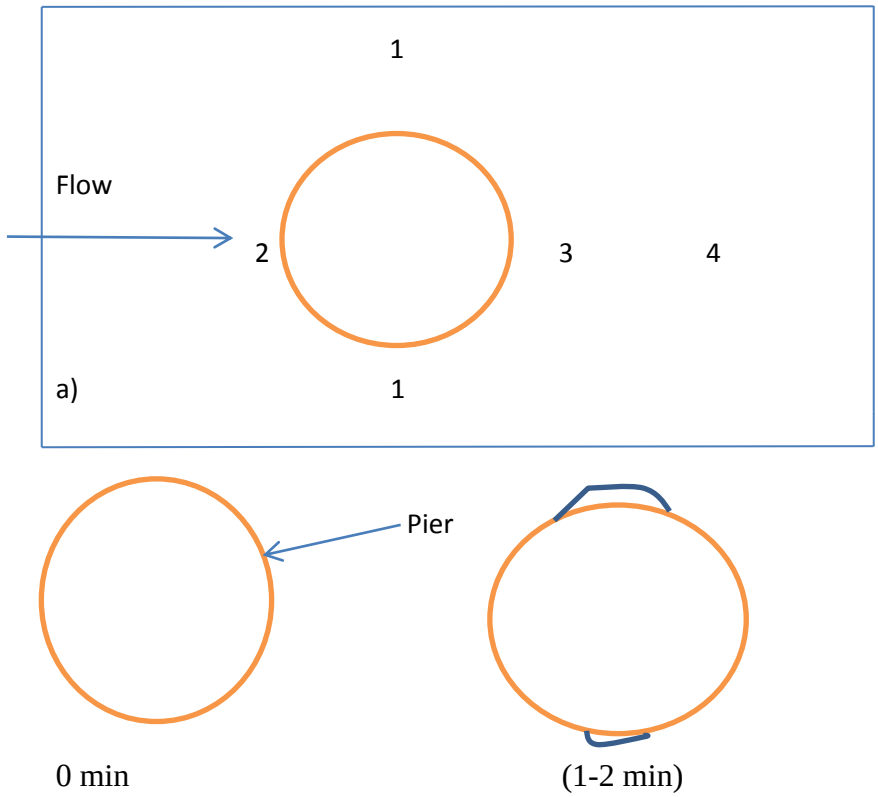

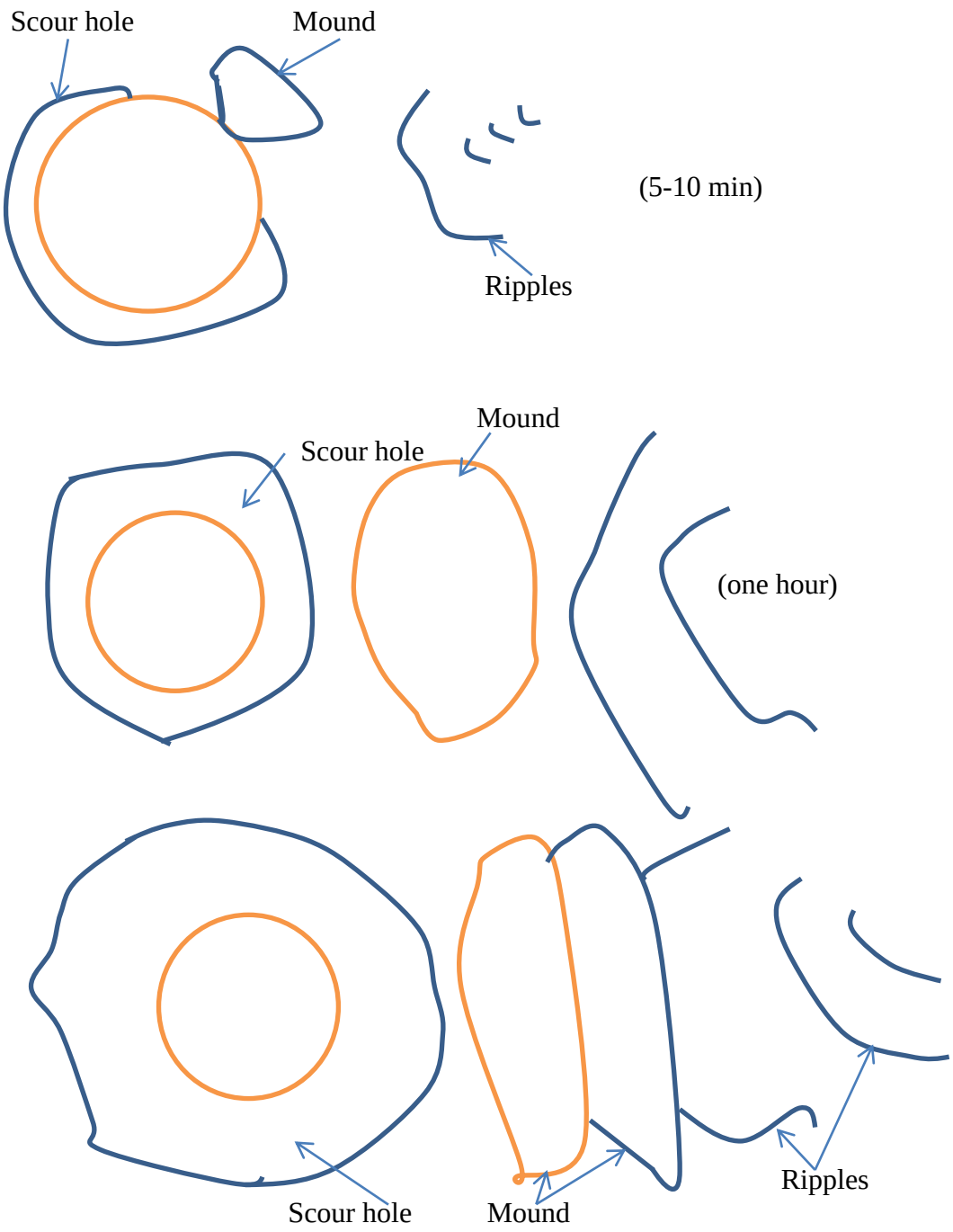

b)

(48 hours)

Fig. 4.14. Schematic illustration of the scour hole development for the plain pier a) scour pattern, and b) sketches of scour hole development with time

To show the temporal evolution of the local scour, time vs. scour (in the point in which the maximum scour is produced) graph has been plotted as shown in Fig. 4.15. It is clearly understood that there are three phases in this process.

i) Active phase

ii) Passive phase

iii) Equilibrium phase

The more interesting phenomenon that occurs during the scour evolution is the continuous collapse of the wall which has occurred in the passive phase. Ettema et al. (2011) stated that small cylinders in laboratory flumes could create asymptotic temporal approach to equilibrium scour depth within a matter of hours. It is difficult to determine the time when the equilibrium scour hole forms in real field conditions, because equilibrium clear-water scour depth is reached asymptotically with time. To solve this problem time to equilibrium is defined as the time at which the scour hole develops to a depth at which the rate of increase of scour does not exceed 5% of the pier diameter in the succeeding 24 hour period. In the present study, the scour rates in the succeeding 24 hours after 48 hours period did not increase more than 1.5%. It is mentioned that for time durations 72, 96, 120, and 144 hours only equilibrium scour depths were measured instead of detailed measurement of scour hole and deposit profiles. Therefore the equilibrium scour depth was considered by conducting experiments for 48 hours duration for all tests. The plot of the temporal development of scour depth for these two experiments clearly shows that the equilibrium scour is not being developed as indicated by the continuous increase of the slope of the plot.

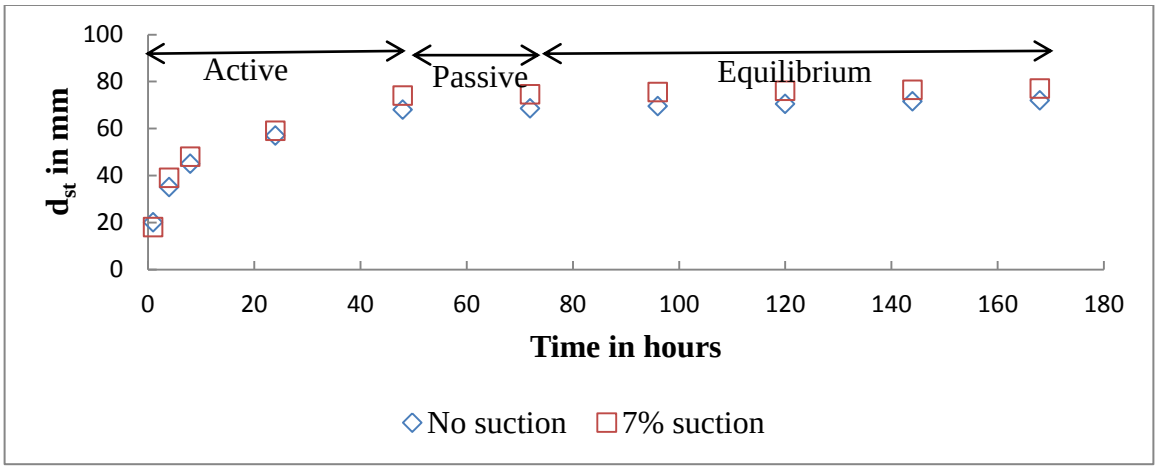

Fig. 4.15. Temporal variation of scour depth for the experiment no. 2 (no suction) and experiment no. 11 (with 7 % suction)

The results show that the scour rate $\frac{dY}{dT}$ was very high in the initial phase and very low near the equilibrium condition which is shown in the Figs. 4.16 and 4.17. It was noted that scour rate for the 7 % suction is larger than no suction condition. The expressions for dimensionless time-dependent scour depth, Y and dimensionless time, T are as follows:

$$Y = \frac{d_{st}}{d_{se}} \qquad (36)$$

$$T = \frac{tU}{D} \qquad (37)$$

where, d_{st} = scour depth at time t, and d_{se}= equilibrium scour depth

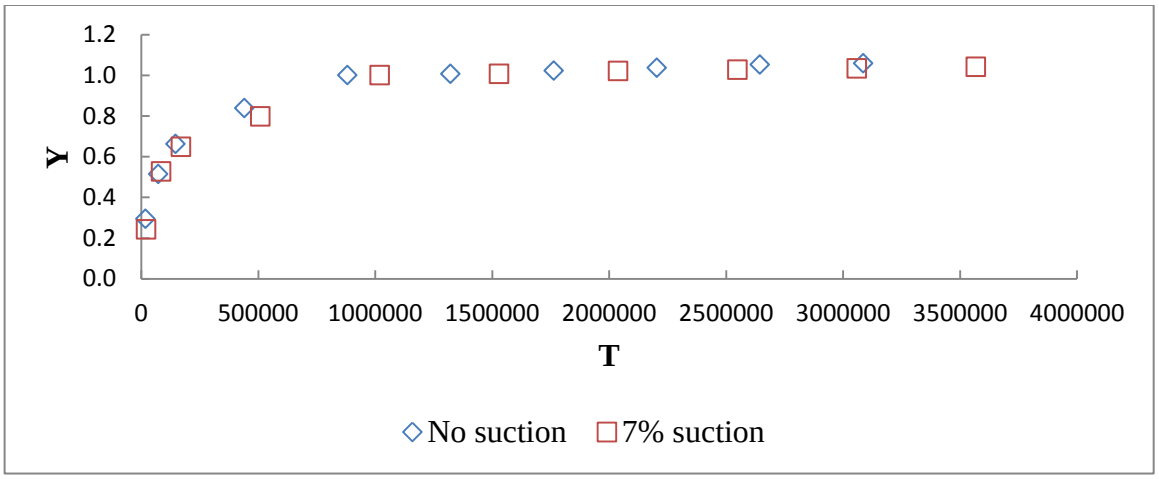

Fig. 4.16. Time evolution of scour depth (Y vs. T) with 7% suction and no suction

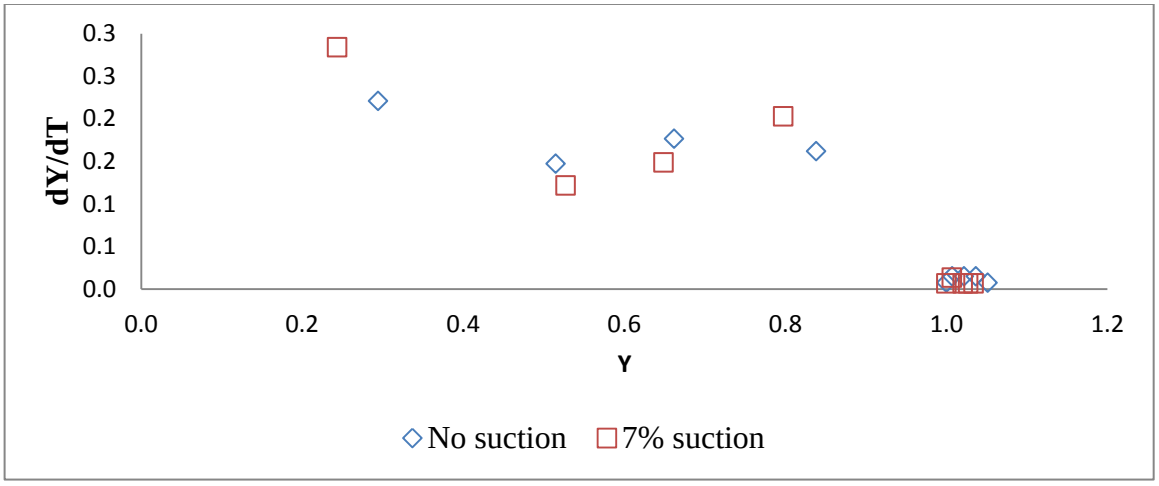

Fig. 4.17. Scour rate for 7% suction and no suction (dY/dT vs. Y)

In the Fig. 4.18 to 4.25, the centerline profiles are shown, which indicate that generally the increasing rates of scour and deposition area of different time durations with 7% suction are higher than those of no suction condition. The 7% suction condition creates larger scour depth and scour hole diameter, more deposit expansion along centerline, but almost same maximum deposit height in comparison to no suction condition after 1 hour

test duration. After 4, 8, and 24 hour test durations, the 7% suction condition creates the scour hole similar to that of 1 hour test duration except the larger maximum deposit height attained in comparison to no suction condition. In case of 24 hours test durations suction condition creates even more deposit expansion along centerline in comparison to 1 hour test duration result.

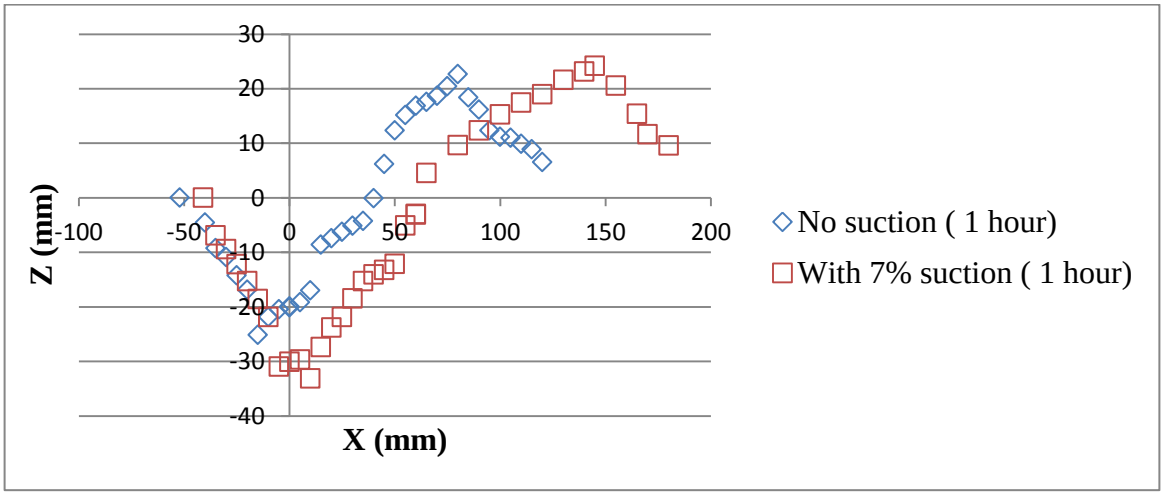

Fig. 4.18. Dimensional centerline profiles for Experiment 2 (no suction) and Experiment 11 (7% suction) after 1 hour

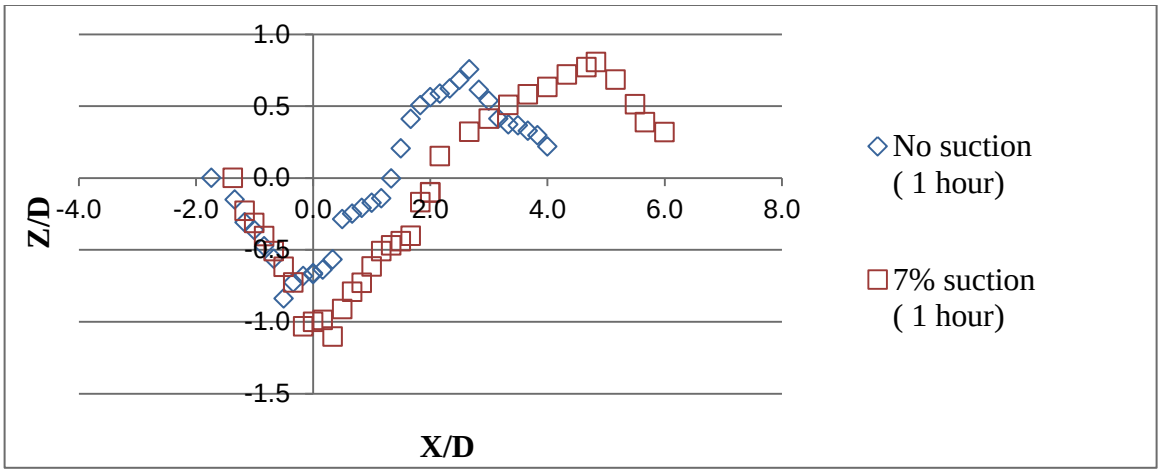

Fig. 4.19. Non-dimensional centerline profiles for Experiment 2 (no suction) and Experiment 11 (7% suction) after 1 hour

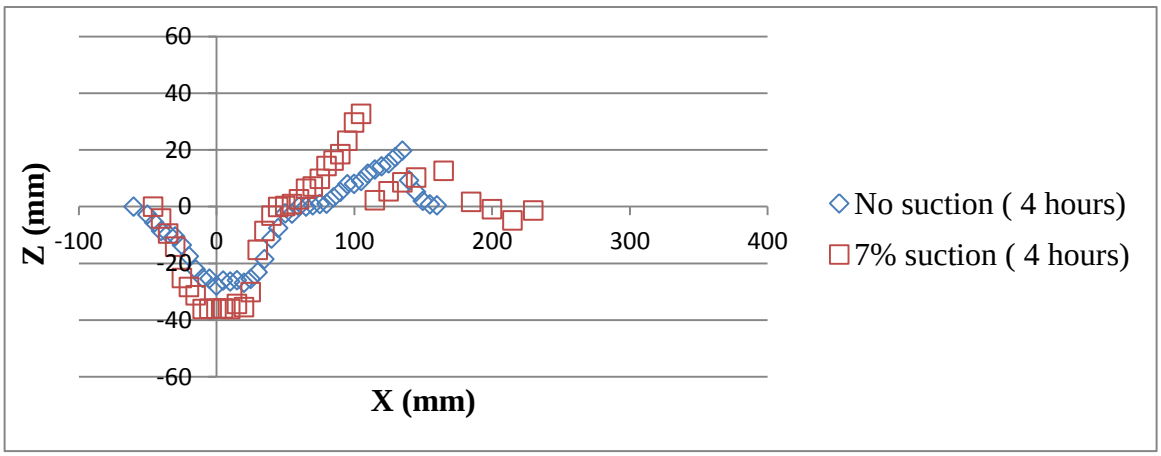

Fig. 4.20. Dimensional centerline profiles for Experiment 2 (no suction) and Experiment 11 (7% suction) after 4 hours

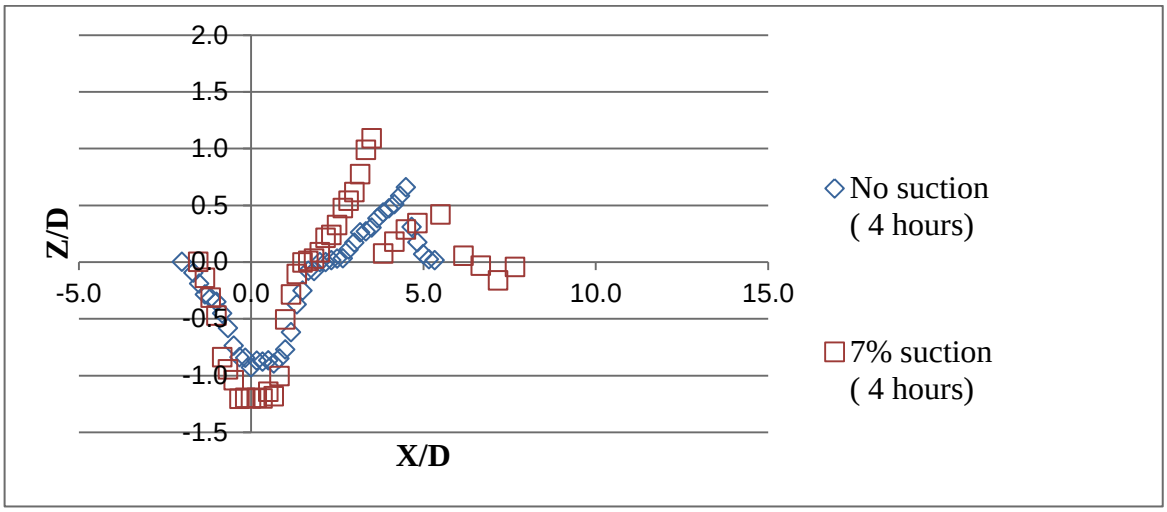

Fig. 4.21. Non-dimensional centerline profiles for Experiment 2 (no suction) and Experiment 11 (7% suction) after 4 hours

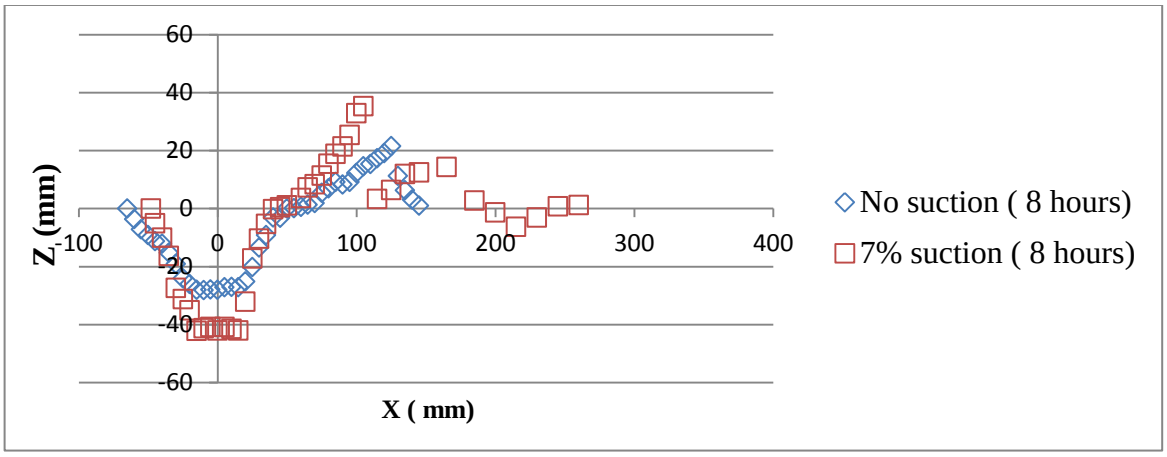

Fig. 4.22. Dimensional centerline profiles for Experiment 2 (no suction) and Experiment 11 (7% suction) after 8 hours

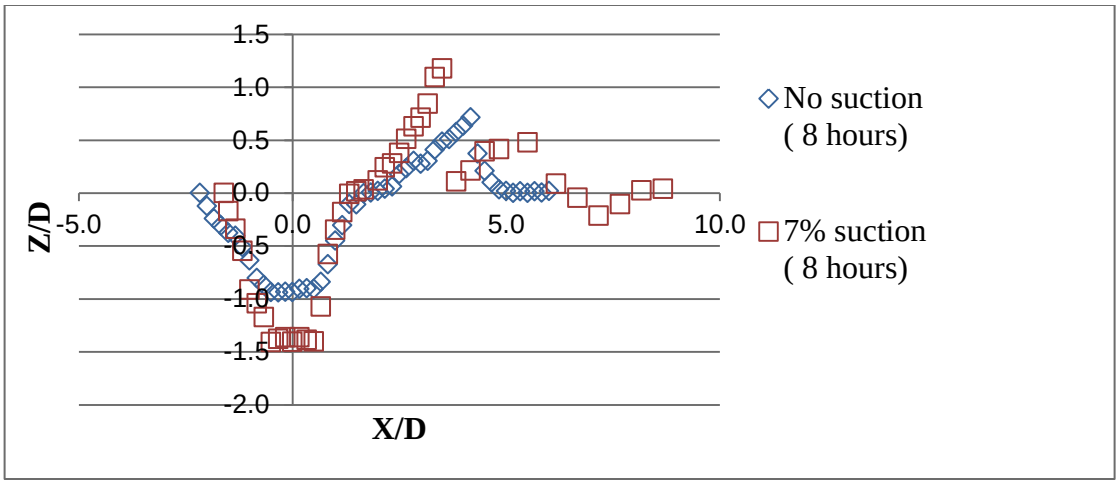

Fig. 4.23. Non-dimensional centerline profiles for Experiment 2 (no suction) and Experiment 11 (7% suction) after 8 hours

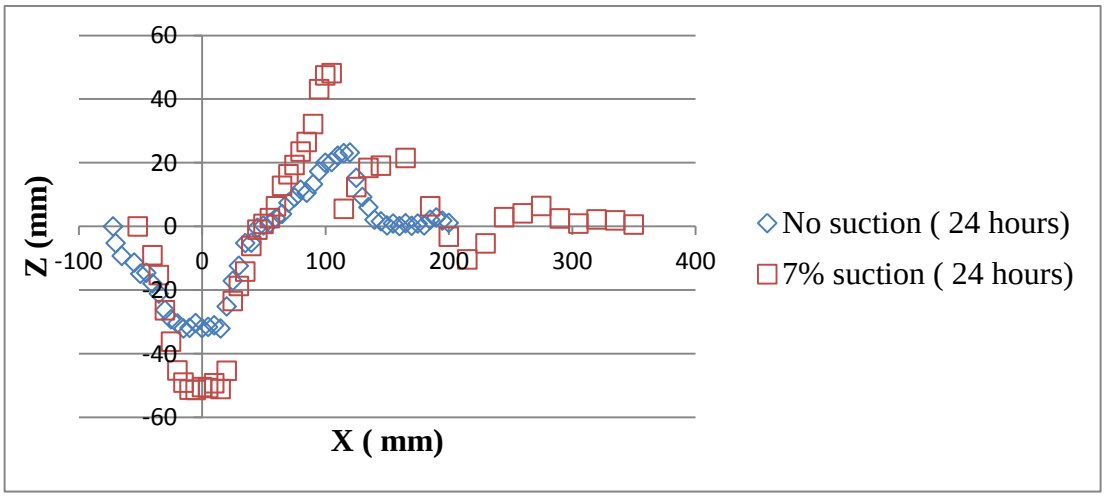

Fig. 4.24. Dimensional centerline profiles for Experiment 2 (no suction) and Experiment 11 (7% suction) after 24 hours

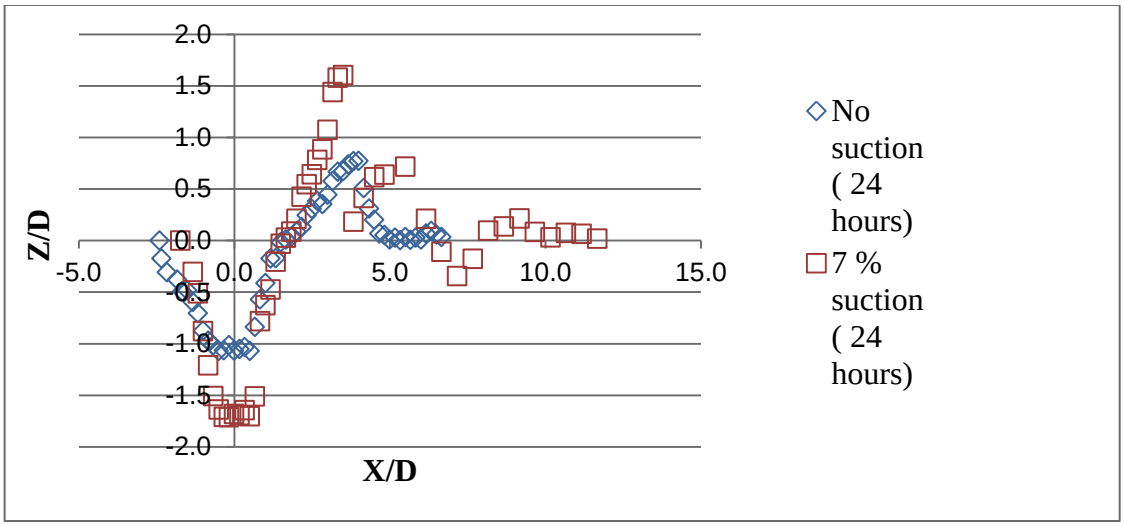

Fig. 4.25. Non-dimensional centerline profiles for Experiment 2 (no suction) and Experiment 11 (7% suction) after 24 hours

It is shown in the Table 4.1 that about 80% of equilibrium scour depth and 93% of equilibrium deposit height were attained with no suction condition, and about 94 % of equilibrium scour depth and 89% of equilibrium deposit height were attained with 7% suction after 50% of the time to equilibrium, and 75% of the equilibrium scour depth attained without suction and 80% of the equilibrium scour depth attained after 17% of the time to equilibrium. The following Table 4.1 shows the relation between percentage of the equilibrium scour depth and deposit with percentage of the time to equilibrium with 7% suction and no suction conditions. About 50-80% of the equilibrium scour depth develops at a stage after 10% of the time to equilibrium, depending on the approaching flow velocity (Melville and Chiew, 1999).

Table 4.1. Percentages of equilibrium scour depth and deposit with 7% suction and no suction for different time durations

% of the time to equilibrium	% of the equilibrium scour depth and deposit with no suction	% of the equilibrium scour depth and deposit with 7% suction
2	62, 68	65, 52
8	69, 76	70, 66
17	75, 81	80, 73
50	80, 93	94, 89

4.4 Suction Effect on Local Scour

Experiments 6 to 12 were performed with different suction rates of 2%, 5%, 6%, 7% and 10%, and the experimental results of velocity profiles and equilibrium scour depths were compared with those of no suction conditions. The mean velocity profiles for no suction and with different suction rates were shown in the Fig. 4.26 to Fig. 4.30. In the experiments with 5-10% suction conditions, the approach velocities were increased in the near bed location and decreased near the free surface. But, for the experiment with 2% suction rate, the results show opposite in nature. The friction velocities were decreased with increasing suction for the experiment 8 to 12 and increased for the experiment 7 in comparison to no suction condition.

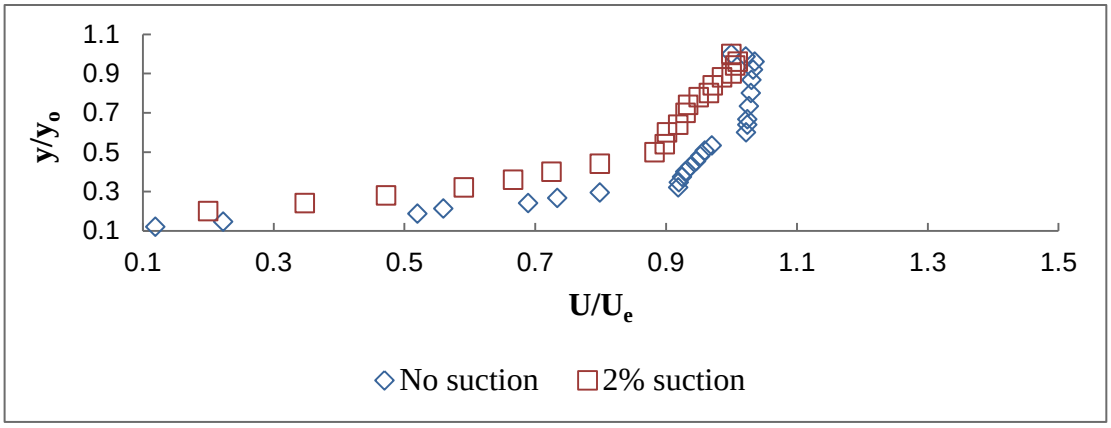

Fig. 4.26. Mean velocity profiles for Experiment 6 (no suction) and Experiment 7 (2% suction)

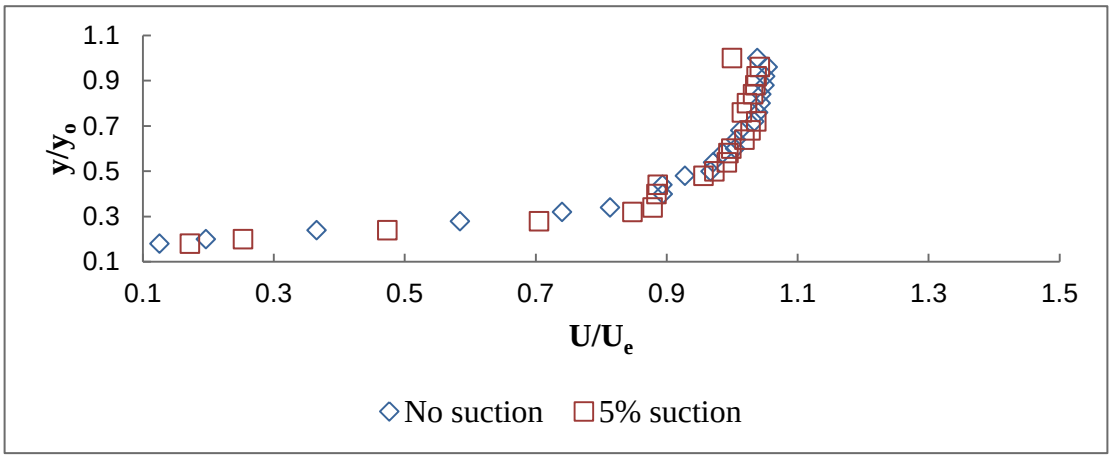

Fig. 4.27. Mean velocity profiles for Experiment 2 (no suction) and Experiment 8 (5 % suction)

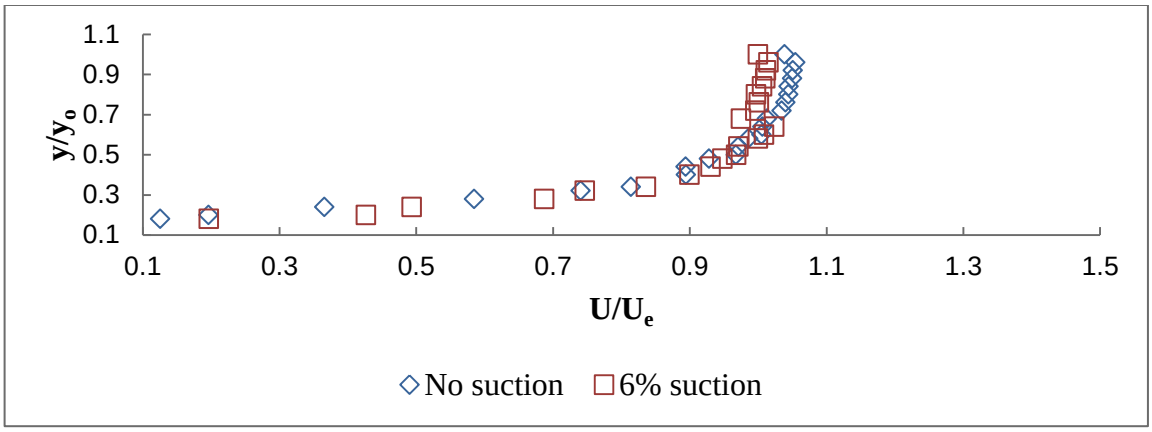

Fig. 4.28. Mean velocity profiles for Experiment 2 (no suction) and Experiment 10 (6 % suction)

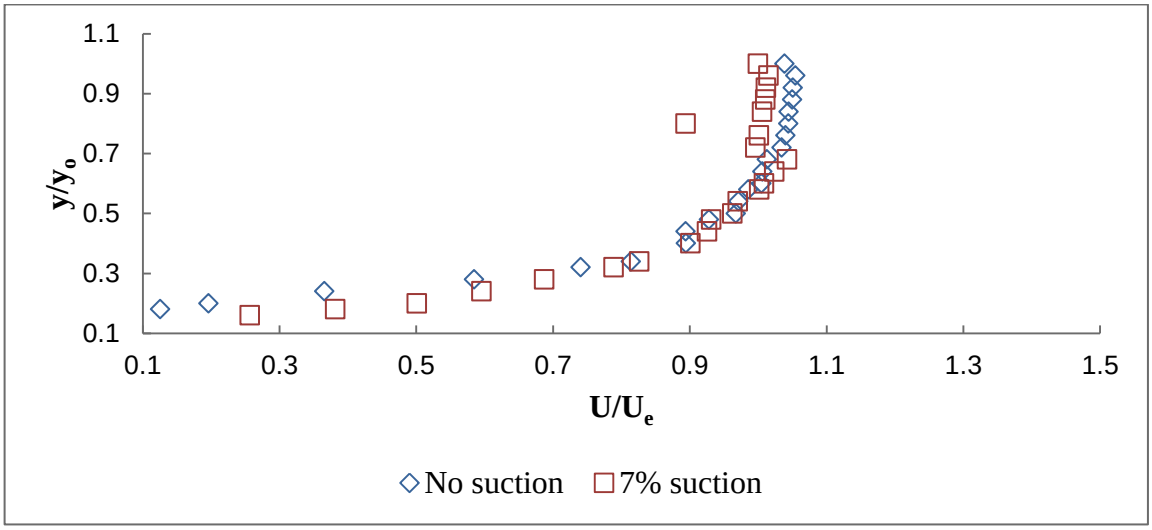

Fig. 4.29. Mean velocity profiles for Experiment 2 (no suction) and Experiment 11 (7 % suction)

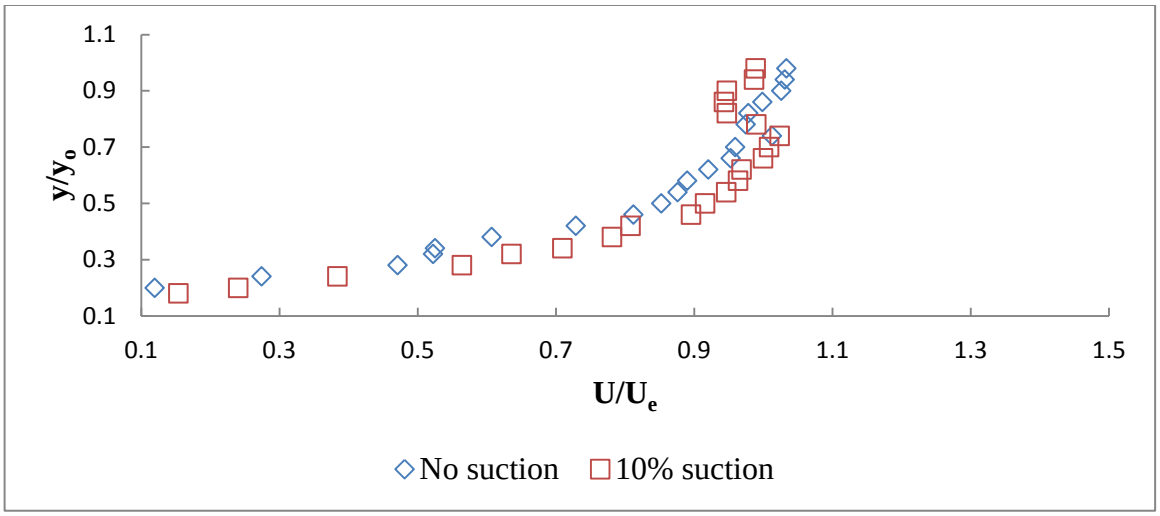

Fig. 4.30. Mean velocity profiles for Experiment 2 (no suction) and Experiment 12 (10 % suction)

After conducting 48 hours tests with no suction and 2%, 5%, 6%, 7%, and 10% suction, the role of suction on equilibrium local scour depth and area as well as deposition height and area were clearly understood from the Fig. 4.31 to 4.36 (centerline profiles and scour hole and deposit profiles). It is shown in the Fig. 4.31 and Fig. 4.32 that the largest and the least scour hole perimeter occurred with no suction, and 2% suction condition respectively. Scour hole perimeter was gradually decreasing from 10% suction to 5% suction condition. From the Fig. 4.33 and Fig. 4.34 it may be seen that the least and largest deposit expansion along centerline occurred for 2% suction, and 10% suction condition respectively. Deposit expansion was gradually increasing from 6% to 10% suction condition in comparison to no suction condition.

It was shown in Fig. 4.35 and Fig. 4.36 the equilibrium local scour depth was the least and the largest for 2% suction, and 10% suction condition, respectively, and gradually it was increasing from 5% suction condition to 10% suction condition in comparison to no suction condition. From the Table 4.2 it was found that maximum equilibrium scour

depth reduced by 39.50% in case of 2% suction condition, and increased by about 23% to 42% in the cases of 5% to 10% suction condition in comparison to no suction condition. From these experimental results it is understood that suction modifies the behaviour of both the flow and sediment transport around a bridge pier and it has profound influence on the equilibrium scour depth.

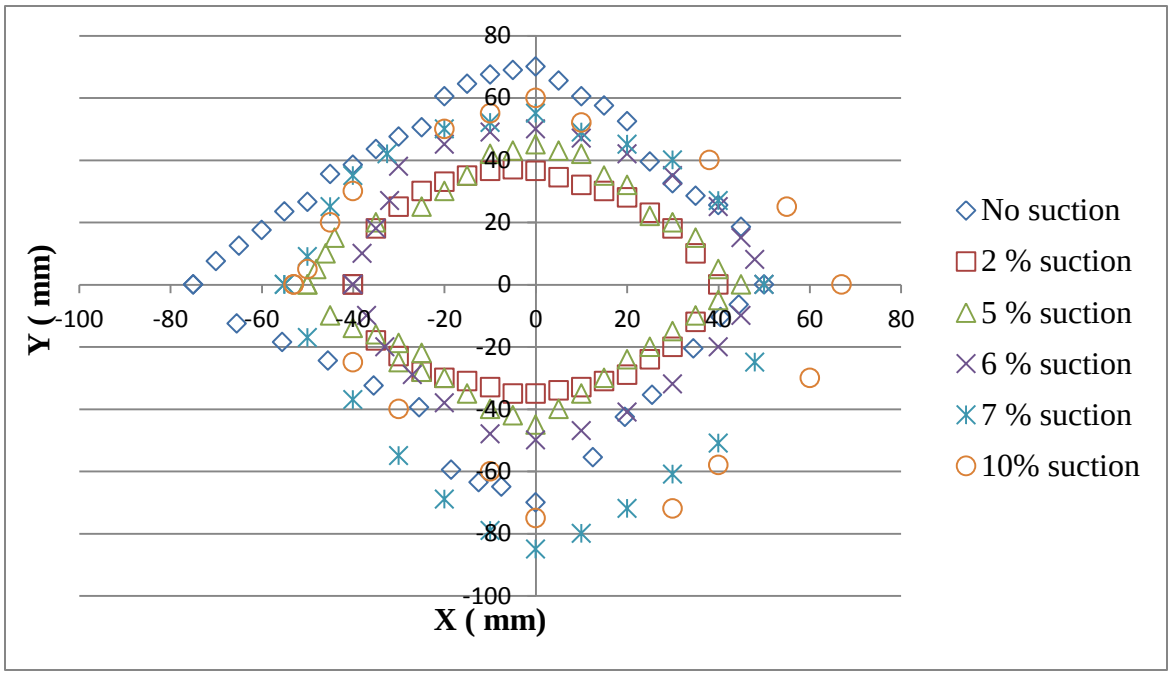

Fig. 4.31. Dimensional scour hole with no suction and 2 %, 5%, 6%, 7%, and 10% suction (48 hours test)

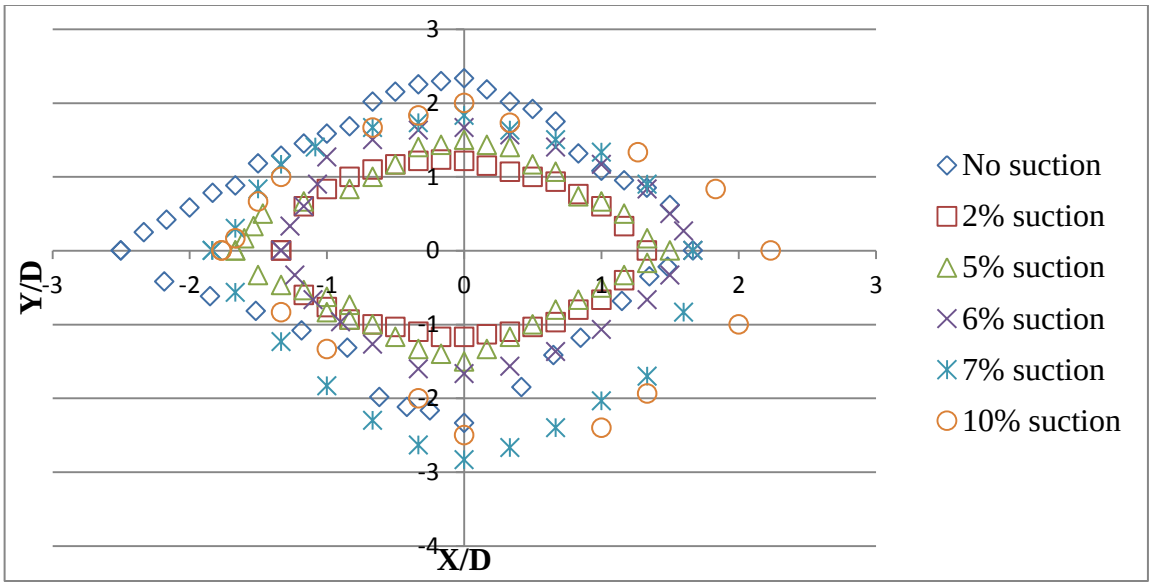

Fig. 4.32. Non-Dimensional scour hole with no suction and 2 %, 5%, 6%, 7%, and 10% suction (48 hours test)

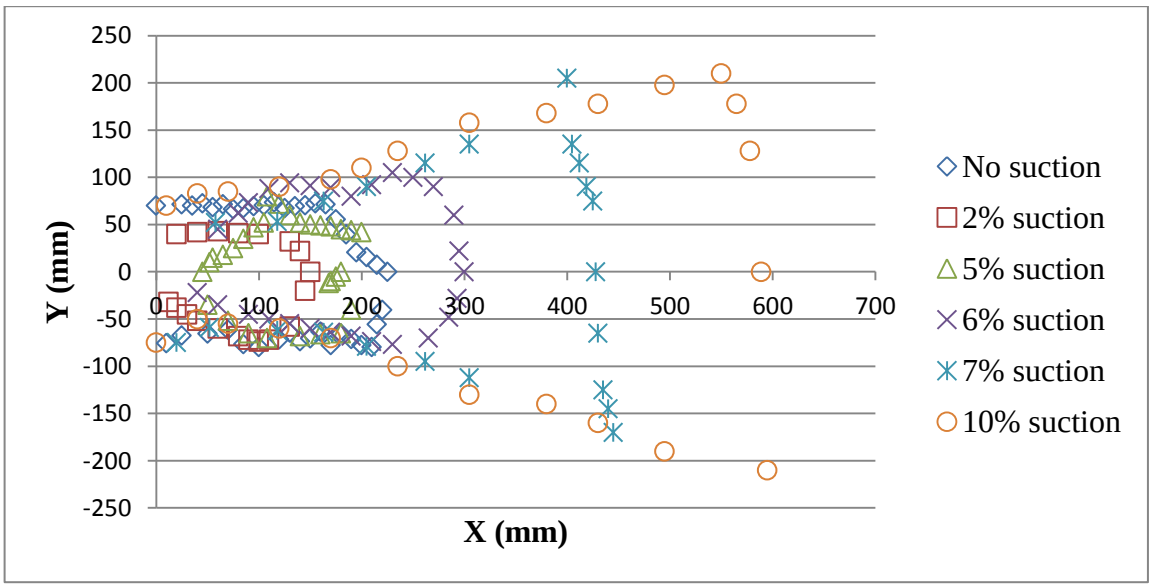

Fig. 4.33. Dimensional deposit profiles for no suction and different suction (2%, 5%, 6%, 7%, and 10%) after 48 hours test duration

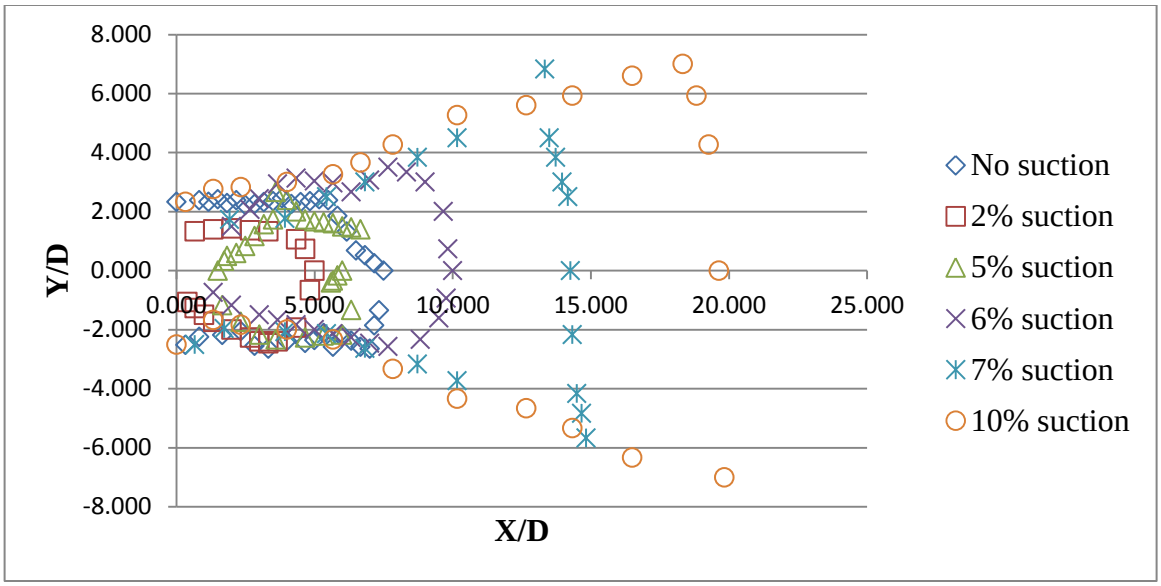

Fig. 4.34. Non-Dimensional deposit profiles for no suction and different suction (2%, 5%, 6%, 7% , and 10%) after 48 hours test duration

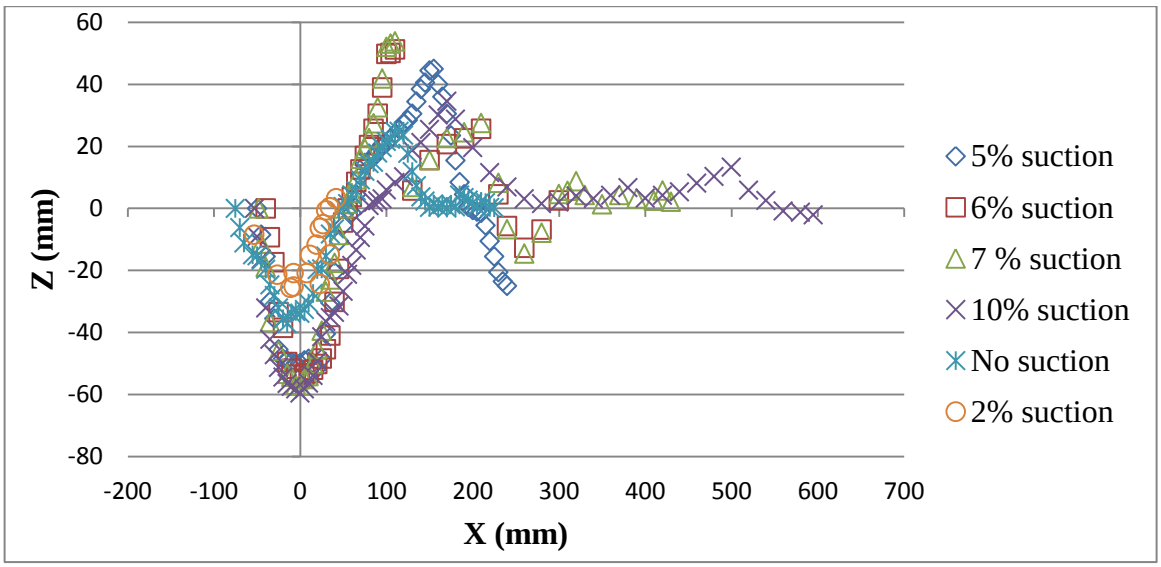

Fig. 4.35. Dimensional centerline profiles for no suction and different suction (2%, 5%, 6%, 7%, and 10%) after 48 hours test duration

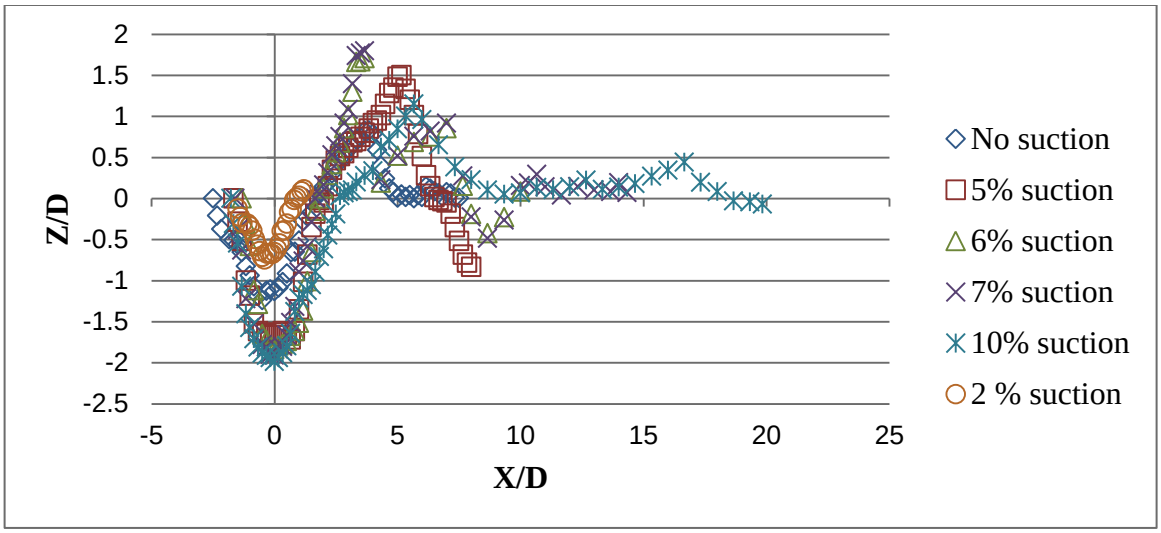

Fig. 4.36. Non-dimensional centerline profiles for no suction and different suction (2%, 5%, 6%, 7%, and 10%) after 48 hours test duration

Table 4.2. Comparisons of percentage change of equilibrium scour depth

Experiment No.	Rate of Suction	% change in equilibrium scour depth
7	2%	-39.50
8	5%	+22.62
9	7%	+27.53
10	6%	+30.91
11	7%	+36.23
12	10%	+41.81

Note: + ve represents increase and –ve represents decrease in comparison to no suction condition

4.5 Summary of Findings

The results from the experimental velocity profiles for experiment 1, 3 and 4 in outer layer and inner layer show that the maximum velocity occurs below the free surface and for the shallow water depth (y_0 = 50 mm) the higher gradient of velocity and shear stress attained near the bottom compared to deep water depth (y_0 = 100 mm). The results also show that turbulent intensity gains a maximum value very close to the bed, and reduces towards the free surface. The turbulence intensity attains almost constant value closer to the free surface. The results from the variations of equilibrium scour depth with Euler number show that with suction (2-10%) conditions Euler number varies from 0.10-0.15, and equilibrium scour depths are increasing with the increase in Euler number, and with no suction condition this number varies from 0.05-0.15.

The results from the variation of scour hole and deposit for different y_0/D with suction and no suction condition show that 2% suction condition creates reduced scour hole and deposit area and 7% suction condition creates larger scour hole and deposit area compared to scour hole and deposit area for no suction conditions.

The temporal variations of scour depth for the experiment no. 2 (no suction condition) and experiment no. 11 (with 7% suction condition) show that scour rate becomes very high in the initial phase and very low near the equilibrium condition, and scour rate for the 7% suction is larger than no suction condition. About 80% of equilibrium scour depth and 93% of equilibrium deposit height were attained after 24 hours with no suction condition, and about 94 % of equilibrium scour depth and 89% of equilibrium deposit height were attained after 24 hours with 7% suction condition.

In the experiments with 5-10% suction conditions, the approach velocities were increased in the near bed location and decreased near the free surface. But, for the experiment with 2% suction rate, the result shows opposite in nature. The friction velocities were decreased with increasing suction for the experiment 8 to 12 and increased for the experiment 7 in comparison to no suction condition. For 2% suction condition equilibrium scour depth was decreased by 39.5% in comparison to no suction condition. Percentage increase of equilibrium scour depth for 5% to 10% suction conditions were 23% to 42% in comparison to no suction condition.

CHAPTER 5

CONCLUSIONS AND RECOMMENDATIONS

5.1 Conclusions

The present study was carried out to review local scour hole and deposit profiles and the maximum equilibrium scour depth by conducting experimental study using laboratory flume varying flow shallowness ratio and test time durations in case of no suction and with different suction rates condition. The main findings are summarized as follows:

1. Irrespective of the suction or no suction condition, the results show that equilibrium scour depth for these experiments (except experiment no.1) depend on both water depth and pier diameter, and does not increase linearly with increase of y_o/D. Introducing different suction rates, equilibrium scour depths increase with the increase of Euler number.
2. Sediment coarseness ratio (D/d_{50}) varies from 50-100 and the bed material is fine relative to pier diameter and scour volume decreases when pier diameter increases. For the same flow shallowness (y_o/D) and sediment coarseness (D/d_{50}) ratio, the suction has a great influence on bridge pier local scour depth. A narrower pier induced larger equilibrium local scour depth in comparison to wider pier in the same flow field irrespective of no suction and with suction condition
3. Irrespective of no suction or with suction condition, the scour rate was very high in the initial phase and very low near the equilibrium condition. The scour rate for the 7% suction condition was larger than that of no suction condition.
4. The largest and the least scour hole perimeter occurred with no suction, and 2% suction condition, and the least and the largest deposit expansion along centerline

occurred for 2% suction, and 10% suction condition, respectively. Although 2% suction reduces local scour depth, the 5-10% suction increases local scour depth; generally suction (5-10%) increases near bed velocity and decreases near surface velocity. The friction velocity decreases while increasing suction (5-10%).

5.2 Recommendations

All the tests were accomplished under clear-water condition maintaining constant flow intensity (0.8). The behaviour of suction on local scour for varying flow intensities should be tested in the further research studies. The effect of injection on local scour may also be investigated. This experimental study may also be conducted under live bed scour condition.

REFERENCES

[1] Ashtiani, A., Ghorghi, B., and Behesti, A. (2009). Experimental investigation of clear-water local scour of compound piers. Journal of Hydraulic Engineering, 136(6), 343-351.

[2] Breusers, H. (1967). Time scale of two dimensional local scour. Proceedings of 12th Congress (IAHR), Ft. Collins, Colorado, 3, 275-282.

[3] Breusers, H., and Raudkivi, A.J. (1991). Scouring: Hydraulic Structures Design Manual Series, Vol 2. Taylor and Francis, International Association of Hydraulic Research.

[4] Breusers, H., Nicollect, G., and Shen, H.W. (1977). Local scour around cylindrical piers. Journal of Hydraulic Research, 15(3), 211-252.

[5] Carollo, F.G., Ferro, V., and Termini, D. (2008). Analyzing turbulence intensity in gravel bed channels. Journal of Hydraulic Engineering, 134, 506-508.

[6] Chen, X., and Chiew, Y. (2004). Velocity distribution of turbulent open-channel flow with bed suction. Journal of Hydraulic Engineering, 130(2), 140-148. doi:10.1061/(ASCE)0733-9429(2004)130:2(140).

[7] Chiew, Y. M., and Melville, B.W. (1987). Local scour around bridge piers. Journal of Hydraulic Research, 25(1), 15-26.

[8] Chiew, M., and Hong, J. (2013). Suction effects on bridge pier scour under clear water conditions. Journal of Hydraulic Engineering, 139(6), 621-629. doi:10.1061/(ASCE)HY.1943-7900.000711.

[9] Clark, J.A. (1968). A study of incompressible turbulent layers in channel flows. Journal of Basic Engineering, ASME, 90: 455-468.

[10] Coleman, N.L. (1967). A theoretical and experimental study of drag and lift forces acting on a sphere resting on hyphothetical stream bed. Proceedings of International Association for Hydraulic Research (IAHR), 3, 185-192.

[11] Copp, H.D., and Johnson, J.P. (1987). Riverbed scour at bridge piers. Washington State Department of Transportation, Final Report No. WA-RD 118.1.

[12] Das, N. (2005). Soil moisture modeling and scaling using passive microwave remote sensing. Master's Thesis, Texas A & M University, College Station, Texas.

[13] Dey, S., and Sarker, A. (2007). Effect of upward seepage on scour and flow downstream of an apron due to submerged jets. Journal of Hydraulic Engineering, 133(1), 59-69. doi: 10.1061/(ASCE)0733-9429(2007)133:1(59).

[14] Ettema, R. (1980). Scour at bridge piers, Auckland University, Auckland, New Zealand.

[15] Ettema, R., Melville, B., and Barkdoll, B. (2001). Scale effects in pier-scour experiments. Journal of Hydraulics Engineering, 124(6), 639-642.

[16] Ettema, R., Kirkil, G., and Muste, M. (2006). Similitude of large-scale turbulence in experiments on local scour at cylinders. Journal of Hydraulic Engineering, ASCE, 132(1), 33-40.

[17] Ettema, R., Constantinescu, G., and Melville, B. (2011). Evaluation of bridge scour research: pier scours processes and predictions. National Cooperative Highway Program, 24-27(01), 1-181. Retrieved from http://onlinepubs.trb.org/onlinepubs/nchrp/nchrp_w175.pdf (Accessed on March 12, 2012).

[18] Faruque, M. A. (2009). Smooth and rough wall open channel flow including effects of seepage and ice cover. University of Windsor, Windsor, Ontario.

[19] Francalanci, S., Parker, G., and Solari, L. (2008). Effect of seepage induced nonhydrostatic pressure distribution on bed load transport and bed morphodynamics. Journal of Hydraulic Engineering, 134(4), 378-389.

[20] Gratiot, N., Mory, M., and Auchere, D. (2000). An acoustic Doppler velocimeter (ADV) for the characterisation of turbulence in concentrated fluid mud. Continental Shelf Research, 20, 1551-1567.

[21] Hafez, Y. (2004). A new analytical bridge pier scour equations. 8th International Water Technology Conference, IWTC8, Alexandria, Egypt, 587-60.

[22] Herbich, H., and Brennan, L. (1967). Prediction of scour at bridges. Ontario Department of Highway, D.H.O. Dept. No. RR 115, 1-135.

[23] Hodi, B. (2009). Effect of blockage and densimetric Froude number on circular bridge pier local scour. Master's thesis, University of Windsor, Windsor, Ontario.

[24] Hoffmans, G., and Pilarczk, K. (1995). Local scour downstream of hydraulic structure. Journal of Hydraulic Engineering, 121(4), 326-340.

[25] Hopkins, G.R., Vance, R.W., and Kasraie, B. (1980). Scour around bridge piers. Report No. FHWA-RD-79-103, Federal Highway Administration, Washington, D.C.

[26] Jain, S.C., and Fischer, E. E. (1980). Scour around bridge piers at high Froude numbers. Report number FHWA-RD-79-104, Federal Highway Administration, Washington, D.C.

[27] Laursen, E.M., and Toch, A. (1956). Scour around bridge piers and abutments. Bull. No. 4, Iowa Hwy. Res. Board, Ames, Iowa.

[28] Lin, Y., Chen, J., Chang, K., Chen, J., and Lai, J. (2004). Real-time monitoring of local scour by using fiber brag grating sensors. Institute of Physics Publishing, 14(05), 664-670. doi: 10.1088/0964-1726/14/4/025.

[29] Liu, X., and Chiew, Y. (2012). Effect of seepage on initiation of cohesionless sediment transport. Acta Geophysica, 60(6), 1778-1796. doi: 10.2478/s 11600-012-0043-7.

[30] Maclean, A.G., and Willets B.B. (1986). Measurement of boundary shear stress in nonuniform open channel flow. Journal of Hydraulic Research, 24(1), 39-51.

[31] Maclean, A.G. (1991). Open channel velocity profiles over a zone of rapid infiltration. Journal of Hydraulic Research, 29(1), 15-27.

[32] Melville, B.W., and Raudkivi, A.J. (1977). Flow characteristics in local scour at bridge piers. Journal of Hydraulic Research, 15, 373-380.

[33] Melville, B.W., and Sutherland, A.J. (1988). Design method for local scour at bridge piers. Journal of Hydraulic Engineering, 114(10), 1210-1226.

[34] Melville, B.W., and Chiew, Y.M. (1999). Time scale for local scour at bridge piers. Journal of Hydraulic Engineering, 125(1), 59-65.

[35] Melville, B.W., and Coleman, S.E. (2000). Bridge Scour. Water Resources Publications, Colorado, USA.

[36] Mia, M., and Nago, H. (2003). Design method of time-dependent local scour at circular bridge pier. Journal of Hydraulic Engineering, 129(6), 420-427.

[37] Mohammed, T., Noor, M., Ghazali, A., Yusuf, B., and Saed, K. (2006). Physical modeling of local scouring around bridge piers in erodible bed. Journal of King Saud University, 19(2), 195-207.

[38] Muzzammil, M., and Gangadhariah, T. (2003). The mean characteristics of horseshoe vortex at a cylindrical pier. Journal of Hydraulic Research, 41(3), 285-297. doi: 10.1080/00221680309499973.

[39] National Transportation Safety Board. (1990). Highway Accident Report. Retrieved from http://www.ntsb.gov/investigations/summary/HAR900/html. (Accessed on July 20, 2012).

[40] Nezu, I., Nakagawa, H., 1993. Turbulence in open-channel flow. Journal of Fluid Mechanics, 269, 373-375, doi:http://dx.doi.org/10.1017/s00221120-94211618.

[41] Nezu, I. (2005). Open-channel flow turbulence and its research prospect in the 21st century. Journal of Hydraulic Engineering, 131(4), 229-246.

[42] Oldenziel, D.M., and Brink, W.E. (1974). Influence of suction and blowing on entertainment of sand particles. Journal of Hydraulics Division, ASCE, 100(7), 935-949.

[43] Pope, S. (2000). Turbulent Flows. Cambridge University Press, Cambridge.

[44] Prinos, P. (1995). Bed-suction effects on structure of turbulent open-channel flow. Journal of Hydraulic Engineering, 121(5), 404-412.

[45] Richardson, J.R., and Richardson, E.V. (1985). Inflow seepage influence on straight alluvial channels. Journal of Irrigation and Drainage Engineering, ASCE, 120(1), 60-79.

[46] Ross, H., Sicking, D, Zimmer, R., and Michie, J. (1993). Recommended procedures for the safety performance evaluation of highway features. National Cooperative Highway Research Program, 22-7 (350), 1-74. Retrieved from http://onlinepubs.trb.org/onlinepubs/nchrp-rpt-350-a.pdf. (Accessed on May18, 2012).

[47] Roussinova, V., Biswas, N., and Balachandar, R. (2006). Revisiting turbulence in smooth uniform open channel flow. Journal of Hydraulic Research, 46 (Extra Issue1), 36-48.

[48] Shen, H., Schneider, V., and Karaki, S. (1969). Local scour around bridge piers. Journal of the Hydraulics Division, ASCE, 95, 1919-1940.

[49] Shields, A. (1936). Application of similarity principles and turbulence research to bed-load movement. Publication No. 167, California Institute of Technology, Pasadena, Calif. (English translation).

[50] St. Anthony Falls Laboratory. (2012). Looking for trouble beneath the water surface. Retrieved from http:// www.safl.ums.edu/featured-story-beneath-water-surface. (Accessed on March 10, 2013).

[51] Truc, N.X., and Khai, N.H. (1982). Local scour at bridge pier and design relation proposed. Transportation Journal, 4, 49-52.

[52] Watters, G.Z., and Rao Manam, V.P. (1971). Hydrodynamic effects of seepage on bed particles. Journal of Hydraulics Division, ASCE, 101(3), 421-439.

[53] Willets, B.B., and Drossos, M.E. (1975). Local erosion caused by rapid infiltration. Journal of Hydraulic Division, ASCE, 101(12), 1477-1488.

[54] Yu, X., and Yu, X. (2010). Laboratory evaluations of time-domain reflectometry for bridge scour measurement: comparison with the ultrasonic method. Journal of Advances in Civil Engineering, 2010(2010),1-12. doi: 10.1155/2010/508172.

[55] Terzaghi, K., Peck, R. and Mesri, G. (1996). Soil Mechanics in Engineering Practice. Third edition, John Wiley and Sons, New York.

[56] Cheng, N. and Chiew, Y. (1998). Turbulent open channel flow with upward seepage. Journal of Hydraulic Research, 36(3), 415-431.

[57] Lu, Y. and Chiew, Y. (2007). Seepage effects on dune dimensions. Journal of Hydraulic Engineering, 133(5), 560-563.

[58] Cheng, N. and Chiew, Y. (1999). Incipient sediment motion with seepge. Journal of Hydraulic Research, 37(5), 665-681.

[59] Rao, A., Subrahmanyam, V., Thayumnavan, S. and Damodaran, N. (1994). Seepage effects on sand-bed channels. Journal of Irrigation and drainage Engineering, 120(1), 60-79. doi: 10.1061/(ASCE)0733-9437(1994)120:1(60).

[60] Dey, S. and Nath, T. (2010) Turbulence characteristics in flows subjected to boundary injection and suction. Journal of Engineering Mechanics, 136(7), 877-888. doi: 10.1061/(ASCE)EM.1943-7889.0000124.

[61] Dey, S. and Zanku, U. (2004). Sediment threshold with upward seepage. Journal of Engineering Mechanics, 130(9), 1118-1123. doi: 10.1061/(ASCE)0733-9399(2004)130:9(1118).

[62] Ali, K., Achterberg, M. and Zhu, Y. (2003). Effect of seepage on sediment transport in channels. Proceedings of International conference on Estuaries and coasts, IAHR, Hanszhou, China, 461-466.

[63] Sreenivasulu, G., Kumar, B. and Rao, A. (2011). Variation of stream power with seepage in sand-bed channels, Journal of Hydraulic Engineering, 37(1), 115-120.

[64] Xie, L., Lei, H., Yu, Y. and Sun, X. (2009). Incipient motion of river bank sediments with outflow seepage. Journal of Hydraulic Engineering, 135(3), 228-233. Doi: 10.1061/ (ASCE)0733-9429(2009)135:3(228).

APPENDICES

APPENDIX- A

Critical velocity determination by using Shields diagram/formulae for the channel bed at water flow depth 100 mm, 75 mm, and 50 mm

Using Shields diagram:

Step 1 : Find the value of third dimensional parameter using the following term

$$\frac{d_{50}}{\nu}[0.1(G.S.-1)gd_{50}]^{1/2}$$

where, d_{50} = 0.51 mm
Specific gravity of sand (G.S.) = 2.65
Accelaration due to gravity, g = 9.81 m/s^2
Kinematic viscosity, ν = 1.349x 10^{-6} m^2/s (at test temperature of water 17.1˚C)

Step2: Using the above parameter value determines the dimensional shear stress, τ_* from Shield diagram

The value of τ_* = 0.029

Step 3 : Determine the critical shear stress from the following formulae:

$$\tau_c = \tau_*(G.S. - 1)\, \gamma d_{50}$$

The value of τ_c = 0.239 N/m^2

Step 4 : Determine the critical shear velocity, U^{*c} from the following equation

$$U_c^* = \left(\frac{\tau_c}{\rho}\right)^{1/2}$$

The value of U_c^* = 0.01546 m/s

Step 5: Find the critical velocity, Uc from the following formulae:

$$\frac{U_c}{U_c^*} = 5.75 \log (5.53\frac{y_0}{d_{50}}) \qquad \text{(i)}$$

The value of U_c for water depth, y_o = 100mm is 0.2698 m/s
The value of U_c for water depth, y_o = 75mm is 0.2587 m/s and
The value of U_c for water depth, y_o = 50mm is 0.2431 m/s

Using only formulae:

U_c^*= 0.03 (d_{50}) (ii)

and U_c^* = 0.0115 + 0.0125(d_{50}) (iii) (for quartz sand in water at 20 °C & 0.1mm<d_{50}< 1mm)

Where, U_c^* is in m/s and d_{50} is in mm

From (i) & (ii) U_c^* = 0.0153 m/s and U_c = 0.2670 m/s from (i) & (iii) U_c^* = 0.01788 m/s and U_c = 0.3120 m/s

APPENDIX- B

UNCERTAINTY ANALYSIS

Appendix B-1

Uncertainty analysis for the sampling rate of 25 Hz and 25 mm depth from channel bed (y_0 = 100 mm):

Bias limit (±B) is the design stage uncertainty of Velocimeter.

Zero-order uncertainty,

U_0 = ±1/2 *Instrument resolution (95%)

Assuming the interval of values in which 95% of the measurements of velocity should lie. As there is no error listed about the resolution, we consider zero-order uncertainty as zero.

Hence,

U_0 = ±0 (95%)

Instrument error, which is the velocity accuracy given by the manufacturer, is ±0.5% of measured value ±1mm/s.

$U_c = \pm\sqrt{\sum_{i=1}^{n} e_i^2}$ *where e_i is error listed by the manufacturer*

$Uc = \pm\sqrt{(0.5\% \times 0.2119)^2} = \pm 1.0595 \times 10^{-3}\ m/s$ (95%)

Therefore, design stage uncertainty Velocimeter is,

$U_{25} = \pm\sqrt{U_0^2 + U_c^2} = \pm\sqrt{0^2 + (1.0595 \times 10^{-3})^2}$

$= \pm 1.0595 \times 10^{-3}\ m/s$

$= \pm 0.0010595\ m/s$ (95%)

Now we will be calculating the estimated design stage uncertainty of the Velocimeter,

$$U_{Velocimeter} = \sqrt{B^2 + (t_{\nu,P} P)^2}$$

where

B is the Bias limit

$t_{\nu,P}$ is student 't' distribution at P% probability and ν is the degrees of freedom

P is the precision index

Precision index, $P = \frac{S_d}{\sqrt{N}} = \frac{0.0592}{\sqrt{20}} = 0.0132375\ m/s$

Degrees of freedom ν = N-1=20-1 =19

Probability, P = 95%

Then, $t_{19,95} = 2.093$ (Table 4.4 from Figliola and Beasely, 1991)

Therefore, $U_{Velocimeter\_25} = \pm\sqrt{(0.0010595)^2 + (0.0132375 \times 2.093)^2}$

$$U_{Velocimeter\_25} = \pm 0.0277263\ m/s \quad (95\%)$$

Appendix B-2

Uncertainty Analysis for the sampling rate of 35 Hz and 25 mm depth from the channel bed (y_0 = 100 mm):

Bias limit (±B) is the design stage uncertainty of Velocimeter.

Zero-order uncertainty,

U_0 = ±1/2 * Instrument resolution (95%)

Assuming the interval of values in which 95% of the measurements of velocity should lie. As there is no error listed about the resolution, we consider zero-order uncertainty as zero.

Hence,

U_0 = ±0 (95%)

Instrument error, which is the velocity accuracy given by the manufacturer, is ±0.5% of measured value ±1mm/s.

$U_c = \pm\sqrt{\sum_{i=1}^{n} e_i^2}$ *where* e_i *is error listed by the manufacturer*

$Uc = \pm\sqrt{(0.5\% \times 0.1843)^2} = \pm 9.215 \times 10^{-4}\ m/s$ (95%)

Therefore, design stage uncertainty Velocimeter is,

$U_{35} = \pm\sqrt{U_0^2 + U_c^2} = \pm\sqrt{0^2 + (9.215 \times 10^{-4})^2}$

$= \pm 9.215 \times 10^{-4}\ m/s$

$= \pm 0.0009215\ m/s$ (95%)

Similarly, the estimated design stage uncertainty for 35 Hz sampling rate can be calculated as follows:

Precision index, $P = \frac{S_d}{\sqrt{N}} = \frac{0.0375}{\sqrt{20}} = 0.00838525\ m/s$

Degrees of freedom ν = N-1=20-1 =19

Probability, P = 95%

Then, $t_{19,95} = 2.093$ (Table 4.4 from Figliola and Beasely, 1991)

Therefore, $U_{Velocimeter\_35} = \pm\sqrt{(0.0009215)^2 + (0.00838525 \times 2.093)^2}$

$$U_{Velocimeter\_35} = \pm 0.0175743\ m/s \quad (95\%)$$

Appendix B-3

Uncertainty analysis for the sampling rate of 100 Hz and 50 mm depth from channel bed (y_0 = 100 mm) :

Bias limit (±B) is the design stage uncertainty of Velocimeter.

Zero-order uncertainty,

U_0 = ±1/2 X Instrument resolution (95%)

Assuming the interval of values in which 95% of the measurements of velocity should lie. As there is no error listed about the resolution, we consider zero-order uncertainty as zero.

Hence,

U_0 = ±0 (95%)

Instrument error, which is the velocity accuracy given by the manufacturer, is ±0.5% of measured value ±1mm/s.

$U_c = \pm\sqrt{\sum_{i=1}^{n} e_i^2}$ *where* e_i *is error listed by the manufacturer*

$Uc = \pm\sqrt{(0.5\% \times 0.2390)^2} = \pm 1.195 \times 10^{-3}\ m/s$ (95%)

Therefore, design stage uncertainty velocimeter is,

$U_{mid\_100} = \pm\sqrt{U_0^2 + U_c^2} = \pm\sqrt{0^2 + (1.195 \times 10^{-3})^2}$

$= \pm 1.195 \times 10^{-3}\ m/s$

$= \pm 0.001195\ m/s$ (95%)

Similarly, the estimated design stage uncertainty for 100 Hz sampling rate at mid-depth (50 mm) can be calculated as follows:

Precision index, $P = \frac{S_d}{\sqrt{N}} = \frac{0.0123}{\sqrt{20}} = 0.00275\ m/s$

Degrees of freedom ν = N-1=20-1 =19

Probability, P = 95%

Then, $t_{19,95} = 2.093$ (Table 4.4 from Figliola and Beasely, 1991)

Therefore, $U_{Velocimeter\_100\_mid} = \pm\sqrt{(0.001195)^2 + (0.00275 \times 2.093)^2}$

$$U_{Velocimeter\_100\_mid} = \pm 0.00058785\ m/s \quad (95\%)$$

Appendix B-4

Uncertainty analysis for the sampling rate of 100 Hz and still water (y_0 = 120 mm)

Bias limit (±B) is the design stage uncertainty of Velocimeter.

Zero-order uncertainty,

U_0 = ±1/2 * Instrument resolution (95%)

Assuming the interval of values in which 95% of the measurements of velocity should lie. As there is no error listed about the resolution, we consider zero-order uncertainty as zero.

Hence,

U_0 = ±0 (95%)

Instrument error, which is the velocity accuracy given by the manufacturer, is ±0.5% of measured value ±1mm/s.

$U_c = \pm\sqrt{\sum_{i=1}^{n} e_i^2}$ *where* e_i *is error listed by the manufacturer*

$Uc = \pm\sqrt{(0.5\% \times 0.0)^2} = \pm 0.0\ m/s$ (95%)

Therefore, design stage uncertainty of velocimeter is,

$U_{still\_120} = \pm\sqrt{U_0^2 + U_c^2} = \pm\sqrt{0^2 + (0)^2}$

$= \pm 0\ m/s$

$= \pm 0\ m/s$ (95%)

Then, the estimated design stage uncertainty for 100 Hz sampling rate in the still water (120 mm depth) can be calculated as follows:

Precision index, $P = \frac{S_d}{\sqrt{N}} = \frac{0.0334}{\sqrt{20}} = 0.0074685\ m/s$

Degrees of freedom ν = N-1=20-1 =19

Probability, P = 95%

Then, $t_{19,95} = 2.093$ (Table 4.4 from Figliola and Beasely, 1991)

Therefore, $U_{Velocimeter\_100\_still} = \pm\sqrt{(0.0)^2 + (0.0074685 \times 2.093)^2}$

$U_{Velocimeter\_100\_still} = \pm 0.0156315\ m/s$ (95%)

APPENDIX C

Calculation of Friction Velocity

For the experiment no. 1

Flow depth y(m)	Velocity U(m/s)
0.007	0.0026
0.008	0.0179
0.009	0.0359
0.01	0.0568
0.012	0.0986
0.014	0.1601
0.016	0.2016
0.017	0.2125
0.02	0.2355
0.022	0.2396
0.024	0.2418
0.025	0.2591
0.027	0.2593
0.029	0.2601
0.03	0.2681
0.032	0.2691
0.034	0.2698
0.036	0.2705
0.038	0.2709
0.04	0.2715
0.042	0.2758
0.044	0.2786
0.046	0.2795
0.048	0.2799
0.05	0.2699

Step 1 : Plot velocity U, versus y

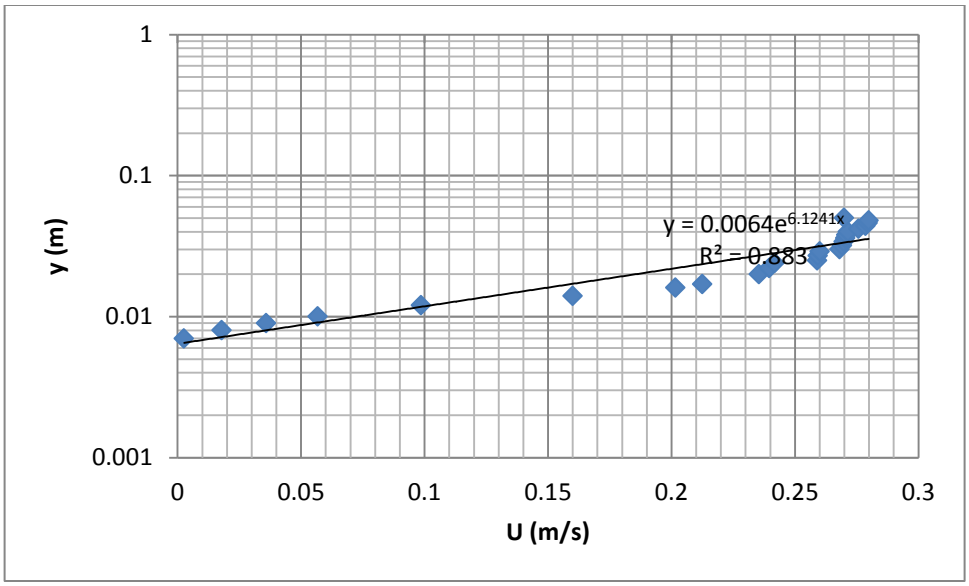

Step 2 :

From the plot, fit a straight line equation of best fit to the data:

$Y = 0.0064e^{6.124x}$

So slope of this straight line = 6.124

Step 3 : The semi-logarithmic average velocity equation is:

$U/U^* = 5.75\log (5.53\ y/d_{50})$ (here U* = friction velocity)

By rearranging the above equation:

$\text{Log}(y) = U/5.75U^* \log (5.53/d_{50})$

So 6.124 = 1/5.75U*

U* = 0.0284 m/s

APPENDIX D

Measurement details for Experiments

Appendix D-1

Data for the Experiment 01

Experiment no. 1 ; Depth of water= 50mm, Pier diameter (mm)= 50.8, no suction, Velocity (m/s) = 0.1642 and Test duration= 48 hours														
y0(mm)	D(mm)	U*	yo/D	D/d50	U(m/s)	dse(mm)	dse/D	U2/gD	Fr					
50	50.8	0.0284	0.98	100	0.1642	37.5	0.74	0.054	0.23					
Scour hole outline								Deposit outline						
X(mm)	Y(mm)	Z(mm)	X/D	Y/D	Z/D			X(mm)	Y(mm)	Z(mm)	X/D	Y/D	Z/D	
-95	0	0	-1.870	0.000	0			12	97	-2.5	0.400	3.233	-0.083	
-90	5.5	0	-1.772	0.108	0			17	99	-1.5	0.567	3.300	-0.050	
-85	7.5	0	-1.673	0.148	0			25	105	-3.5	0.833	3.500	-0.117	
-80	15.5	0	-1.575	0.305	0			35	106	-2.5	1.167	3.533	-0.083	
-75	20.5	0	-1.476	0.404	0			45	108	-1	1.500	3.600	-0.033	
-70	25.5	0	-1.378	0.502	0			55	110	-2.5	1.833	3.667	-0.083	
-65	40.5	0	-1.280	0.797	0			65	112	-0.5	2.167	3.733	-0.017	
-60	55	0	-1.181	1.083	0			75	114	-4.5	2.500	3.800	-0.150	
-55	60	0	-1.083	1.181	0			85	115.5	-2.5	2.833	3.850	-0.083	
-50	62	0	-0.984	1.220	0			95	117	-3.5	3.167	3.900	-0.117	
-45	65	0	-0.886	1.280	0			105	120	-2.5	3.500	4.000	-0.083	
-40	70	0	-0.787	1.378	0			115	122	-5.5	3.833	4.067	-0.183	
-35	77	0	-0.689	1.516	0			125	123	-2.5	4.167	4.100	-0.083	
-30	80	0	-0.591	1.575	0			135	125	-3.5	4.500	4.167	-0.117	
-25	83	0	-0.492	1.634	0			140	127	-4.5	4.667	4.233	-0.150	
-20	86	0	-0.394	1.693	0			150	120	-1.5	5.000	4.000	-0.050	
-15	88	0	-0.295	1.732	0			160	118	-3.5	5.333	3.933	-0.117	
-10	89	0	-0.197	1.752	0			170	100	-2.5	5.667	3.333	-0.083	
-5	89.5	0	-0.098	1.762	0			180	90	-1.5	6.000	3.000	-0.050	
0	90	0	0.000	1.772	0			190	82	-3.5	6.333	2.733	-0.117	
88.5	6.5	0	1.742	0.128	0			200	65	-4.5	6.667	2.167	-0.150	
80.5	15.5	0	1.585	0.305	0			210	52	-1.5	7.000	1.733	-0.050	
70	20	0	1.378	0.394	0			220	36	-3.5	7.333	1.200	-0.117	
60	35	0	1.181	0.689	0			230	18	-1.5	7.667	0.600	-0.050	
50	45	0	0.984	0.886	0			240	0	-0.5	8.000	0.000	-0.017	
40	49	0	0.787	0.965	0			235	5	-1.5	7.833	0.167	-0.050	
30	58	0	0.591	1.142	0			220	25	-0.5	7.333	0.833	-0.017	
20	67	0	0.394	1.319	0			210	45	-2.5	7.000	1.500	-0.083	
15	77	0	0.295	1.516	0			200	60	-1.5	6.667	2.000	-0.050	
10	85	0	0.197	1.673	0			190	65	-0.5	6.333	2.167	-0.017	
5	92	0	0.098	1.811	0			180	75	-0.2	6.000	2.500	-0.007	
0	95	0	0.000	1.870	0			170	80	-0.5	5.667	2.667	-0.017	
90	-10	0	1.772	-0.197	0			160	77	-1.5	5.333	2.567	-0.050	
80	-20	0	1.575	-0.394	0			150	75	-2.5	5.000	2.500	-0.083	
70	-30	0	1.378	-0.591	0			140	74	-3.5	4.667	2.467	-0.117	
60	-35.5	0	1.181	-0.699	0			130	72	-0.5	4.333	2.400	-0.017	
50	-45.5	0	0.984	-0.896	0			120	69	0.75	4.000	2.300	0.025	
40	-50.5	0	0.787	-0.994	0			110	67	-4.5	3.667	2.233	-0.150	
30	-52.5	0	0.591	-1.033	0			100	66.5	-3.5	3.333	2.217	-0.117	
20	-55.5	0	0.394	-1.093	0			90	65.5	-2.5	3.000	2.183	-0.083	
10	-58.5	0	0.197	-1.152	0			80	65	-5.5	2.667	2.167	-0.183	
5	-59	0	0.098	-1.161	0			70	64.5	-4.5	2.333	2.150	-0.150	
0	-60	0	0.000	-1.181	0			60	64	-2.5	2.000	2.133	-0.083	
-5	-55	0	-0.098	-1.083	0			50	63.5	-0.5	1.667	2.117	-0.017	
-15	-45	0	-0.295	-0.886	0			40	63	-1.5	1.333	2.100	-0.050	
-25	-42	0	-0.492	-0.827	0			30	62.5	-3.6	1.000	2.083	-0.120	
-35	-48	0	-0.689	-0.945	0			20	62	-4.5	0.667	2.067	-0.150	
-45	-52	0	-0.886	-1.024	0			10	61.5	-5.5	0.333	2.050	-0.183	
-55	-56	0	-1.083	-1.102	0			5	61	-0.5	0.167	2.033	-0.017	
-65	-57	0	-1.280	-1.122	0			0	60	-2.5	0.000	2.000	-0.083	
-75	-58	0	-1.476	-1.142	0									
-85	-59	0	-1.673	-1.161	0									
-95	-60	0	-1.870	-1.181	0									

Appendix D-2

Data for the Experiment 02

Experiment no. 2 ; Depth of water= 50mm, Pier diameter (mm)= 30, no suction, Velocity (m/s) = 0.1604 and Test duration= 48 hours												
y0(mm)	D(mm)	U*	yo/D	D/d50	U(m/s)	dse(mm)	dse/D	U2/gD	Fr			
50	30	0.0286	1.67	59	0.1604	42	1.40	0.087	0.23			
Scour hole outline												
							Deposit outline(no suction)					
X(mm)	Y(mm)	Z(mm)	X/D	Y/D	Z/D							
-75	0	0	-2.500	0.000	0		X(mm)	Y(mm)	Z(mm)	X/D	Y/D	Z/D
-70	7.5	0	-2.333	0.250	0		10	-75.5	2.33	0.333	-2.517	0.078
-65	12.5	0	-2.167	0.417	0		25	-67.5	-1.56	0.833	-2.250	-0.052
-60	17.5	0	-2.000	0.583	0		50	-65.5	-3.98	1.667	-2.183	-0.133
-55	23.5	0	-1.833	0.783	0		70	-61.5	-1.50	2.333	-2.050	-0.050
-50	26.5	0	-1.667	0.883	0		85	-76.5	-4.78	2.833	-2.550	-0.159
-45	35.5	0	-1.500	1.183	0		100	-79.5	-2.65	3.333	-2.650	-0.088
-40	38.5	0	-1.333	1.283	0		120	-71.5	-0.50	4.000	-2.383	-0.017
-35	43.5	0	-1.167	1.450	0		130	-64.5	-2.50	4.333	-2.150	-0.083
-30	47.5	0	-1.000	1.583	0		140	-73.5	-0.50	4.667	-2.450	-0.017
-25	50.5	0	-0.833	1.683	0		150	-70.5	-1.50	5.000	-2.350	-0.050
-20	60.5	0	-0.667	2.017	0		160	-63.5	-2.00	5.333	-2.117	-0.067
-15	64.5	0	-0.500	2.150	0		170	-77.5	-1.50	5.667	-2.583	-0.050
-10	67.5	0	-0.333	2.250	0		180	-65.5	-0.50	6.000	-2.183	-0.017
-5	68.9	0	-0.167	2.297	0		190	-71.25	-1.00	6.333	-2.375	-0.033
0	70	0	0.000	2.333	0		200	-77.5	-1.50	6.667	-2.583	-0.050
5	65.5	0	0.167	2.183	0		210	-79.5	-1.00	7.000	-2.650	-0.033
10	60.5	0	0.333	2.017	0		215	-55.5	-0.50	7.167	-1.850	-0.017
15	57.5	0	0.500	1.917	0		220	-40.5	-1.00	7.333	-1.350	-0.033
20	52.5	0	0.667	1.750	0		225	0	-0.50	7.500	0.000	-0.017
25	39.5	0	0.833	1.317	0		215	7.5	-1.00	7.167	0.250	-0.033
30	32.5	0	1.000	1.083	0		205	15.5	-2.00	6.833	0.517	-0.067
35	28.5	0	1.167	0.950	0		195	20.5	-1.50	6.500	0.683	-0.050
40	25.5	0	1.333	0.850	0		185	39.5	-2.00	6.167	1.317	-0.067
45	18.5	0	1.500	0.617	0		175	55.5	-0.50	5.833	1.850	-0.017
50	0	0	1.667	0.000	0		165	71.5	-1.50	5.500	2.383	-0.050
44.5	-6.5	0	1.483	-0.217	0		155	72.5	-2.00	5.167	2.417	-0.067
40.5	-10.5	0	1.350	-0.350	0		145	70.5	-1.50	4.833	2.350	-0.050
34.5	-20.5	0	1.150	-0.683	0		135	69.5	-2.00	4.500	2.317	-0.067
25.5	-35.5	0	0.850	-1.183	0		125	67.5	-1.00	4.167	2.250	-0.033
19.5	-42.5	0	0.650	-1.417	0		115	73.5	-1.00	3.833	2.450	-0.033
12.5	-55.5	0	0.417	-1.850	0		105	70.5	-1.50	3.500	2.350	-0.050
0	-70	0	0.000	-2.333	0		95	69.5	-3.56	3.167	2.317	-0.119
-7.5	-65	0	-0.250	-2.167	0		85	67.5	-2.78	2.833	2.250	-0.093
-12.5	-63.5	0	-0.417	-2.117	0		75	66.5	-1.69	2.500	2.217	-0.056
-18.5	-59.5	0	-0.617	-1.983	0		65	71.5	-1.50	2.167	2.383	-0.050
-25.5	-39.5	0	-0.850	-1.317	0		55	68.5	-2.65	1.833	2.283	-0.088
-35.5	-32.5	0	-1.183	-1.083	0		45	72.5	-1.36	1.500	2.417	-0.045
-45.5	-24.5	0	-1.517	-0.817	0		35	70	-3.98	1.167	2.333	-0.133
-55.5	-18.5	0	-1.850	-0.617	0		25	71.5	-0.97	0.833	2.383	-0.032
-65.5	-12.5	0	-2.183	-0.417	0		0	70	-0.36	0.000	2.333	-0.012
-75	0	0	-2.500	0.000	0							

Centerline Profiles							Mid Profile					
X(mm)	Y(mm)	Z(mm)	X/D	Y/D	Z/D		X(mm)	Y(mm)	Z(mm)	X/D	Y/D	Z/D
-75	0	0	-2.5	0	0		-75	-35	-0.26	-2.5	-1.167	-0.009
-70	0	-6.21	-2.333	0	-0.207		-70	-35	-4.78	-2.333	-1.167	-0.159
-65	0	-11.12	-2.167	0	-0.371		-65	-35	-6.22	-2.167	-1.167	-0.207
-55	0	-14.94	-1.833	0	-0.498		-55	-35	-8.25	-1.833	-1.167	-0.275
-50	0	-15.26	-1.667	0	-0.509		-50	-35	-10.25	-1.667	-1.167	-0.342
-45	0	-16.77	-1.5	0	-0.559		-45	-35	-12.11	-1.5	-1.167	-0.404
-40	0	-19.59	-1.333	0	-0.653		-40	-35	-12.89	-1.333	-1.167	-0.43
-35	0	-24.68	-1.167	0	-0.823		-35	-35	-14.45	-1.167	-1.167	-0.482
-30	0	-28.12	-1	0	-0.937		-30	-35	-14.98	-1	-1.167	-0.499
-25	0	-32.08	-0.833	0	-1.069		-25	-35	-15.11	-0.833	-1.167	-0.504
-20	0	-35.62	-0.667	0	-1.187		-20	-35	-15.68	-0.667	-1.167	-0.523
-15	0	-37.18	-0.5	0	-1.239		-15	-35	-16.85	-0.5	-1.167	-0.562
-10	0	-33.7	-0.333	0	-1.123		-10	-35	-17.54	-0.333	-1.167	-0.585
-5	0	-33.21	-0.167	0	-1.107		-5	-35	-18.89	-0.167	-1.167	-0.63
0	0	-33.87	0	0	-1.129		0	-35	-20.69	0	-1.167	-0.69
5	0	-32.57	0.167	0	-1.086		5	-35	-19.56	0.167	-1.167	-0.652
10	0	-30.6	0.333	0	-1.02		10	-35	-18.45	0.333	-1.167	-0.615
15	0	-27.46	0.5	0	-0.915		15	-35	-18.11	0.5	-1.167	-0.604
20	0	-19.75	0.667	0	-0.658		20	-35	-17.12	0.667	-1.167	-0.571
25	0	-19.47	0.833	0	-0.649		25	-35	-16.79	0.833	-1.167	-0.56
30	0	-15.36	1	0	-0.512		30	-35	-13.28	1	-1.167	-0.443
35	0	-8.28	1.167	0	-0.276		35	-35	-6.28	1.167	-1.167	-0.209
40	0	-6.64	1.333	0	-0.221		40	-35	-4.29	1.333	-1.167	-0.143
45	0	-0.84	1.5	0	-0.028		45	-35	-0.25	1.5	-1.167	-0.008
50	0	0.58	1.667	0	0.019		50	-35	0.36	1.667	-1.167	0.012
55	0	1.57	1.833	0	0.052		55	-35	1.02	1.833	-1.167	0.034
60	0	4.29	2	0	0.143		60	-35	2.98	2	-1.167	0.099
65	0	5.63	2.167	0	0.188		65	-35	4.56	2.167	-1.167	0.152
70	0	9.2	2.333	0	0.307		70	-35	7.46	2.333	-1.167	0.249
75	0	11.97	2.5	0	0.399		75	-35	9.56	2.5	-1.167	0.319
80	0	14.48	2.667	0	0.483		80	-35	11.34	2.667	-1.167	0.378
85	0	14.88	2.833	0	0.496		85	-35	12.44	2.833	-1.167	0.415
90	0	17.79	3	0	0.593		90	-35	14.55	3	-1.167	0.485
95	0	19.61	3.167	0	0.654		95	-35	15.39	3.167	-1.167	0.513
100	0	21.55	3.333	0	0.718		100	-35	16.87	3.333	-1.167	0.562
105	0	22.31	3.5	0	0.744		105	-35	17.64	3.5	-1.167	0.588
110	0	24.72	3.667	0	0.824		110	-35	18.45	3.667	-1.167	0.615
115	0	24.88	3.833	0	0.829		115	-35	20.21	3.833	-1.167	0.674
120	0	23.62	4	0	0.787		120	-35	20.03	4	-1.167	0.668
125	0	17.69	4.167	0	0.59		125	-35	14.86	4.167	-1.167	0.495
130	0	11.82	4.333	0	0.394		130	-35	9.45	4.333	-1.167	0.315
135	0	7.33	4.5	0	0.244		135	-35	5.69	4.5	-1.167	0.19
140	0	3.72	4.667	0	0.124		140	-35	1.99	4.667	-1.167	0.066
145	0	2.33	4.833	0	0.078		145	-35	2.02	4.833	-1.167	0.067
150	0	0.33	5	0	0.011		150	-35	0.15	5	-1.167	0.005
155	0	1.45	5.167	0	0.048		155	-35	1.06	5.167	-1.167	0.035
160	0	0.49	5.333	0	0.016		160	-35	0.28	5.333	-1.167	0.009
165	0	1.24	5.5	0	0.041		165	-35	0.98	5.5	-1.167	0.033
170	0	0.09	5.667	0	0.003		170	-35	0.06	5.667	-1.167	0.002
175	0	1.24	5.833	0	0.041		175	-35	0.85	5.833	-1.167	0.028
180	0	0.51	6	0	0.017		180	-35	0.36	6	-1.167	0.012
185	0	4.35	6.167	0	0.145		185	-35	2.97	6.167	-1.167	0.099
190	0	3.53	6.333	0	0.118		190	-35	2.22	6.333	-1.167	0.074
195	0	2.65	6.5	0	0.088		195	-35	-3.08	6.5	-1.167	-0.103
200	0	1.89	6.667	0	0.063		200	-35	-4.56	6.667	-1.167	-0.152
205	0	0.59	6.833	0	0.02		205	-35	-3.65	6.833	-1.167	-0.122
210	0	2.25	7	0	0.075		210	-35	-2.56	7	-1.167	-0.085
215	0	1.87	7.167	0	0.062		215	-35	-5.12	7.167	-1.167	-0.171
220	0	0.25	7.333	0	0.008		220	-35	-4.99	7.333	-1.167	-0.166
225	0	0.15	7.5	0	0.005		225	-35	-5.52	7.5	-1.167	-0.184

Experiment no. 2; Depth of water = 50 mm, Pier Diameter (mm) = 30, no suction, Velocity (m/s) = 0.1608 and Test duration = 48 hours

Perpendicular Profile

X (mm)	Y (mm)	Z (mm)	X/D	Y/D	Z/D
0.00	70.00	0.00	0.00	2.33	0.00
0.00	65.00	-3.17	0.00	2.17	-0.11
0.00	60.00	-6.89	0.00	2.00	-0.23
0.00	55.00	10.75	0.00	1.83	0.36
0.00	50.00	-12.45	0.00	1.67	-0.42
0.00	45.00	-14.80	0.00	1.50	-0.49
0.00	40.00	-25.48	0.00	1.33	-0.85
0.00	35.00	-33.65	0.00	1.17	-1.12
0.00	30.00	-35.40	0.00	1.00	-1.18
0.00	25.00	-33.25	0.00	0.83	-1.11
0.00	20.00	-29.85	0.00	0.67	-1.00
0.00	15.00	-29.32	0.00	0.50	-0.98
0.00	10.00	-28.26	0.00	0.33	-0.94
0.00	5.00	-29.11	0.00	0.17	-0.97
0.00	0.00	-30.45	0.00	0.00	-1.02
0.00	-5.00	-93.31	0.00	-0.17	-3.11
0.00	-10.00	-23.06	0.00	-0.33	-0.77
0.00	-15.00	-19.89	0.00	-0.50	-0.66
0.00	-20.00	-13.89	0.00	-0.67	-0.46
0.00	-25.00	-14.25	0.00	-0.83	-0.48
0.00	-30.00	-15.57	0.00	-1.00	-0.52
0.00	-35.00	-14.66	0.00	-1.17	-0.49
0.00	-40.00	-12.78	0.00	-1.33	-0.43
0.00	-45.00	-11.56	0.00	-1.50	-0.39
0.00	-50.00	-8.05	0.00	-1.67	-0.27
0.00	-55.00	-3.56	0.00	-1.83	-0.12
0.00	-60.00	-4.85	0.00	-2.00	-0.16
0.00	-65.00	-4.96	0.00	-2.17	-0.17
0.00	-70.00	2.04	0.00	-2.33	0.07

Appendix D-3

Data for the Experiment 03

Experiment no. 3 ; Depth of water= 75mm, Pier diameter (mm)= 30, no suction, Velocity (m/s) = 0.2159 and Test duration= 48 hours

y0(mm)	D(mm)	U*	yo/D	D/d50	U(m/s)	dse(mm)	dse/D	U2/gD	Fr
75	30	0.0116	2.5	59	0.2159	48	1.60	0.158	0.25

Scour hole outline

X(mm)	Y(mm)	Z(mm)	X/D	Y/D	Z/D
-58	0	0	-1.933	0.000	0
-53	5.5	0	-1.767	0.183	0
-48	16.5	0	-1.600	0.550	0
-40	22.5	0	-1.333	0.750	0
-35	30.5	0	-1.167	1.017	0
-30	40.5	0	-1.000	1.350	0
-25	50	0	-0.833	1.667	0
-20	53	0	-0.667	1.767	0
-10	55	0	-0.333	1.833	0
-5	58	0	-0.167	1.933	0
0	60	0	0.000	2.000	0
5	57	0	0.167	1.900	0
10	51	0	0.333	1.700	0
15	48	0	0.500	1.600	0
20	40	0	0.667	1.333	0
25	35	0	0.833	1.167	0
30	29	0	1.000	0.967	0
35	22.5	0	1.167	0.750	0
40	20	0	1.333	0.667	0
45	15	0	1.500	0.500	0
50	12.5	0	1.667	0.417	0
55	5.5	0	1.833	0.183	0
57	0	0	1.900	0.000	0
50	-5.5	0	1.667	-0.183	0
45	-12.5	0	1.500	-0.417	0
40	-18.5	0	1.333	-0.617	0
35	-25.5	0	1.167	-0.850	0
30	-31.5	0	1.000	-1.050	0
25	-42.5	0	0.833	-1.417	0
20	-49.5	0	0.667	-1.650	0
15	-52.5	0	0.500	-1.750	0
10	-53.5	0	0.333	-1.783	0
5	-54.5	0	0.167	-1.817	0
0	-57	0	0.000	-1.900	0
-5.5	-55.5	0	-0.183	-1.850	0
-14.5	-49.5	0	-0.483	-1.650	0
-19.5	-39.5	0	-0.650	-1.317	0
-25.5	-32.5	0	-0.850	-1.083	0
-35.5	-24.5	0	-1.183	-0.817	0
-45.5	-18.5	0	-1.517	-0.617	0
-51.5	-12.5	0	-1.717	-0.417	0
-53.5	-6.5	0	-1.783	-0.217	0
-58	0		-1.933	0.000	0

Deposit outline(no suction)

X(mm)	Y(mm)	Z(mm)	X/D	Y/D	Z/D
10	60	2.33	0.333	2.000	0.078
20	62.5	-1.56	0.667	2.083	-0.052
30	64.5	-3.98	1.000	2.150	-0.133
40	66.5	-1.50	1.333	2.217	-0.050
50	67.5	-4.78	1.667	2.250	-0.159
60	68.5	-2.65	2.000	2.283	-0.088
70	69.5	-0.50	2.333	2.317	-0.017
80	72.5	-2.50	2.667	2.417	-0.083
90	71.5	-0.50	3.000	2.383	-0.017
100	69.5	-1.50	3.333	2.317	-0.050
110	74.5	-2.00	3.667	2.483	-0.067
120	75.5	-1.50	4.000	2.517	-0.050
130	74.5	-0.50	4.333	2.483	-0.017
140	73.5	-1.00	4.667	2.450	-0.033
150	75.5	-1.50	5.000	2.517	-0.050
160	78.5	-1.00	5.333	2.617	-0.033
170	77.5	-0.50	5.667	2.583	-0.017
180	75.5	-1.00	6.000	2.517	-0.033
190	79.5	-0.50	6.333	2.650	-0.017
200	78.5	-1.00	6.667	2.617	-0.033
210	75.5	-2.00	7.000	2.517	-0.067
220	70.5	-1.50	7.333	2.350	-0.050
230	62.5	-2.00	7.667	2.083	-0.067
240	55.5	-0.50	8.000	1.850	-0.017
250	53.5	-1.50	8.333	1.783	-0.050
260	50.5	-2.00	8.667	1.683	-0.067
260	40.5	-1.50	8.667	1.350	-0.050
260	31.5	-2.00	8.667	1.050	-0.067
260	25.5	-1.00	8.667	0.850	-0.033
260	20.5	-1.00	8.667	0.683	-0.033
260	12.5	-1.50	8.667	0.417	-0.050
260	0	-3.56	8.667	0.000	-0.119
260	-10.5	-2.78	8.667	-0.350	-0.093
260	-15.5	-1.69	8.667	-0.517	-0.056
260	-25.5	-1.50	8.667	-0.850	-0.050
260	-38.5	-2.65	8.667	-1.283	-0.088
260	-50.5	-1.36	8.667	-1.683	-0.045
260	-65.5	-3.98	8.667	-2.183	-0.133
260	-75.5	-0.97	8.667	-2.517	-0.032
250	-72.5	-0.36	8.333	-2.417	-0.012
240	-71.5	-1.00	8.000	-2.383	-0.033
230	-69.5	-1.50	7.667	-2.317	-0.050
220	-68.5	-2.50	7.333	-2.283	-0.083
210	-67.5	-3.50	7.000	-2.250	-0.117
200	-67	-1.00	6.667	-2.233	-0.033
190	-66.5	-0.50	6.333	-2.217	-0.017
180	-66	-1.50	6.000	-2.200	-0.050
170	-65.5	-2.00	5.667	-2.183	-0.067
160	-65	-2.50	5.333	-2.167	-0.083
150	-64.5	-0.50	5.000	-2.150	-0.017
140	-64	-0.75	4.667	-2.133	-0.025
130	-63.5	-4.50	4.333	-2.117	-0.150
120	-63	-5.50	4.000	-2.100	-0.183
110	-62.5	-1.50	3.667	-2.083	-0.050
115	-62	-3.50	3.833	-2.067	-0.117
105	-61.5	-4.50	3.500	-2.050	-0.150
90	-60.5	-6.50	3.000	-2.017	-0.217
80	-59.5	-2.00	2.667	-1.983	-0.067
70	-59	-1.50	2.333	-1.967	-0.050
60	-58	-2.50	2.000	-1.933	-0.083
50	-57	-1.50	1.667	-1.900	-0.050
40	-56.5	-1.00	1.333	-1.883	-0.033
0	55	-3.50	0.000	1.833	-0.117

Appendix D-4

Data for the Experiment 04

Experiment no. 4 ; Depth of water= 100mm, Pier diameter (mm)= 30, no suction, Velocity (m/s) = 0.1974 and Test duration= 48 hours													
y0(mm)	D(mm)	U*	yo/D	D/d50	U(m/s)	dse(mm)	dse/D	U2/gD	Fr				
100	30	0.0264	3.33	59	0.1974	54	1.80	0.132	0.20				
Scour hole outline													
							Deposit outline(no suction)						
X(mm)	Y(mm)	Z(mm)	X/D	Y/D	Z/D								
-62	0	0	-2.067	0.000	0		X(mm)	Y(mm)	Z(mm)	X/D	Y/D	Z/D	
-55	8.5	0	-1.833	0.283	0		10	59	2.33	0.333	1.967	0.078	
-50	15.5	0	-1.667	0.517	0		20	58.5	-1.56	0.667	1.950	-0.052	
-45	20.5	0	-1.500	0.683	0		30	55.5	-3.98	1.000	1.850	-0.133	
-40	25.5	0	-1.333	0.850	0		40	54.5	-1.50	1.333	1.817	-0.050	
-35	34.5	0	-1.167	1.150	0		50	60.5	-4.78	1.667	2.017	-0.159	
-30	45	0	-1.000	1.500	0		60	62.5	-2.65	2.000	2.083	-0.088	
-25	46.5	0	-0.833	1.550	0		70	63.5	-0.50	2.333	2.117	-0.017	
-20	48.5	0	-0.667	1.617	0		80	59.5	-2.50	2.667	1.983	-0.083	
-10	52.5	0	-0.333	1.750	0		90	65.5	-0.50	3.000	2.183	-0.017	
-5	53.5	0	-0.167	1.783	0		100	67.5	-1.50	3.333	2.250	-0.050	
0	55	0	0.000	1.833	0		110	68.5	-2.00	3.667	2.283	-0.067	
10	53	0	0.333	1.767	0		120	69.5	-1.50	4.000	2.317	-0.050	
15	47	0	0.500	1.567	0		130	65.5	-0.50	4.333	2.183	-0.017	
20	41	0	0.667	1.367	0		140	66.5	-1.00	4.667	2.217	-0.033	
25	35	0	0.833	1.167	0		150	62.5	-1.50	5.000	2.083	-0.050	
30	31	0	1.000	1.033	0		160	63.5	-1.00	5.333	2.117	-0.033	
35	23.5	0	1.167	0.783	0		170	68.5	-0.50	5.667	2.283	-0.017	
40	21	0	1.333	0.700	0		180	65.5	-1.00	6.000	2.183	-0.033	
45	16	0	1.500	0.533	0		190	64.5	-0.50	6.333	2.150	-0.017	
50	13.5	0	1.667	0.450	0		200	62.5	-1.00	6.667	2.083	-0.033	
55	6.5	0	1.833	0.217	0		210	61.5	-2.00	7.000	2.050	-0.067	
60	4.5	0	2.000	0.150	0		220	60.5	-1.50	7.333	2.017	-0.050	
65	0	0	2.167	0.000	0		230	64.5	-2.00	7.667	2.150	-0.067	
60	-10.5	0	2.000	-0.350	0		240	61.5	-0.50	8.000	2.050	-0.017	
55	-19.5	0	1.833	-0.650	0		240	60	-1.50	8.000	2.000	-0.050	
50	-26.5	0	1.667	-0.883	0		240	55	-2.00	8.000	1.833	-0.067	
45	-33.5	0	1.500	-1.117	0		240	45	-1.50	8.000	1.500	-0.050	
35	-44.5	0	1.167	-1.483	0		240	35	-2.00	8.000	1.167	-0.067	
25	-51.5	0	0.833	-1.717	0		240	25	-1.00	8.000	0.833	-0.033	
15	-57.5	0	0.500	-1.917	0		240	10	-1.00	8.000	0.333	-0.033	
10	-59.5	0	0.333	-1.983	0		240	0	-1.50	8.000	0.000	-0.050	
5	-65	0	0.167	-2.167	0		240	-10	-3.56	8.000	-0.333	-0.119	
0	-66	0	0.000	-2.200	0		240	-20	-2.78	8.000	-0.667	-0.093	
-5.5	-62	0	-0.183	-2.067	0		240	-30	-1.69	8.000	-1.000	-0.056	
-20	-55	0	-0.667	-1.833	0		240	-45	-1.50	8.000	-1.500	-0.050	
-25	-50	0	-0.833	-1.667	0		240	-55	-2.65	8.000	-1.833	-0.088	
-35	-40	0	-1.167	-1.333	0		240	-65	-1.36	8.000	-2.167	-0.045	
-45	-30	0	-1.500	-1.000	0		240	-75	-3.98	8.000	-2.500	-0.133	
-55	-25	0	-1.833	-0.833	0		220	-74.5	-0.97	7.333	-2.483	-0.032	
-60	-12.5	0	-2.000	-0.417	0		210	-74	-0.36	7.000	-2.467	-0.012	
-62	0	0	-2.067	0.000	0		200	-73.5	-1.00	6.667	-2.450	-0.033	
							190	-73	-1.50	6.333	-2.433	-0.050	
							220	-72.5	-2.50	7.333	-2.417	-0.083	
							210	-72	-3.50	7.000	-2.400	-0.117	
							200	-71.5	-1.00	6.667	-2.383	-0.033	
							190	-71	-0.50	6.333	-2.367	-0.017	
							180	-70.5	-1.50	6.000	-2.350	-0.050	
							140	-70	-2.00	4.667	-2.333	-0.067	
							130	-69.5	-2.50	4.333	-2.317	-0.083	
							120	-69	-0.50	4.000	-2.300	-0.017	
							100	-68.5	-0.75	3.333	-2.283	-0.025	
							80	-68	-4.50	2.667	-2.267	-0.150	
							60	-67.5	-5.50	2.000	-2.250	-0.183	
							40	-67	-1.50	1.333	-2.233	-0.050	
							20	-66.5	-3.50	0.667	-2.217	-0.117	
							0	-66	-4.50	0.000	-2.200	-0.150	

Appendix D-5

Data for the Experiment 05

Experiment no. 5 ; Depth of water= 100mm, Pier diameter (mm)= 38, no suction, Velocity (m/s) = 0.1994 and Test duration= 48 hours

y0(mm)	D(mm)	U*	yo/D	D/d50	U(m/s)	dse(mm)	dse/D	U2/gD	Fr
100	30	0.015	2.63	75	0.1974	57	1.50	0.105	0.20

Scour hole outline

X(mm)	Y(mm)	Z(mm)	X/D	Y/D	Z/D
-65	0	0	-2.167	0.000	0
-63	20	0	-2.100	0.667	0
-55	40	0	-1.833	1.333	0
-45	58	0	-1.500	1.933	0
-30	68	0	-1.000	2.267	0
-12	72	0	-0.400	2.400	0
0	75	0	0.000	2.500	0
18	71.5	0	0.600	2.383	0
30	65	0	1.000	2.167	0
40	58	0	1.333	1.933	0
49	50	0	1.633	1.667	0
57	39	0	1.900	1.300	0
60	30	0	2.000	1.000	0
59	20	0	1.967	0.667	0
65	0	0	2.167	0.000	0
58	-15	0	1.933	-0.500	0
52	-30	0	1.733	-1.000	0
42	-42	0	1.400	-1.400	0
32	-52	0	1.067	-1.733	0
22	-60	0	0.733	-2.000	0
10	-70	0	0.333	-2.333	0
0	-75	0	0.000	-2.500	0
-10	-71	0	-0.333	-2.367	0
-20	-69	0	-0.667	-2.300	0
-29	-65	0	-0.967	-2.167	0
-40	-58	0	-1.333	-1.933	0
-50	-48	0	-1.667	-1.600	0
-55	-30	0	-1.833	-1.000	0
-65	0	0	-2.167	0.000	0

Deposit outline(no suction)

X(mm)	Y(mm)	Z(mm)	X/D	Y/D	Z/D
20	80	2.33	0.667	2.667	0.078
30	81	-1.56	1.000	2.700	-0.052
60	79	-3.98	2.000	2.633	-0.133
90	80	-1.50	3.000	2.667	-0.050
120	78	-4.78	4.000	2.600	-0.159
125	77	-2.65	4.167	2.567	-0.088
210	79	-0.50	7.000	2.633	-0.017
220	69	-2.50	7.333	2.300	-0.083
220	49	-0.50	7.333	1.633	-0.017
220	45	-1.50	7.333	1.500	-0.050
220	0	-2.00	7.333	0.000	-0.067
220	-30	-1.50	7.333	-1.000	-0.050
220	-50	-0.50	7.333	-1.667	-0.017
220	-70	-1.00	7.333	-2.333	-0.033
190	-90	-1.50	6.333	-3.000	-0.050
160	-92	-1.00	5.333	-3.067	-0.033
130	-85	-0.50	4.333	-2.833	-0.017
100	-83	-1.00	3.333	-2.767	-0.033
70	-79	-0.50	2.333	-2.633	-0.017
40	-77	-1.00	1.333	-2.567	-0.033
20	-75	-2.00	0.667	-2.500	-0.067
0	-74	-1.50	0.000	-2.467	-0.050

Appendix D-6

Data for the Experiment 06

Experiment no. 6 ; Depth of water= 75mm, Pier diameter (mm)= 38, no suction, Velocity (m/s) = 0.1619 and Test duration= 48 hours

y0(mm)	D(mm)	U*	yo/D	D/d50	U(m/s)	dse(mm)	dse/D	U2/gD	Fr
75	38	0.0211	1.97	75	0.1619	49.4	1.30	0.070	0.19

Scour hole outline

X(mm)	Y(mm)	Z(mm)	X/D	Y/D	Z/D
-70	0	0	-2.333	0.000	0
-68	10	0	-2.267	0.333	0
-60	30	0	-2.000	1.000	0
-44	45	0	-1.467	1.500	0
-35	57	0	-1.167	1.900	0
-25	68	0	-0.833	2.267	0
-10	75	0	-0.333	2.500	0
0	80	0	0.000	2.667	0
10	78	0	0.333	2.600	0
18	72	0	0.600	2.400	0
30	65	0	1.000	2.167	0
39	59	0	1.300	1.967	0
50	48	0	1.667	1.600	0
55	38	0	1.833	1.267	0
60	30	0	2.000	1.000	0
65	22	0	2.167	0.733	0
68	12	0	2.267	0.400	0
70	0	0	2.333	0.000	0
66	-10	0	2.200	-0.333	0
60	-20	0	2.000	-0.667	0
55	-30	0	1.833	-1.000	0
45	-48	0	1.500	-1.600	0
40	-56	0	1.333	-1.867	0
35	-60	0	1.167	-2.000	0
30	-66	0	1.000	-2.200	0
22	-69	0	0.733	-2.300	0
15	-75	0	0.500	-2.500	0
10	-78	0	0.333	-2.600	0
0	-81	0	0.000	-2.700	0
-9	-79	0	-0.300	-2.633	0
-14	-71	0	-0.467	-2.367	0
-20	-66	0	-0.667	-2.200	0
-26	-60	0	-0.867	-2.000	0
-30	-55	0	-1.000	-1.833	0
-50	-41	0	-1.667	-1.367	0
-60	-28	0	-2.000	-0.933	0
-65	-15	0	-2.167	-0.500	0
-70	0	0	-2.333	0.000	0

Deposit outline(no suction)

X(mm)	Y(mm)	Z(mm)	X/D	Y/D	Z/D
30	80	2.33	1.000	2.667	0.078
60	79	-1.56	2.000	2.633	-0.052
80	81	-3.98	2.667	2.700	-0.133
100	82	-1.50	3.333	2.733	-0.050
130	81	-4.78	4.333	2.700	-0.159
150	78	-2.65	5.000	2.600	-0.088
170	79	-0.50	5.667	2.633	-0.017
190	77	-2.50	6.333	2.567	-0.083
190	67	-0.50	6.333	2.233	-0.017
190	47	-1.50	6.333	1.567	-0.050
190	10	-2.00	6.333	0.333	-0.067
190	0	-1.50	6.333	0.000	-0.050
190	-15	-0.50	6.333	-0.500	-0.017
185	-35	-1.00	6.167	-1.167	-0.033
180	-70	-1.50	6.000	-2.333	-0.050
165	-92	-1.00	5.500	-3.067	-0.033
130	-94	-0.50	4.333	-3.133	-0.017
110	-90	-1.00	3.667	-3.000	-0.033
80	-88	-0.50	2.667	-2.933	-0.017
60	-82	-1.00	2.000	-2.733	-0.033
40	-81	-2.00	1.333	-2.700	-0.067
0	-81	-1.50	0.000	-2.700	-0.050

Appendix D-7

Data for the Experiment 07

Experiment no. 7 ; Depth of water= 75 mm, Pier diameter (mm)= 38, 2% suction, Velocity (m/s) = 0.1686 and Test duration= 48 hours

y0(mm)	D(mm)	U*	yo/D	D/d50	U(m/s)	dse(mm)	dse/D	U2/gD	Fr
75	38	0.0264	1.97	75	0.1689	29.89	0.79	0.077	0.20

Scour hole outline

X(mm)	Y(mm)	Z(mm)	X/D	Y/D	Z/D
-40	0	0	-1.333	0.000	0
-35	18	0	-1.167	0.600	0
-30	25	0	-1.000	0.833	0
-25	30	0	-0.833	1.000	0
-20	33	0	-0.667	1.100	0
-15	35	0	-0.500	1.167	0
-10	36.5	0	-0.333	1.217	0
-5	37	0	-0.167	1.233	0
0	36.5	0	0.000	1.217	0
5	34.5	0	0.167	1.150	0
10	32	0	0.333	1.067	0
15	30	0	0.500	1.000	0
20	28	0	0.667	0.933	0
25	23	0	0.833	0.767	0
30	18	0	1.000	0.600	0
35	10	0	1.167	0.333	0
40	0	0	1.333	0.000	0
35	-12	0	1.167	-0.400	0
30	-20	0	1.000	-0.667	0
25	-24	0	0.833	-0.800	0
20	-29	0	0.667	-0.967	0
15	-31	0	0.500	-1.033	0
10	-33	0	0.333	-1.100	0
5	-34	0	0.167	-1.133	0
0	-35	0	0.000	-1.167	0
-5	-35	0	-0.167	-1.167	0
-10	-33	0	-0.333	-1.100	0
-15	-31	0	-0.500	-1.033	0
-20	-30	0	-0.667	-1.000	0
-25	-28	0	-0.833	-0.933	0
-30	-23	0	-1.000	-0.767	0
-35	-18	0	-1.167	-0.600	0
-40	0	0	-1.333	0.000	0

Deposit outline(no suction)

X(mm)	Y(mm)	Z(mm)	X/D	Y/D	Z/D
20	40	1.54	0.667	1.333	0.051
40	42	-0.89	1.333	1.400	-0.030
60	43	-1.25	2.000	1.433	-0.042
80	41	-0.50	2.667	1.367	-0.017
100	40	3.14	3.333	1.333	0.105
130	32	-1.45	4.333	1.067	-0.048
140	22	-0.78	4.667	0.733	-0.026
150	0	-1.46	5.000	0.000	-0.049
145	-20	-0.75	4.833	-0.667	-0.025
130	-58	-2.30	4.333	-1.933	-0.077
110	-72	-1.50	3.667	-2.400	-0.050
100	-74	-0.65	3.333	-2.467	-0.022
90	-72	-0.95	3.000	-2.400	-0.032
80	-68	-2.68	2.667	-2.267	-0.089
60	-60	-3.47	2.000	-2.000	-0.116
40	-52	-4.57	1.333	-1.733	-0.152
30	-45	-1.50	1.000	-1.500	-0.050
20	-38	1.00	0.667	-1.267	0.033
12	-32	-0.25	0.400	-1.067	-0.008

Appendix D-8

Data for the Experiment 08

Experiment no. 8; Depth of water= 50mm, Pier diameter (mm)= 30, 5% suction, Velocity (m/s) = 0.1768 and Test duration= 48 hours												
Centerline Profiles							Mid Profile					
X(mm)	Y(mm)	Z(mm)	X/D	Y/D	Z/D		X(mm)	Y(mm)	Z(mm)	X/D	Y/D	Z/D
-50	0	0	-1.667	0	0.000		-50	30	0	-1.667	1.000	0.000
-45	0	-8.5	-1.500	0	-0.283		-45	30	-5.5	-1.500	1.000	-0.183
-40	0	-15.5	-1.333	0	-0.517		-40	30	-20.5	-1.333	1.000	-0.683
-35	0	-30	-1.167	0	-1.000		-35	30	-25.5	-1.167	1.000	-0.850
-30	0	-35.5	-1.000	0	-1.183		-30	30	-28.5	-1.000	1.000	-0.950
-25	0	-45.5	-0.833	0	-1.517		-25	30	-30.5	-0.833	1.000	-1.017
-20	0	-48.5	-0.667	0	-1.617		-20	30	-33.5	-0.667	1.000	-1.117
-15	0	-49	-0.500	0	-1.633		-15	30	-35	-0.500	1.000	-1.167
-10	0	-49.5	-0.333	0	-1.650		-10	30	-34.5	-0.333	1.000	-1.150
-5	0	-50	-0.167	0	-1.667		-5	30	-30.5	-0.167	1.000	-1.017
0	0	-50	0.000	0	-1.667		0	30	-32.5	0.000	1.000	-1.083
5	0	-49	0.167	0	-1.633		5	30	-29.5	0.167	1.000	-0.983
10	0	-48.5	0.333	0	-1.617		10	30	-28.5	0.333	1.000	-0.950
15	0	-50	0.500	0	-1.667		15	30	-25.5	0.500	1.000	-0.850
20	0	-51.5	0.667	0	-1.717		20	30	-36.5	0.667	1.000	-1.217
25	0	-48.5	0.833	0	-1.617		25	30	-38.5	0.833	1.000	-1.283
30	0	-40.5	1.000	0	-1.350		30	30	-33.5	1.000	1.000	-1.117
35	0	-30.5	1.167	0	-1.017		35	30	-31.5	1.167	1.000	-1.050
40	0	-20.5	1.333	0	-0.683		40	30	-18.5	1.333	1.000	-0.617
45	0	-10.5	1.500	0	-0.350		45	30	-9.5	1.500	1.000	-0.317
50	0	-5.5	1.667	0	-0.183		50	30	-4.5	1.667	1.000	-0.150
55	0	-0.5	1.833	0	-0.017		55	30	-0.5	1.833	1.000	-0.017
60	0	-1.5	2.000	0	-0.050		60	30	-1	2.000	1.000	-0.033
65	0	4.5	2.167	0	0.150		65	30	3.5	2.167	1.000	0.117
70	0	10.5	2.333	0	0.350		70	30	8.5	2.333	1.000	0.283
75	0	14	2.500	0	0.467		75	30	12	2.500	1.000	0.400
80	0	15.5	2.667	0	0.517		80	30	14	2.667	1.000	0.467
85	0	16.5	2.833	0	0.550		85	30	15	2.833	1.000	0.500
90	0	18.5	3.000	0	0.617		90	30	17	3.000	1.000	0.567
95	0	20.5	3.167	0	0.683		95	30	19	3.167	1.000	0.633
100	0	21	3.333	0	0.700		100	30	20	3.333	1.000	0.667
105	0	22.5	3.500	0	0.750		105	30	21	3.500	1.000	0.700
110	0	24	3.667	0	0.800		110	30	22.5	3.667	1.000	0.750
115	0	25.5	3.833	0	0.850		115	30	24	3.833	1.000	0.800
120	0	27.5	4.000	0	0.917		120	30	25.5	4.000	1.000	0.850
125	0	28.5	4.167	0	0.950		125	30	26.5	4.167	1.000	0.883
130	0	30.5	4.333	0	1.017		130	30	28.5	4.333	1.000	0.950
135	0	34.5	4.500	0	1.150		135	30	30.5	4.500	1.000	1.017
140	0	38.5	4.667	0	1.283		140	30	35	4.667	1.000	1.167
145	0	40.5	4.833	0	1.350		145	30	38	4.833	1.000	1.267
150	0	44.5	5.000	0	1.483		150	30	40	5.000	1.000	1.333
155	0	45	5.167	0	1.500		155	30	42	5.167	1.000	1.400
160	0	40	5.333	0	1.333		160	30	39	5.333	1.000	1.300
165	0	36	5.500	0	1.200		165	30	31.5	5.500	1.000	1.050
170	0	30.5	5.667	0	1.017		170	30	28.5	5.667	1.000	0.950
175	0	23.5	5.833	0	0.783		175	30	21.5	5.833	1.000	0.717
180	0	15.5	6.000	0	0.517		180	30	12.5	6.000	1.000	0.417
185	0	8.5	6.167	0	0.283		185	30	6.5	6.167	1.000	0.217
190	0	4.5	6.333	0	0.150		190	30	2.5	6.333	1.000	0.083
195	0	0.5	6.500	0	0.017		195	30	0.5	6.500	1.000	0.017
200	0	-0.5	6.667	0	-0.017		200	30	-0.5	6.667	1.000	-0.017
205	0	-1	6.833	0	-0.033		205	30	-2	6.833	1.000	-0.067
210	0	-1.5	7.000	0	-0.050		210	30	-1	7.000	1.000	-0.033
215	0	-5.5	7.167	0	-0.183		215	30	-4.5	7.167	1.000	-0.150
220	0	-10.5	7.333	0	-0.350		220	30	-8.5	7.333	1.000	-0.283
225	0	-15.5	7.500	0	-0.517		225	30	-14.5	7.500	1.000	-0.483
230	0	-20.5	7.667	0	-0.683		230	30	-19.5	7.667	1.000	-0.650
235	0	-23.5	7.833	0	-0.783		235	30	-22.5	7.833	1.000	-0.750
240	0	-25	8.000	0	-0.833		240	30	-23	8.000	1.000	-0.767

Experiment no. 8; Depth of water= 50mm, Pier diameter (mm)= 30, 5% suction, Velocity (m/s) = 0.1768 and Test duration= 48 hours												
Perpendicular profile							Scour hole outline					
X(mm)	Y(mm)	Z(mm)	X/D	Y/D	Z/D		X(mm)	Y(mm)	Z(mm)	X/D	Y/D	Z/D
0	45	-0.5	0	1.500	-0.017		-50	0	0	-1.667	0	0
0	40	-5.5	0	1.333	-0.183		-48	5	0	-1.600	0.167	0
0	35	-12.5	0	1.167	-0.417		-46	10	0	-1.533	0.333	0
0	30	-18.5	0	1.000	-0.617		-44	15	0	-1.467	0.5	0
0	25	-30.5	0	0.833	-1.017		-35	20	0	-1.167	0.667	0
0	20	-35.5	0	0.667	-1.183		-25	25	0	-0.833	0.833	0
0	15	-45.5	0	0.500	-1.517		-20	30	0	-0.667	1	0
0	10	-46	0	0.333	-1.533		-15	35	0	-0.500	1.167	0
0	5	-47.5	0	0.167	-1.583		-10	42	0	-0.333	1.4	0
0	0	-47.5	0	0	-1.583		-5	43	0	-0.167	1.433	0
0	-5	-51.5	0	-0.167	-1.717		0	45	0	0.000	1.5	0
0	-10	-52	0	-0.333	-1.733		5	43	0	0.167	1.433	0
0	-15	-52.5	0	-0.500	-1.750		10	42	0	0.333	1.4	0
0	-20	-48.5	0	-0.667	-1.617		15	35	0	0.500	1.167	0
0	-25	-35.5	0	-0.833	-1.183		20	32	0	0.667	1.067	0
0	-30	-25.5	0	-1.000	-0.850		25	22	0	0.833	0.733	0
0	-35	-13.5	0	-1.167	-0.450		30	20	0	1.000	0.667	0
40	-45	-2.5	1.333	-1.500	-0.083		35	15	0	1.167	0.5	0
							40	5	0	1.333	0.167	0
							45	0	0	1.500	0	0
							40	-5	0	1.333	-0.167	0
							35	-10	0	1.167	-0.333	0
							30	-15	0	1.000	-0.5	0
							25	-20	0	0.833	-0.667	0
							20	-24	0	0.667	-0.8	0
							15	-30	0	0.500	-1	0
							10	-35	0	0.333	-1.167	0
							5	-40	0	0.167	-1.333	0
							0	-45	0	0.000	-1.5	0
							-5	-42	0	-0.167	-1.4	0
							-10	-40	0	-0.333	-1.333	0
							-15	-35	0	-0.500	-1.167	0
							-20	-30	0	-0.667	-1	0
							-25	-28	0	-0.833	-0.933	0
							-30	-25	0	-1.000	-0.833	0
							-25	-22	0	-0.833	-0.733	0
							-30	-18.8	0	-1.000	-0.627	0
							-35	-16	0	-1.167	-0.533	0
							-40	-14	0	-1.333	-0.467	0
							-45	-10	0	-1.500	-0.333	0
							-50	0	0	-1.667	0	0

Experiment no. 8; Depth of water = 50 mm, Pier Diameter (mm) = 30, 5% suction, Velocity (m/s) = 0.1768 and Test duration = 48 hours

Deposit outline (5% suction)

X (mm)	Y (mm)	Z (mm)	X/D	Y/D	Z/D
52	10	1.50	1.73	0.33	0.05
55	15	-0.50	1.83	0.50	-0.02
65	18	-1.50	2.17	0.60	-0.05
75	25	-2.50	2.50	0.83	-0.08
85	35	-3.50	2.83	1.17	-0.12
95	47	-2.50	3.17	1.57	-0.08
105	52	-0.50	3.50	1.73	-0.02
108	80	-2.50	3.60	2.67	-0.08
120	72	-0.50	4.00	2.40	-0.02
130	60	-1.50	4.33	2.00	-0.05
140	52	-2.00	4.67	1.73	-0.07
150	50	-1.50	5.00	1.67	-0.05
160	49	-0.50	5.33	1.63	-0.02
170	48	-1.00	5.67	1.60	-0.03
180	45	-1.50	6.00	1.50	-0.05
190	44	-1.00	6.33	1.47	-0.03
200	42	-0.50	6.67	1.40	-0.02
180	0	-1.00	6.00	0.00	-0.03
175	-5	-0.50	5.83	-0.17	-0.02
170	-10	-1.00	5.67	-0.33	-0.03
168	-12	-0.50	5.60	-0.40	-0.02
190	-40	-2.00	6.33	-1.33	-0.07
180	-65	-0.50	6.00	-2.17	-0.02
160	-66	-1.50	5.33	-2.20	-0.05
140	-68	-2.00	4.67	-2.27	-0.07
108	-70	-1.50	3.60	-2.33	-0.05
90	-65	2.00	3.00	-2.17	0.07
70	-52	1.00	2.33	-1.73	0.03
50	-35	-1.00	1.67	-1.17	-0.03
45	0	-1.50	1.50	0.00	-0.05

Appendix D-9

Data for the Experiment 09

Experiment no. 9 ; Depth of water= 75 mm, Pier diameter (mm)= 38, 7% suction, Velocity (m/s) = 0.2242 and Test duration= 48 hours

y0(mm)	D(mm)	U*	yo/D	D/d50	U(m/s)	dse(mm)	dse/D	U2/gD	Fr
75	38	0.0185	1.97	75	0.2242	63	1.66	0.135	0.26

Scour hole outline

X(mm)	Y(mm)	Z(mm)	X/D	Y/D	Z/D
-55	0	0	-1.833	0.000	0
-50	15	0	-1.667	0.500	0
-40	33	0	-1.333	1.100	0
-30	44	0	-1.000	1.467	0
-20	51	0	-0.667	1.700	0
-10	59	0	-0.333	1.967	0
0	62	0	0.000	2.067	0
10	58	0	0.333	1.933	0
20	52	0	0.667	1.733	0
30	44	0	1.000	1.467	0
40	35	0	1.333	1.167	0
50	20	0	1.667	0.667	0
57	0	0	1.900	0.000	0
50	-28	0	1.667	-0.933	0
40	-46	0	1.333	-1.533	0
30	-57	0	1.000	-1.900	0
20	-64	0	0.667	-2.133	0
10	-67	0	0.333	-2.233	0
0	-70	0	0.000	-2.333	0
-10	-62	0	-0.333	-2.067	0
-20	-51	0	-0.667	-1.700	0
-30	-41	0	-1.000	-1.367	0
-40	-31	0	-1.333	-1.033	0
-50	-12	0	-1.667	-0.400	0
-55	0	0	-1.833	0.000	0

Deposit outline(no suction)

X(mm)	Y(mm)	Z(mm)	X/D	Y/D	Z/D
0	60	2.33	0.000	2.000	0.078
30	59	-1.56	1.000	1.967	-0.052
60	56	-3.98	2.000	1.867	-0.133
90	50	-1.50	3.000	1.667	-0.050
110	54	-4.78	3.667	1.800	-0.159
130	59	-2.65	4.333	1.967	-0.088
150	58	-0.50	5.000	1.933	-0.017
170	56	-2.50	5.667	1.867	-0.083
190	52	-0.50	6.333	1.733	-0.017
210	45	-1.50	7.000	1.500	-0.050
220	40	-2.00	7.333	1.333	-0.067
228	20	-1.50	7.600	0.667	-0.050
230	0	-0.50	7.667	0.000	-0.017
228	-12	-1.00	7.600	-0.400	-0.033
220	-50	-1.50	7.333	-1.667	-0.050
210	-66	-1.00	7.000	-2.200	-0.033
190	-83	-0.50	6.333	-2.767	-0.017
170	-88	-1.00	5.667	-2.933	-0.033
150	-89	-0.50	5.000	-2.967	-0.017
130	-90	-1.00	4.333	-3.000	-0.033
110	-89	-2.00	3.667	-2.967	-0.067
90	-85	-1.50	3.000	-2.833	-0.050
60	-82	-1.50	2.000	-2.733	-0.050
30	-78	-1.50	1.000	-2.600	-0.050
0	-70	-1.50	0.000	-2.333	-0.050

Experiment no. 9; Depth of water = 75 mm, Pier diameter (mm) = 38, 7% suction, Velocity (m/s) = 0.2242 and Test duration = 48 hours												
Centerline Profile							Mid profile					
X (mm)	Y (mm)	Z (mm)	X/D	Y/D	Z/D		X (mm)	Y (mm)	Z (mm)	X/D	Y/D	Z/D
-55	0	0.00	-1.45	0	0.00		-55	31	0	-1.45	0.82	0.00
-50	0	-6.70	-1.32	0	-0.18		-50	31	-5.1	-1.32	0.82	-0.13
-40	0	-17.50	-1.05	0	-0.46		-40	31	-15.2	-1.05	0.82	-0.40
-30	0	-31.50	-0.79	0	-0.83		-30	31	-23.1	-0.79	0.82	-0.61
-20	0	-35.60	-0.53	0	-0.94		-20	31	-29.6	-0.53	0.82	-0.78
-10	0	-51.60	-0.26	0	-1.36		-10	31	-45.2	-0.26	0.82	-1.19
0	0	-61.20	0.00	0	-1.61		0	31	-50.5	0.00	0.82	-1.33
10	0	-63.00	0.26	0	-1.66		10	31	-52.6	0.26	0.82	-1.38
20	0	-49.50	0.53	0	-1.30		20	31	-40.5	0.53	0.82	-1.07
30	0	-36.30	0.79	0	-0.96		30	31	-30.1	0.79	0.82	-0.79
40	0	-20.60	1.05	0	-0.54		40	31	-18.2	1.05	0.82	-0.48
50	0	-15.30	1.32	0	-0.40		50	31	-12.1	1.32	0.82	-0.32
60	0	-4.50	1.58	0	-0.12		60	31	-2.5	1.58	0.82	-0.07
70	0	1.25	1.84	0	0.03		70	31	0.26	1.84	0.82	0.01
80	0	5.69	2.11	0	0.15		80	31	2.6	2.11	0.82	0.07
90	0	14.26	2.37	0	0.38		90	31	10.56	2.37	0.82	0.28
100	0	18.26	2.63	0	0.48		100	31	14.5	2.63	0.82	0.38
110	0	28.36	2.89	0	0.75		110	31	21.6	2.89	0.82	0.57
120	0	39.90	3.16	0	1.05		120	31	30.1	3.16	0.82	0.79
130	0	25.30	3.42	0	0.67		130	31	21.3	3.42	0.82	0.56
140	0	8.50	3.68	0	0.22		140	31	5.6	3.68	0.82	0.15
150	0	-2.60	3.95	0	-0.07		150	31	-1.3	3.95	0.82	-0.03
160	0	-15.50	4.21	0	-0.41		160	31	-10.5	4.21	0.82	-0.28
170	0	-23.10	4.47	0	-0.61		170	31	-19.1	4.47	0.82	-0.50
180	0	-26.00	4.74	0	-0.68		180	31	-20.5	4.74	0.82	-0.54
190	0	-32.00	5.00	0	-0.84		190	31	-22.1	5.00	0.82	-0.58
200	0	-20.50	5.26	0	-0.54		200	31	-15.3	5.26	0.82	-0.40
210	0	-15.60	5.53	0	-0.41		210	31	-13.6	5.53	0.82	-0.36
220	0	-19.30	5.79	0	-0.51		220	31	-14.2	5.79	0.82	-0.37
230	0	-24.00	6.05	0	-0.63		230	31	-21	6.05	0.82	-0.55

Appendix D-10

Data for the Experiment 10

Experiment no. 10; Depth of water= 50mm, Pier diameter (mm)= 30, 6% suction, Velocity (m/s) = 0.1540 and Test duration= 48 hours												
Centerline Profiles							Mid Profile					
X(mm)	Y(mm)	Z(mm)	X/D	Y/D	Z/D		X(mm)	Y(mm)	Z(mm)	X/D	Y/D	Z/D
-40	0	0	-1.333	0	0.000		-50	30	0	-1.667	1.000	0.000
-35	0	-9.25	-1.167	0	-0.308		-45	30	-5.5	-1.500	1.000	-0.183
-30	0	-17.36	-1.000	0	-0.579		-40	30	-20.5	-1.333	1.000	-0.683
-25	0	-33.45	-0.833	0	-1.115		-35	30	-25.5	-1.167	1.000	-0.850
-20	0	-38.5	-0.667	0	-1.283		-30	30	-28.5	-1.000	1.000	-0.950
-15	0	-49.56	-0.500	0	-1.652		-25	30	-30.5	-0.833	1.000	-1.017
-10	0	-51.68	-0.333	0	-1.723		-20	30	-33.5	-0.667	1.000	-1.117
-5	0	-53.57	-0.167	0	-1.786		-15	30	-35	-0.500	1.000	-1.167
0	0	-54.98	0.000	0	-1.833		-10	30	-34.5	-0.333	1.000	-1.150
5	0	-53.69	0.167	0	-1.790		-5	30	-30.5	-0.167	1.000	-1.017
10	0	-53.12	0.333	0	-1.771		0	30	-32.5	0.000	1.000	-1.083
15	0	-52.05	0.500	0	-1.735		5	30	-29.5	0.167	1.000	-0.983
20	0	-50.18	0.667	0	-1.673		10	30	-28.5	0.333	1.000	-0.950
25	0	-48.35	0.833	0	-1.612		15	30	-25.5	0.500	1.000	-0.850
30	0	-45.38	1.000	0	-1.513		20	30	-36.5	0.667	1.000	-1.217
35	0	-40.96	1.167	0	-1.365		25	30	-38.5	0.833	1.000	-1.283
40	0	-30.17	1.333	0	-1.006		30	30	-33.5	1.000	1.000	-1.117
45	0	-19.56	1.500	0	-0.652		35	30	-31.5	1.167	1.000	-1.050
50	0	-4.56	1.667	0	-0.152		40	30	-18.5	1.333	1.000	-0.617
55	0	0	1.833	0	0.000		45	30	-9.5	1.500	1.000	-0.317
60	0	3.69	2.000	0	0.123		50	30	-4.5	1.667	1.000	-0.150
65	0	8.57	2.167	0	0.286		55	30	-0.5	1.833	1.000	-0.017
70	0	12.54	2.333	0	0.418		60	30	-1	2.000	1.000	-0.033
75	0	16.89	2.500	0	0.563		65	30	3.5	2.167	1.000	0.117
80	0	20.44	2.667	0	0.681		70	30	8.5	2.333	1.000	0.283
85	0	25.69	2.833	0	0.856		75	30	12	2.500	1.000	0.400
90	0	30.48	3.000	0	1.016		80	30	14	2.667	1.000	0.467
95	0	38.94	3.167	0	1.298		85	30	15	2.833	1.000	0.500
100	0	49.86	3.333	0	1.662		90	30	17	3.000	1.000	0.567
105	0	50.12	3.500	0	1.671		95	30	19	3.167	1.000	0.633
110	0	51.26	3.667	0	1.709		100	30	20	3.333	1.000	0.667
130	0	5.8	4.333	0	0.193		105	30	21	3.500	1.000	0.700
150	0	15.56	5.000	0	0.519		110	30	22.5	3.667	1.000	0.750
170	0	20.68	5.667	0	0.689		115	30	24	3.833	1.000	0.800
190	0	22.56	6.333	0	0.752		120	30	25.5	4.000	1.000	0.850
210	0	25.69	7.000	0	0.856		125	30	26.5	4.167	1.000	0.883
230	0	4.56	7.667	0	0.152		130	30	28.5	4.333	1.000	0.950
240	0	-5.68	8.000	0	-0.189		135	30	30.5	4.500	1.000	1.017
260	0	-12.68	8.667	0	-0.423		140	30	35	4.667	1.000	1.167
280	0	-6.85	9.333	0	-0.228		145	30	38	4.833	1.000	1.267
300	0	2.56	10.000	0	0.085		150	30	40	5.000	1.000	1.333

Experiment no. 10; Depth of water= 50mm, Pier diameter (mm)= 30, 6% suction, Velocity (m/s) = 0.1797 and Test duration= 48 hours

Perpendicular profile						Scour hole outline					
X(mm)	Y(mm)	Z(mm)	X/D	Y/D	Z/D	X(mm)	Y(mm)	Z(mm)	X/D	Y/D	Z/D
0	50	-0.69	0	1.667	-0.023	-40	0	0	-1.333	0	0
0	45	-7.59	0	1.500	-0.253	-38	10	0	-1.267	0.333	0
0	40	-15.59	0	1.333	-0.520	-35	18	0	-1.167	0.600	0
0	35	-20.68	0	1.167	-0.689	-32	27	0	-1.067	0.9	0
0	30	-33.63	0	1.000	-1.121	-30	38	0	-1.000	1.267	0
0	25	-40.35	0	0.833	-1.345	-20	45	0	-0.667	1.500	0
0	20	-46.85	0	0.667	-1.562	-10	49	0	-0.333	1.633333	0
0	25	-48.36	0	0.833	-1.612	0	50	0	0.000	1.667	0
0	20	-49.47	0	0.667	-1.649	10	47	0	0.333	1.566667	0
0	15	-51.45	0	0.5	-1.715	20	42	0	0.667	1.400	0
0	10	-52.69	0	0.333	-1.756	30	35	0	1.000	1.166667	0
0	5	-53.22	0	0.167	-1.774	40	25	0	1.333	0.833	0
0	0	-53.87	0	0.000	-1.796	45	15	0	1.500	0.5	0
0	-5	-51.78	0	-0.167	-1.726	48	8	0	1.600	0.267	0
0	-10	-50.33	0	-0.333	-1.678	50	0	0	1.667	0.000	0
0	-15	-44.69	0	-0.500	-1.490	45	-10	0	1.500	-0.333	0
0	-20	-30.45	0	-0.667	-1.015	40	-20	0	1.333	-0.667	0
0	-25	-20.11	0.000	-0.833	-0.670	30	-32	0	1.000	-1.06667	0
0	-30	-16.35	0	-1.000	-0.545	20	-41	0	0.667	-1.367	0
0	-35	-12.56	0	-1.167	-0.419	10	-47	0	0.333	-1.56667	0
0	-45	-9.06	0	-1.500	-0.302	0	-50	0	0.000	-1.667	0
40	-50	-0.36	1.333333	-1.667	-0.012	-10	-48	0	-0.333	-1.600	0
						-20	-38	0	-0.667	-1.26667	0
						-27	-29	0	-0.900	-0.967	0
						-33	-20	0	-1.100	-0.66667	0
						-37	-10	0	-1.233	-0.33333	0
						-40	0	0	-1.333	0.000	0

Appendix D-11

Data for the Experiment 11

Experiment no. 11; Depth of water= 50mm, Pier diameter (mm)= 30, 7% suction, Velocity (m/s) = 0.1797 and Test duration= 48 hours

Centerline Profiles						Mid Profile						Deposit outline(7% suction)					
X(mm)	Y(mm)	Z(mm)	X/D	Y/D	Z/D	X(mm)	Y(mm)	Z(mm)	X/D	Y/D	Z/D	X(mm)	Y(mm)	Z(mm)	X/D	Y/D	Z/D
-48	0	0	-1.600	0	0.000	-48	42.5	0	-1.600	1.417	0.000	58	52	-2.50	1.933	1.733	-0.083
-45	0	-11.36	-1.500	0	-0.379	-45	42.5	-9.63	-1.500	1.417	-0.321	118	53	-0.50	3.933	1.767	-0.017
-40	0	-18.89	-1.333	0	-0.630	-40	42.5	-15.56	-1.333	1.417	-0.519	163	75	-1.50	5.433	2.500	-0.050
-35	0	-36.69	-1.167	0	-1.223	-35	42.5	-26.58	-1.167	1.417	-0.886	205	90	-2.50	6.833	3.000	-0.083
-25	0	-45.88	-0.833	0	-1.529	-25	42.5	-39.98	-0.833	1.417	-1.333	262	115	-3.50	8.733	3.833	-0.117
-15	0	-53.36	-0.500	0	-1.779	-15	42.5	-42.25	-0.500	1.417	-1.408	305	135	-2.50	10.167	4.500	-0.083
-10	0	-54.25	-0.333	0	-1.808	-10	42.5	-43.87	-0.333	1.417	-1.462	430	205	-0.50	14.333	6.833	-0.017
-5	0	-56.91	-0.167	0	-1.897	-5	42.5	-44.12	-0.167	1.417	-1.471	430	135	-2.50	14.333	4.500	-0.083
0	0	-57.22	0.000	0	-1.907	0	42.5	-45.79	0.000	1.417	-1.526	430	115	-0.50	14.333	3.833	-0.017
5	0	-55.05	0.167	0	-1.835	5	42.5	-43.56	0.167	1.417	-1.452	430	90	-1.50	14.333	3.000	-0.050
10	0	-54.11	0.333	0	-1.804	10	42.5	-39.79	0.333	1.417	-1.326	430	75	-2.00	14.333	2.500	-0.067
15	0	-50.03	0.500	0	-1.668	15	42.5	-33.46	0.500	1.417	-1.115	430	0	-1.50	14.333	0.000	-0.050
20	0	-45.33	0.667	0	-1.511	20	42.5	-30.15	0.667	1.417	-1.005	430	-65	-0.50	14.333	-2.167	-0.017
25	0	-39.44	0.833	0	-1.315	25	42.5	-26.15	0.833	1.417	-0.872	430	-125	-1.00	14.333	-4.167	-0.033
30	0	-26.88	1.000	0	-0.896	30	42.5	-22.85	1.000	1.417	-0.762	430	-145	-1.50	14.333	-4.833	-0.050
35	0	-22.87	1.167	0	-0.762	35	42.5	-18.74	1.167	1.417	-0.625	430	-170	-1.00	14.333	-5.667	-0.033
40	0	-17.56	1.333	0	-0.585	40	42.5	-11.25	1.333	1.417	-0.375	305	-112	-0.50	10.167	-3.733	-0.017
45	0	-8.55	1.500	0	-0.285	45	42.5	-5.56	1.500	1.417	-0.185	262	-95	-1.00	8.733	-3.167	-0.033
50	0	0	1.667	0	0.000	50	42.5	-1.23	1.667	1.417	-0.041	205	-79	-0.50	6.833	-2.633	-0.017
55	0	1.56	1.833	0	0.052	55	42.5	0.89	1.833	1.417	0.030	163	-64	-1.00	5.433	-2.133	-0.033
60	0	4.98	2.000	0	0.166	60	42.5	2.36	2.000	1.417	0.079	118	-62	-2.00	3.933	-2.067	-0.067
65	0	9.36	2.167	0	0.312	65	42.5	7.56	2.167	1.417	0.252	52	-59	-1.50	1.733	-1.967	-0.050
70	0	15.97	2.333	0	0.532	70	42.5	11.26	2.333	1.417	0.375	20	-75	-2.00	0.667	-2.500	-0.067
75	0	19.25	2.500	0	0.642	75	42.5	14.89	2.500	1.417	0.496						
80	0	22.65	2.667	0	0.755	80	42.5	17.35	2.667	1.417	0.578						
85	0	27.47	2.833	0	0.916	85	42.5	20.45	2.833	1.417	0.682						
90	0	32.56	3.000	0	1.085	90	42.5	22.64	3.000	1.417	0.755						
95	0	41.89	3.167	0	1.396	95	42.5	30.58	3.167	1.417	1.019						
100	0	52.14	3.333	0	1.738	100	42.5	42.56	3.333	1.417	1.419						
105	0	53.11	3.500	0	1.770	105	42.5	46.36	3.500	1.417	1.545						
110	0	53.89	3.667	0	1.796	110	42.5	47.11	3.667	1.417	1.570						
130	0	6.87	4.333	0	0.229	130	42.5	2.56	4.333	1.417	0.085						
150	0	15.56	5.000	0	0.519	150	42.5	10.58	5.000	1.417	0.353						
170	0	22.69	5.667	0	0.756	170	42.5	18.45	5.667	1.417	0.615						
190	0	24.58	6.333	0	0.819	190	42.5	20.78	6.333	1.417	0.693						
210	0	27.58	7.000	0	0.919	210	42.5	22.98	7.000	1.417	0.766						
230	0	8.26	7.667	0	0.275	230	42.5	7.69	7.667	1.417	0.256						
240	0	-6.74	8.000	0	-0.225	240	42.5	-5.69	8.000	1.417	-0.190						
260	0	-14.56	8.667	0	-0.485	260	42.5	-10.79	8.667	1.417	-0.360						
280	0	-7.89	9.333	0	-0.263	280	42.5	-4.68	9.333	1.417	-0.156						
300	0	4.68	10.000	0	0.156	300	42.5	2.67	10.000	1.417	0.089						
310	0	5.68	10.333	0	0.189	310	42.5	5.87	10.333	1.417	0.196						
320	0	8.79	10.667	0	0.293	320	42.5	6.11	10.667	1.417	0.204						
330	0	4.28	11.000	0	0.143	330	42.5	1.56	11.000	1.417	0.052						
350	0	1.28	11.667	0	0.043	350	42.5	0.85	11.667	1.417	0.028						
370	0	4.35	12.333	0	0.145	370	42.5	1.58	12.333	1.417	0.053						
390	0	3.15	13.000	0	0.105	390	42.5	1.11	13.000	1.417	0.037						
410	0	2.47	13.667	0	0.082	410	42.5	1.98	13.667	1.417	0.066						
420	0	5.78	14.000	0	0.193	420	42.5	2.57	14.000	1.417	0.086						
430	0	2.14	14.333	0	0.071	430	42.5	0.98	14.333	1.417	0.033						

Experiment no. 11; Depth of water= 50mm, Pier diameter (mm)= 30, 7% suction, Velocity (m/s) = 0.1797 and Test duration= 48 hours

Perpendicular profile							Scour hole outline					
X(mm)	Y(mm)	Z(mm)	X/D	Y/D	Z/D		X(mm)	Y(mm)	Z(mm)	X/D	Y/D	Z/D
0	55	0.85	0.00	1.833	0.028		-55	0	0	-1.833	0	0
0	50	-9.15	0.00	1.667	-0.305		-50	9	0	-1.667	0.300	0
0	45	-17.12	0.00	1.500	-0.571		-45	25	0	-1.500	0.833	0
0	40	-22.45	0.00	1.333	-0.748		-40	35	0	-1.333	1.166667	0
0	35	-35.18	0.00	1.167	-1.173		-32.5	42	0	-1.083	1.400	0
0	30	-40.66	0.00	1.000	-1.355		-20	50	0	-0.667	1.667	0
0	25	-48.35	0.00	0.833	-1.612		-10	52	0	-0.333	1.733333	0
0	20	-50.24	0.00	0.667	-1.675		0	55	0	0.000	1.833	0
0	15	-53.45	0.00	0.500	-1.782		10	49	0	0.333	1.633333	0
0	10	-54.36	0.00	0.333	-1.812		20	45	0	0.667	1.500	0
0	5	-54.89	0.00	0.167	-1.830		30	40	0	1.000	1.333333	0
0	0	-55.48	0.00	0.000	-1.849		40	27	0	1.333	0.900	0
0	-5	-56.45	0.00	-0.167	-1.882		50	0	0	1.667	0	0
0	-10	-53.18	0.00	-0.333	-1.773		48	-25	0	1.600	-0.833	0
0	-15	-52.65	0.00	-0.500	-1.755		40	-51	0	1.333	-1.700	0
0	-20	-46.38	0.00	-0.667	-1.546		30	-61	0	1.000	-2.033	0
0	-25	-32.78	0.00	-0.833	-1.093		20	-72	0	0.667	-2.400	0
0	-30	-22.79	0.00	-1.000	-0.760		10	-80	0	0.333	-2.66667	0
0	-35	-18.55	0.00	-1.167	-0.618		0	-85	0	0.000	-2.833	0
0	-40	-14.89	0.00	-1.333	-0.496		-10	-79	0	-0.333	-2.63333	0
0	-45	-11.15	0.00	-1.500	-0.372		-20	-69	0	-0.667	-2.300	0
0	-50	-9.15	0.00	-1.667	-0.305		-30	-55	0	-1.000	-1.833	0
0	-55	-7.55	0.00	-1.833	-0.252		-40	-37	0	-1.333	-1.23333	0
0	-60	-5.15	0.00	-2.000	-0.172		-50	-17	0	-1.667	-0.567	0
0	-65	-4.55	0.00	-2.167	-0.152		-55	0	0	-1.833	0	0
0	-70	-3.99	0.00	-2.333	-0.133							
0	-75	-2.59	0.00	-2.500	-0.086							
0	-80	-1.45	0.00	-2.667	-0.048							
50	-85	-0.87	1.67	-2.833	-0.029							

Appendix D-12

Data for the Experiment 12

Experiment no. 12; Depth of water= 50mm, Pier diameter (mm)= 30, 10% suction, Velocity (m/s) = 0.1878 and Test duration= 48 hours												
Centerline Profiles							Mid Profile					
X(mm)	Y(mm)	Z(mm)	X/D	Y/D	Z/D		X(mm)	Y(mm)	Z(mm)	X/D	Y/D	Z/D
-53	0	0	-1.767	0	0.000		-53	37.5	0	-1.767	1.250	0.000
-50	0	-9.14	-1.667	0	-0.305		-50	37.5	-5.24	-1.667	1.250	-0.175
-45	0	-16.35	-1.500	0	-0.545		-45	37.5	-14.11	-1.500	1.250	-0.470
-40	0	-32.15	-1.333	0	-1.072		-40	37.5	-25.34	-1.333	1.250	-0.845
-35	0	-42.19	-1.167	0	-1.406		-35	37.5	-31.69	-1.167	1.250	-1.056
-30	0	-47.16	-1.000	0	-1.572		-30	37.5	-34.25	-1.000	1.250	-1.142
-25	0	-51.28	-0.833	0	-1.709		-25	37.5	-41.05	-0.833	1.250	-1.368
-20	0	-54.36	-0.667	0	-1.812		-20	37.5	-39.13	-0.667	1.250	-1.304
-15	0	-56.48	-0.500	0	-1.883		-15	37.5	-43.26	-0.500	1.250	-1.442
-10	0	-57.35	-0.333	0	-1.912		-10	37.5	-45.55	-0.333	1.250	-1.518
-5	0	-58.17	-0.167	0	-1.939		-5	37.5	-46.11	-0.167	1.250	-1.537
0	0	-59.56	0.000	0	-1.985		0	37.5	-47.23	0.000	1.250	-1.574
5	0	-58.17	0.167	0	-1.939		5	37.5	-45.36	0.167	1.250	-1.512
10	0	-56.38	0.333	0	-1.879		10	37.5	-40.25	0.333	1.250	-1.342
15	0	-53.89	0.500	0	-1.796		15	37.5	-38.16	0.500	1.250	-1.272
20	0	-49.28	0.667	0	-1.643		20	37.5	-30.06	0.667	1.250	-1.002
25	0	-41.36	0.833	0	-1.379		25	37.5	-25.33	0.833	1.250	-0.844
30	0	-36.47	1.000	0	-1.216		30	37.5	-21.24	1.000	1.250	-0.708
35	0	-35.15	1.167	0	-1.172		35	37.5	-19.25	1.167	1.250	-0.642
40	0	-33.56	1.333	0	-1.119		40	37.5	-18.27	1.333	1.250	-0.609
45	0	-31.45	1.500	0	-1.048		45	37.5	-17.11	1.500	1.250	-0.570
50	0	-26.78	1.667	0	-0.893		50	37.5	-16.35	1.667	1.250	-0.545
55	0	-21.25	1.833	0	-0.708		55	37.5	-12.25	1.833	1.250	-0.408
60	0	-18.39	2.000	0	-0.613		60	37.5	-10.27	2.000	1.250	-0.342
65	0	-13.42	2.167	0	-0.447		65	37.5	-6.11	2.167	1.250	-0.204
70	0	-9.45	2.333	0	-0.315		70	37.5	-4.23	2.333	1.250	-0.141
75	0	-5.68	2.500	0	-0.189		75	37.5	-1.99	2.500	1.250	-0.066
80	0	0.96	2.667	0	0.032		80	37.5	0.11	2.667	1.250	0.004
85	0	1.99	2.833	0	0.066		85	37.5	0.25	2.833	1.250	0.008
90	0	2.45	3.000	0	0.082		90	37.5	0.74	3.000	1.250	0.025
95	0	3.11	3.167	0	0.104		95	37.5	1.24	3.167	1.250	0.041
100	0	5.97	3.333	0	0.199		100	37.5	3.16	3.333	1.250	0.105
110	0	8.39	3.667	0	0.280		110	37.5	4.28	3.667	1.250	0.143
120	0	10.16	4.000	0	0.339		120	37.5	5.24	4.000	1.250	0.175
130	0	18.77	4.333	0	0.626		130	37.5	12.47	4.333	1.250	0.416
140	0	21.25	4.667	0	0.708		140	37.5	14.18	4.667	1.250	0.473
150	0	25.45	5.000	0	0.848		150	37.5	16.33	5.000	1.250	0.544
160	0	30.11	5.333	0	1.004		160	37.5	19.27	5.333	1.250	0.642
170	0	34.59	5.667	0	1.153		170	37.5	25.17	5.667	1.250	0.839
180	0	28.78	6.000	0	0.959		180	37.5	26.14	6.000	1.250	0.871
200	0	19.54	6.667	0	0.651		200	37.5	14.11	6.667	1.250	0.470
220	0	11.56	7.333	0	0.385		220	37.5	9.25	7.333	1.250	0.308
240	0	6.89	8.000	0	0.230		240	37.5	2.54	8.000	1.250	0.085
260	0	3.11	8.667	0	0.104		260	37.5	1.74	8.667	1.250	0.058
280	0	1.55	9.333	0	0.052		280	37.5	0.76	9.333	1.250	0.025
300	0	2.06	10.000	0	0.069		300	37.5	1.11	10.000	1.250	0.037
320	0	3.99	10.667	0	0.133		320	37.5	1.56	10.667	1.250	0.052
340	0	3.17	11.333	0	0.106		340	37.5	1.34	11.333	1.250	0.045
360	0	4.25	12.000	0	0.142		360	37.5	1.98	12.000	1.250	0.066
380	0	6.68	12.667	0	0.223		380	37.5	4.11	12.667	1.250	0.137
400	0	3.28	13.333	0	0.109		400	37.5	0.89	13.333	1.250	0.030
420	0	4.17	14.000	0	0.139		420	37.5	1.24	14.000	1.250	0.041
440	0	5.39	14.667	0	0.180		440	37.5	2.33	14.667	1.250	0.078
460	0	8.15	15.333	0	0.272		460	37.5	4.28	15.333	1.250	0.143
480	0	10.29	16.000	0	0.343		480	37.5	5.67	16.000	1.250	0.189
500	0	13.26	16.667	0	0.442		500	37.5	8.55	16.667	1.250	0.285
520	0	5.89	17.333	0	0.196		520	37.5	2.17	17.333	1.250	0.072
540	0	2.55	18.000	0	0.085		540	37.5	1.87	18.000	1.250	0.062
560	0	-0.87	18.667	0	-0.029		560	37.5	-0.25	18.667	1.250	-0.008
580	0	-1.24	19.333	0	-0.041		580	37.5	-0.37	19.333	1.250	-0.012
595	0	-2.05	19.833	0	-0.068		595	37.5	-1.04	19.833	1.250	-0.035

Experiment no. 12; Depth of water= 50mm, Pier diameter (mm)= 30, 10% suction, Velocity (m/s) = 0.1878 and Test duration= 48 hours

Perpendicular profile

X(mm)	Y(mm)	Z(mm)	X/D	Y/D	Z/D
0	60	0	0.00	2.000	0.000
0	55	-11.25	0.00	1.833	-0.375
0	50	-19.11	0.00	1.667	-0.637
0	45	-24.11	0.00	1.500	-0.804
0	40	-37.15	0.00	1.333	-1.238
0	35	-44.25	0.00	1.167	-1.475
0	30	-50.24	0.00	1.000	-1.675
0	25	-52.18	0.00	0.833	-1.739
0	20	-55.39	0.00	0.667	-1.846
0	15	-57.16	0.00	0.500	-1.905
0	10	-58.99	0.00	0.333	-1.966
0	5	-59.17	0.00	0.167	-1.972
0	0	-60.14	0.00	0.000	-2.005
0	-5	-58.17	0.00	-0.167	-1.939
0	-10	-56.26	0.00	-0.333	-1.875
0	-15	-54.16	0.00	-0.500	-1.805
0	-20	-50.13	0.00	-0.667	-1.671
0	-25	-40.27	0.00	-0.833	-1.342
0	-30	-35.18	0.00	-1.000	-1.173
0	-35	-25.18	0.00	-1.167	-0.839
0	-40	-17.18	0.00	-1.333	-0.573
0	-45	-12.11	0.00	-1.500	-0.404
0	-50	-8.47	0.00	-1.667	-0.282
0	-55	-6.33	0.00	-1.833	-0.211
0	-60	-5.14	0.00	-2.000	-0.171
0	-65	-2.33	0.00	-2.167	-0.078
0	-70	-1.99	0.00	-2.333	-0.066
50	-75	-0.89	1.67	-2.500	-0.030

Scour hole outline

X(mm)	Y(mm)	Z(mm)	X/D	Y/D	Z/D
-53	0	0	-1.767	0	0
-50	5	0	-1.667	0.167	0
-45	20	0	-1.500	0.667	0
-40	30	0	-1.333	1	0
-20	50	0	-0.667	1.667	0
-10	55	0	-0.333	1.833	0
0	60	0	0.000	2	0
10	52	0	0.333	1.733	0
38	40	0	1.267	1.333333	0
55	25	0	1.833	0.833	0
67	0	0	2.233	0	0
60	-30	0	2.000	-1.000	0
40	-58	0	1.333	-1.93333	0
30	-72	0	1.000	-2.400	0
0	-75	0	0.000	-2.500	0
-10	-60	0	-0.333	-2.000	0
-30	-40	0	-1.000	-1.333	0
-40	-25	0	-1.333	-0.83333	0
-53	0	0	-1.767	0.000	0

Deposit outline(10% suction)

X(mm)	Y(mm)	Z(mm)	X/D	Y/D	Z/D
10	70	-2.50	0.333	2.333	-0.083
40	83	-0.50	1.333	2.767	-0.017
70	85	-1.50	2.333	2.833	-0.050
120	90	-2.50	4.000	3.000	-0.083
170	98	-3.50	5.667	3.267	-0.117
200	110	-2.50	6.667	3.667	-0.083
235	128	-0.50	7.833	4.267	-0.017
305	158	-2.50	10.167	5.267	-0.083
380	168	-0.50	12.667	5.600	-0.017
430	178	-1.50	14.333	5.933	-0.050
495	198	-2.00	16.500	6.600	-0.067
595	210	-1.50	19.833	7.000	-0.050
595	178	-0.50	19.833	5.933	-0.017
595	128	-1.00	19.833	4.267	-0.033
595	0	-1.50	19.833	0.000	-0.050
595	-210	-1.00	19.833	-7.000	-0.033
495	-190	-0.50	16.500	-6.333	-0.017
430	-160	-1.00	14.333	-5.333	-0.033
380	-140	-0.50	12.667	-4.667	-0.017
305	-130	-1.00	10.167	-4.333	-0.033
235	-100	-2.00	7.833	-3.333	-0.067
170	-70	-1.50	5.667	-2.333	-0.050
120	-60	-2.00	4.000	-2.000	-0.067
70	-55	-0.89	2.333	-1.833	-0.030
40	-50	-1.15	1.333	-1.667	-0.038
0	-75	-0.33	0.000	-2.500	-0.011

VITA AUCTORIS

Name	:	Mohammed Showkat Jahan
Place of Birth	:	Mohongonj, Netrokona, Bangladesh
Year of Birth	:	1968
Education	:	Bangladesh University of Engineering and Technology (BUET) 1988-1993 B.Sc. in Civil Engineering University of Windsor 2009-2010 Master of Engineering in Civil Engineering University of Windsor 2010- Present M.A.Sc. in Civil Engineering